EXPLORING PLANT INNATE IMMUNE SIGNALING NETWORK: LAYERED POST-TRANSLATIONAL MODIFICATIONS IN PLAY

A Dissertation

by

XIYU MA

Submitted to the Office of Graduate and Professional Studies of
Texas A&M University
in partial fulfillment of the requirements for the degree of

DOCTOR OF PHILOSOPHY

Chair of Committee,	Ping He
Committee Members,	Martin Dickman
	Tatyana Igumenova
	Craig Kaplan
Head of Department,	Gregory D. Reinhart

December 2017

Major Subject: Biochemistry

ABSTRACT

Prompt activation of pattern recognition receptors (PRRs) upon microbial infection is essential for hosts to defend against pathogen attacks. Plant Botrytis-induced kinase 1 (BIK1) family receptor-like cytoplasmic kinases are key immune regulators associated with multiple PRRs, including the flagellin receptor complex FLS2-BAK1 in arabidopsis (*Arabidopsis thaliana*). Upon flagellin perception, BAK1 directly phosphorylates BIK1, leading to BIK1 dissociation from the FLS2-BAK1 complex to relay immune signaling. How BIK1 activation is regulated and how the signal is transduced downstream remain largely elusive.

In this dissertation, we found that flagellin perception triggers rapid monoubiquitination of BIK1 and its homolog PBL1 *in planta*. Time course and mutational analyses suggest that flagellin-induced BIK1 phosphorylation precedes BIK1 monoubiquitination. We further identified an RING-type E3 ligase LUCKY1 that interacts with BIK1 and monoubiquitinates BIK1 at multiple sites. Mass spectrometry and mutational analyses uncovered that the $BIK1^{9KR}$ mutant with nine lysine residues mutated into arginine eliminated ubiquitination without sacrificing BIK1 kinase activity. Phenotypic analysis with transgenic plants expressing $BIK1^{9KR}$ suggested that ubiquitination of BIK1 positively regulates BIK1 function as well as plant immune responses. Moreover, we found that flg22-triggered ubiquitination of BIK1 does not regulate BIK1 stability but controls ligand-induced BIK1 dissociation from receptor FLS2.

Recognition of pathogen-associated molecular patterns (PAMPs) via PRRs triggers a transient spike of secondary messengers such as Ca^{2+} and phosphatidic acid (PA) in plant. How lipid signaling is tightly controlled to modulate PA production in immunity remains largely unknown. Here we show a PA synthesis diacylglycerol kinase DGK5 functions positively in plant immunity and is differentially regulated by two phosphorylation events. Upon PAMP activation, the PRR-associated cytoplasmic kinase BIK1 directly interacts with DGK5 and phosphorylates DGK5 at Ser-506. In addition, PAMP-activated MAP kinase 4 (MPK4) phosphorylates DGK5 at Thr-446 independently of BIK1. Interestingly, phosphorylation at Ser-506 by BIK1 appears to positively regulate DGK5 function while MPK4-mediated Thr-446 phosphorylation possesses a negative impact. Our findings reveal a mechanism that how PRR complex activation directly switches on lipid signaling to orchestrate innate immunity.

This dissertation is dedicated to my dearest parents and grandparents

ACKNOWLEDGEMENTS

I deeply appreciate my PIs, Dr. Ping He and Dr. Libo Shan, for giving me the great opportunity to study in their lab, and for their tremendous input on training me how to become an independent scientist in the future from every aspects. I clearly understand how I have transformed from that rotation student who almost had no any idea about research in biochemisty/molecular biology/genetics to what I am today. Their patience, encourage and support kept me studying hard on research and inspired me to look forward on academia. Words can't express my appreciation enough and I sincerely thank them for everything they have done in the past years.

I wound give special thanks to my committee Dr. Martin Dickman, Dr. Craig Kaplan and Dr. Tatyana Igumenova for their continuous help and support in the past 6 years. They are always caring about me and my research, bring up constructive comments and suggestions and keep patient and encouraging. I would also like to thank Dr. Timothy Devaranne and Devaranne lab members especially Dr. Hem Thapa for comments and suggestions during our joint group meeting as well as support for our collaborative projects. Also special thanks to other collaborators Dr. Sixue Chen, Dr. Junmin Peng, Dr. Tuen Munnick and Dr. Richard Viestra.

Lots of thanks give to past and current lab members from Dr. He and Dr. Shan lab especially Dr. Bo Li for contribution to DGK5 project and Mr. Yanyan Huang for collaborating in other project. I also really appreciate the guidance I got from several past lab members including Dr. Dongping Lu, Dr. Xiquan Gao and Dr. Baomin Feng.

I also sincerely thank Dr. Xiuren Zhang, Dr. Pingwei Li for their kind mentoring during lab rotations and all other faculty members in TAMU who have taught me during my Ph.D. study.

And great thanks give to department staff and BGA for making my life here easy, warm and pleasant. Also I would like to thank my classmates and friends in College Station who made the past years so enjoyable.

Finally, I can never appreciate my family enough, especially my dad, mom, and my grandparents. I won't be here today without their love, encouragement and unconditional support. And deep appreciation to my wife for her love, understanding, patience for every single day we have spent together. Definitely thank my little Jenny, my life just got so beautiful with you around, I love you.

CONTRIBUTORS AND FUNDING SOURCES

This work was supervised by a dissertation committee consisting of Professors Ping He, Craig Kaplan, and Tatyana Igumenova of the Department of Biochemistry and Biophysics and Professor Martin Dickman of the Department of Plant Pathology and Microbiology.

The data for Chapter II was in part by Jinggeng Zhou (Fig 2.1A). The data for Chapter III was in part by Professor Junmin Peng (Fig 3.5A, B). The data for Chapter IV was in part by Dr. Bo Li (Fig 4.1B, C, 4.2, 4.3B, C, 4.6D, 4.9 B,C), Drs. Hem Thapa and Timothy Devarenne, (Fig 4.9A), Dr. Sixue Chen (Fig 4.7A). Dr. Tuen Munnick provided technical assistance and was involved in various discussions for Chapter IV. All other work presented in the dissertation was conducted by the student independently.

This work was made possible in part by NIH (R01GM092893) and NSF (IOS-1252539) to P.H.

TABLE OF CONTENTS

Page

ABSTRACT ii

DEDICATION iv

ACKNOWLEDGEMENTS v

CONTRIBUTORS AND FUNDING SOURCES vii

TABLE OF CONTENTS viii

LIST OF FIGURES xi

CHAPTER I INTRODUCTION AND LITERATURE REVIEW 1

1.1 Introduction 1
1.2 PAMPs/MAMPs/DAMPs are perceived by membrane-localized pattern recognition receptors 3
1.3 Receptors and co-receptors in plant immunity 6
1.4 Receptor complex formation upon ligand perception 6
1.5 Activation of BIK1 and homologous RLCKs 9
1.6 Activation of MAPK cascade 11
1.7 Ca^{2+} spike and activation of CDPKs 12
1.8 Early defense responses lead to rapid transcriptome reprogramming 14
1.9 BIK1 substrates 15
1.10 Ubiquitin and ubiquitination 16
1.11 Function of ubiquitination 18
1.12 Ubiquitination in innate immunity 22
1.13 Overview of research focus 23

CHAPTER II FLAGELLIN-INDUCED MONOUBIQUITINATION OF BIK1 REGULATES ARABIDOPSIS INNATE IMMUNITY 26

2.1 Introduction 26
2.2 Materials and methods 29
2.2.1 Plant material and growth conditions 29
2.2.2 Plasmid construction and generation of transgenic plants 30
2.2.3 Construction of the *UBQK0* plasmid 30
2.2.4 Pathogen infection assays 31

2.2.5 Protoplast transient expression assay and co-immunoprecipitation (co-IP) assay 32
2.2.6 *In vivo* ubiquitination assay 32
2.2.7 *In vitro* ubiquitination assay 33
2.2.8 MAPK assay 33
2.2.9 Detection of ROS production 33
2.2.10 Recombinant protein isolation and *in vitro* kinase assays 34
2.3 Results 35
2.3.1 Ubiquitination inhibitor PYR-41 blocks flg22-triggered early immune responses 35
2.3.2 Flg22 perception induces BIK1 monoubiquitination 39
2.3.3 Flg22-induced BIK1 phosphorylation occurs temporally prior to ubiquitination 42
2.3.4 $BIK1^{K204}$ is important in flg22-induced BIK1 ubiquitination and phosphorylation 45
2.3.5 $BIK1^{K204}$ positively regulates BIK1-mediated plant immune responses 48
2.4 Discussion 49

CHAPTER III MONOUBIQUITINATION OF BIK1 BY A RING-TYPE E3 LIGASE LUCKY1 MEDIATES BIK1 FUNCTION IN PLANT IMMUNITY 53

3.1 Introduction 53
3.2 Materials and methods 56
3.2.1 Plant material and growth conditions 56
3.2.2 Plasmid construction and generation of transgenic plants 56
3.2.3 Yeast two-hybrid screen 58
3.2.4 Pathogen infection assays 59
3.2.5 Protoplast transient expression assay and co-immunoprecipitation assay 59
3.2.6 *In vivo* ubiquitination assay 60
3.2.7 *In vitro* ubiquitination assay 60
3.2.8 *In vitro* GST pull-down assay 61
3.2.9 Mass spectrometry analysis of ubiquitination sites 61
3.3 Results 62
3.3.1 Y2H screen identified a putative E3 ligase for BIK1 ubiquitination 62
3.3.2. BIK1 phosphorylates LUCKY1 *in vitro* 65
3.3.3. LUCKY1 monoubiquitinates BIK1 65
3.3.4. LUCKY1 is able to ubiquitinate BIK1 at multiple sites 68
3.3.5. Monoubiquitination is required for BIK1 function in innate immunity 70
3.3.6. Monoubiquitination mediates BIK1 dissociation from FLS2 71
3.4 Discussion 73

CHAPTER IV DIFFERENTIAL PHOSPHORYLATION OF DIACYL-GLYCEROL KINASE DGK5 REGULATES PLANT INNATE IMMUNITY AND CONCLUSIONS 78

4.1 Introduction 78
4.2 Materials and methods 82
4.2.1 Plant material and growth conditions 82
4.2.2 Plasmid construction and generation of transgenic plants 83
4.2.3 Pathogen infection assays 84
4.2.4 Protoplast transient expression assay and co-immunoprecipitation assay 85
4.2.5 MAPK assay 85
4.2.6 Detection of ROS production 86
4.2.7 Recombinant protein isolation and *in vitro* kinase assays 86
4.2.8 Yeast two-hybrid screen 87
4.2.9 *In vitro* GST pull-down assay 87
4.2.10 Mass spectrometry analysis of phosphorylation sites 88
4.2.11 *In vitro* DGK activity assay 88
4.3 Results 89
4.3.1 Identification of DGK5 as a novel BIK1 interacting protein 89
4.3.2 DGK5 is a positive regulator of plant immunity 93
4.3.3 PAMPs induce rapid phosphorylation of DGK5 96
4.3.4 BIK1 phosphorylates DGK5 at Ser-506 99
4.3.5 MPK4 phosphorylates DGK5 at Thr-446 101
4.3.6 DGK5 is an active diacylglycerol kinase and phosphorylation of DGK5 at Ser-506 and Thr-446 oppositely regulate DGK5 activity 105
4.3.7 Phosphorylation at Ser-506 and Thr-446 oppositely regulates DGK5 function in ROS and immunity 107
4.4 Discussion and conclusions 108

REFERENCES 113

APPENDIX SUPPLEMENTAL DATA 128

LIST OF FIGURES

FIGURE		Page
1.1	Model of plant innate immunity: PAMP-triggered immunity (PTI) and effector-triggered immunity (ETI).	2
1.2	Immune responses in plant	5
1.3	FLS2 signaling pathways	11
1.4	Ubiquitination cascade	17
1.5	Organization and function mechanism of E3 ligases in arabidopsis	18
2.1	PYR-41 is an efficient ubiquitination inhibitor.	36
2.2	Ubiquitination inhibitor PYR-41 blocks flg22 signaling	37
2.3	FLS2 and BIK1 *in vivo* ubiquitination	39
2.4	PAMP perception induces BIK1 monoubiquitination	40
2.5	Flg22-induced BIK1 phosphorylation precedes its ubiquitination	44
2.6	BIK1 ubiquitination site screen	46
2.7	$BIK1^{K204}$ is required for flg22-induced BIK1 ubiquitination	46
2.8	$BIK1^{K204}$ has impaired kinase activity	47
2.9	$BIK1^{K204}$ plays an essential role in BIK1-mediated immune responses	49
3.1	BIK1 interacts with a novel E3 ligase LUCKY1	64
3.2	BIK1 phosphorylates LUCKY1 *in vitro*	65
3.3	LUCKY1 monoubiquitinates BIK1 *in vitro* and *in vivo*	66
3.4	WB screen of amiRNA for LUCKY1/2	68

3.5 LUCKY1 ubiquitinates BIK1 at multiple sites *in vitro* and BIK1^{9KR} blocks monoubquitination 69

3.6 BIK1^{9KR} has normal kinase activity 70

3.7 Monoubiquitination is required for BIK1 function in innate immunity..... 71

3.8 Monoubiquitination mediates BIK1 dissociation from FLS2 upon flg22 perception 72

4.1 BIK1 interacts with a positive defense regulator DGK5..... 91

4.2 BIK1 interacts with DGK5..... 93

4.3 DGK5 plays a positive role in defense against bacterial infection..... 94

4.4 Flg22-triggered MAPK activation is not altered in *dgk5* 96

4.5 Flg22 induces phosphorylation of DGK5 98

4.6 BIK1 phosphorylates DGK5 at Ser-506..... 100

4.7 MPK4 phosphorylates DGK5 at Thr-446 102

4.8 MPK4 phosphorylates DGK5 and interacts with DGK5 *in vivo* 104

4.9 Phosphorylation at Ser-506 and Thr-446 oppositely regulates DGK5 function in ROS and immunity..... 106

4.10 Model: Inverse regulation of DGK5 by protein kinase BIK1- and MPK4-mediated phosphorylation governs flg22-triggered PA Signaling..... 109

CHAPTER I

INTRODUCTION AND LITERATURE REVIEW[*]

1.1 Introduction

Being sessile, plants have evolved complex defense mechanisms to cope with potential microbial invasions while maintaining and maximizing their growth and development. In addition to physical and mechanical barriers, the innate immune system is an essential part of formidable plant defenses confronting most of the microbial menace. In contrast to animals, plants lack a sophisticated adaptive immune system. However, plants have evolved an effective "danger"-detecting surveillance system by expanding a staggering number of membrane-resident receptor proteins or receptor kinases (RKs) that function as radar antennas to sense the presence of microbial components, termed as microbe or pathogen-associated molecular patterns (MAMPs or PAMPs) (Ausubel, 2005; Boller and Felix, 2009; Shiu and Bleecker, 2001, 2003). One of the first lines of plant inducible defense is initiated by the recognition of MAMPs or PAMPs via cell surface-resident pattern recognition receptors (PRRs) and is termed PAMP-triggered immunity (PTI) (Jones and Dangl, 2006). As part of a basal defense to fend off a broad spectrum of microbial invasions, the elicitation of PTI is accompanied

[*] Part of this chapter is reprinted with permission from "Big Roles of Small Kinases: The Complex Functions of Receptor-Like Cytoplasmic Kinases in Plant Immunity and Development" by Wenwei Lin, Xiyu Ma, Libo Shan, Ping He. *Journal of Integrative Plant Biology*, Vol. 55, (12): 1188-1197. Part of this chapter is reprinted with permission from "SERKing Coreceptors for Receptors" by Xiyu Ma, Guangyuan Xu, Ping He, Libo Shan. *Trends in Plant Science*, Vol. 21, (12): 1017-1033.

by profound transcriptional reprogramming, production of reactive oxygen species (ROS), deposition of callose to reinforce the cell wall and stomatal closure to block pathogen entry (Boller and Felix, 2009; Monaghan and Zipfel, 2012; Schwessinger and Ronald, 2012).

To achieve an effective infection, successful pathogens have further evolved various virulence mechanisms to dampen host immune systems or interfere with host physiological and cellular responses. For instance, many Gram-negative bacteria have obtained the ability to inject a repertoire of virulence effector proteins into host cells through type III secretion system (TTSS) to block immune responses (Feng and Zhou, 2012; Shan et al., 2007). To confine or eliminate infection, certain plants have evolutionarily acquired polymorphic intracellular receptors, also termed as disease resistance proteins (R proteins), to directly or indirectly recognize effectors and elicit a

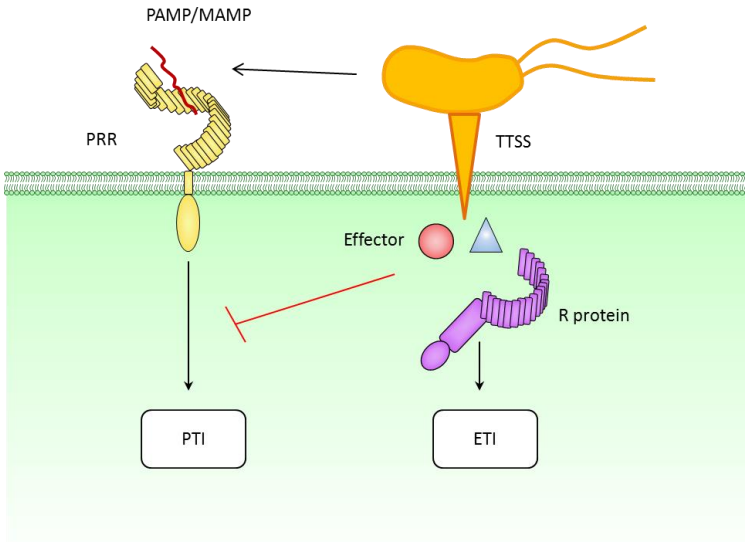

Figure 1.1 Model of plant innate immunity: PAMP-triggered immunity (PTI) and effector-triggered immunity (ETI).

second line of plant inducible defense defined as effector-triggered immunity (ETI), which often accompanied by the hypersensitive response (HR), a localized programmed cell death to restrict the spread of pathogens (Fig. 1.1) (Jones and Dangl, 2006).

1.2 PAMPs/MAMPs/DAMPs are perceived by membrane-localized pattern recognition receptors

Specific and precise recognition of PAMPs/MAMPs by membrane-localized receptors or co-receptor complexes initiate innate immune signaling. Various PAMPs/MAMPs from different microbes have been identified over the past two decades (Couto and Zipfel, 2016). One of the best studied PAMP is bacterial flagellin, the building block of bacterial flagella. Flagellin, or a conserved N-terminal 22 amino acid peptide flg22, elicit strong defense responses in arabidopsis (*Arabidopsis thaliana*) and pre-treatment of flg22 enables enhanced resistance towards subsequent pathogenic bacterial infections (Felix et al., 1999; Gomez-Gomez and Boller, 2000). Other components from bacteria such as elongation factor Tu (EF-Tu), peptidoglycan (PGN) or lipopolysaccharide (LPS), as well as components from fungi such as chitin or peptide nlp20 from bacteria/fungi/oomycetes all trigger robust immune responses (Albert et al., 2015a; Cao et al., 2014; Ranf et al., 2015; Willmann et al., 2011b; Zipfel et al., 2006). In addition to PAMPs/MAMPs from microbes, plant-derived signal molecules termed damage-associated molecular pattern (DAMP) alarm the plants during ongoing damaging, likely caused by pathogen invasion. When plant cell membrane integrity is compromised, DAMPs such as extracellular ATP (eATP) or peptide AtPEP1 will be

released into extracellular space and potently ignite plant defense responses similar to PAMPs (Choi et al., 2014; Krol et al., 2010; Yamaguchi et al., 2006).

Tremendous efforts in plant innate immunity research have focused on how PAMPs/MAMPs/DAMPs are perceived and dozens of PRRs have been characterized in great details. Most of those receptors are either receptor-like kinases (RLKs) or receptor-like proteins (RLPs) (Yu et al., 2017). Typical plant RLKs consist of a signal peptide sequence, an extracellular motif, a single transmembrane region and a cytoplasmic kinase domain, which is structurally similar to mammalian receptor tyrosine kinases (RTKs) (Example: FLS2, EFR in Fig. 1.2) (Antolin-Llovera et al., 2012; Shiu and Bleecker, 2001). RLPs are similar to RLKs with an extracellular domain and a transmembrane domain, but have relatively short cytoplasmic regions that lack a kinase domain (Example: RLP23 in Fig. 1.2) (Shiu and Bleecker, 2003; Wang et al., 2008). In contrast to the limited number of RTKs or Toll-like receptors (TLRs) that perceive hormones, cytokines or MAMPs in mammals, plants have evolved a large repertoire of RLKs and RLPs that form the largest family of plant membrane receptors with more than 600 members in arabidopsis and 1,100 members in rice (Shiu et al., 2004). In addition to the involvement of many RLKs/RLPs in immunity, many RLKs have been found to play fundamental roles in a wide range of physiological processes from development to stress responses (De Smet et al., 2009).

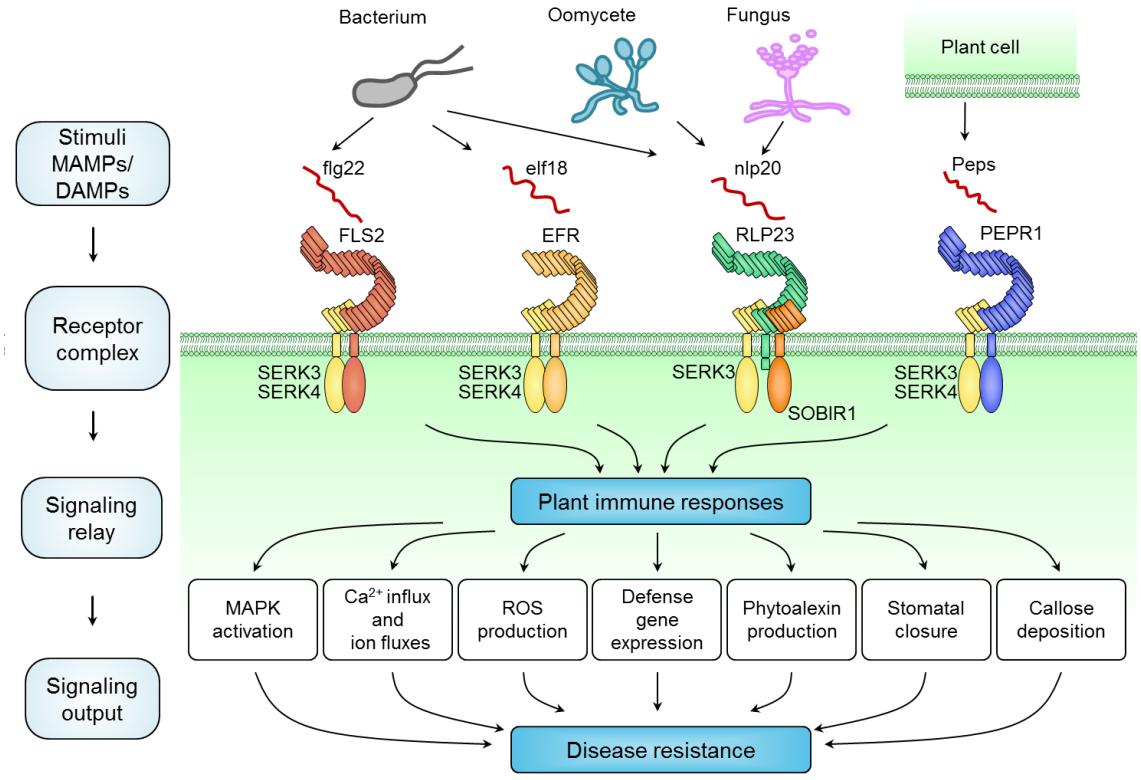

Figure 1.2 Immune receptors and responses in plant. PAMPs/MAMPs or plant endogenous DAMPs are perceived by the cognate RLK or RLP receptors, which recruit co-receptors SERKs to trigger a series of defense responses including MAPK activation, Ca^{2+} influx, ROS production, transcriptional reprograming of defense genes, phytoalexin production, stomatal closure and callose deposition. Bacterial flagellin (flg22) and EF-Tu (elf18) are perceived by FLS2 and EFR respectively. nlp20, a conserved MAMP from bacteria, oomycetes and fungi, is recognized by RLP23, which constitutively interacts with SOBIR1. Endogenous DAMP Peps are perceived by PEPR1 and PERP2.

1.3 Receptors and co-receptors in plant immunity

The arabidopsis genome encodes more than 600 *RLKs* and *RLPs*. The largest group of RLKs and RLPs contains an extracellular leucine-rich repeat (LRR) domain with more than 200 members in arabidopsis (Shiu and Bleecker, 2003). Several LRR-RLKs are known to function as PRRs. For instance, flagellin-sensing 2 (FLS2) and PEP1 receptor 1 (PEPR1) perceive bacterial flagellin and arabidopsis Pep1, respectively (Chinchilla et al., 2006; Yamaguchi et al., 2010). Interestingly, despite distinct ligands, several LRR-RLKs such as FLS2 and PEPR1 heterodimerize with another LRR-RLK, BRI1-associated receptor kinase 1 (BAK1), also known as somatic embryogenesis receptor kinase 3 (SERK3), and other SERK members upon cognate ligand perception (Chinchilla et al., 2007b; Heese et al., 2007b; Li et al., 2002; Nam and Li, 2002; Roux et al., 2011). In addition, SERKs complex with several RLP receptors including receptor-like protein 23 (RLP23), which perceives necrosis- and ethylene-inducing peptide 1 (nep1)-like proteins (NLPs) secreted by various plant-associated microorganisms (Albert et al., 2015b). Thus, SERKs appear to function as a shared signaling node that connects complex signaling networks via association with various RLKs and RLPs (Fig. 1.2).

1.4 Receptor complex formation upon ligand perception

As discussed above, SERKs usually dimerize with receptors upon perception of the cognate ligand. It was previously proposed that BAK1 functions as a signaling partner of LRR-RLK receptors because BAK1 appears to not be involved in flg22 binding to FLS2 (Chinchilla et al., 2007b; Kinoshita et al., 2005). Recent protein

structural studies have provided insights into the mechanisms of "ligand-receptor-co-receptor" complex formation and activation (Han et al., 2014). Structural analyses of the extracellular domains of flg22-FLS2-BAK1 complex revealed that BAK1 is engaged in flg22 perception via contacting the flg22-FLS2 binding interface, (Santiago et al., 2013; Sun et al., 2013a; Sun et al., 2013b). Flg22 induce FLS2-BAK1 heterodimerization by directly contacting the N-terminus of the LRR domain of BAK1 and forming a composite interface with FLS2, which is crucial for assembling the stable heterodimeric complex (Han et al., 2014). However, flg22 is recognized by BAK1 only upon the ligand binding to their cognate receptors, which explains why BAK1 is not required for flg22-FLS2 binding. Thus, SERKs function as co-receptors that interact directly with the ligand-receptor complexes. Notably, flg22-induced FLS2-BAK1 complex formation appears to not trigger significant conformational changes in the extracellular domain or homo-oligomerization of FLS2 (Santiago et al., 2013; Sun et al., 2013a; Sun et al., 2013b). A similar mechanism of the complex formation and activation of the flg22-induced FLS2-BAK1 also extends to the Pep1-induced PEPR1-BAK1 complex (Tang et al., 2015).

Due to the lack of an intracellular kinase domain, several LRR-RLPs complex with, and require, suppressor of bir1-1 (SOBIR1), an LRR-RLK, for signaling activation (Liebrand et al., 2014). Recent studies indicate that the activation of RLP-SOBIR1 complex requires the ligand-dependent association with SERKs (Gust and Felix, 2014; Liebrand et al., 2014). NLPs secreted by a wide range of microbes, including bacteria, fungi, and oomycetes, induce rapid plant tissue necrosis and promote pathogenicity

while also triggering host defense responses. A conserved 20-amino acid peptide derived from NLPs (nlp20) acts as a MAMP to initiate defense responses against different pathogens without inducing necrosis (Bohm et al., 2014; Oome et al., 2014). The arabidopsis LRR-RLP RLP23 functions as the receptor of nlp20 (Albert et al., 2015b). RLP23 constitutively complexes with SOBIR1 and recruits SERKs upon nlp20 perception (Albert et al., 2015b) (Fig. 1.2). It appears that nlp20-RLP23-mediated signaling requires two LRR-RLKs, SOBIR1 and BAK1, both of which have a short extracellular LRR domain. It remains unknown whether they are also involved in the direct binding of nlp20 in a concerted action with RLP23.

It is worth noting that SERKs may not be required for all PRRs-ligand perception. For example, recognition of fungal chitin by putative receptor LysM domain-containing RLK CERK1 leads to homodimerization of CERK1 (Liu et al., 2012). Interestingly, another LysM-RLK LYK5 with higher chitin-binding affinity heterodimerize with CERK1 (Cao et al., 2014). It is likely LYK5 and CERK1 functions as receptor-co-receptor to perceive chitin. Similarly, two LysM domain-containing RLPs LYM1 and LYM3 bind to PGNs and play indispensable roles in PGN-mediated signaling (Willmann et al., 2011a). CERK1 is also involved in PGN-mediated signaling suggesting it might serve as co-receptor for LYM1/3, although evidence for direct binding is lacking.

1.5 Activation of BIK1 and homologous RLCKs

Receptor-like cytoplasmic kinases (RLCKs) are small kinases belonging to the RLK superfamily, but lacking extracellular domains. In mammals, RLCKs IL-1 receptor-associated protein kinases (IRAKs) play essential roles in TLR-mediated innate immunity. MAMP perceptions via TLRs lead to the recruitment of adaptor protein Myeloid differentiation factor 88 (MyD88), and IRAK1 and IRAK 4. Once IRAK1 associates with MyD88, it is phosphorylated by the activated IRAK4, and subsequently released from MyD88 to propagate the signal by association with an E3 ubiquitin ligase (Smith et al., 2009; Takeuchi and Akira, 2010). Significantly, a plant RLCK, BIK1 (Botrytis-induced kinase 1), is rapidly phosphorylated upon flagellin perception in an FLS2- and BAK1-dependent manner (Lu et al., 2010a; Zhang et al., 2010) (Fig. 1.3). The *bik1* mutants are compromised in both diverse flagellin-mediated responses and immunity to non-pathogenic bacterial infection. In addition to flagellin signaling, BIK1 is also involved in EF-Tu- and endogenous peptide AtPep1-mediated immune responses (Zhang et al., 2010). Accordingly, BIK1 interacts with FLS2, EF-Tu receptor EFR, and Pep1 receptor PEPR1, suggesting that BIK1 resembles mammalian IRAKs as a convergent component involved in signaling triggered by multiple MAMPs/DAMPs. Both FLS2 and EFR are non-RD kinases with little kinase activity, whereas BAK1 is a RD kinase with strong *in vitro* kinase activity (Schwessinger et al., 2011). BAK1 phosphorylates BIK1 *in vitro* and *in vivo*. Interestingly, BIK1 also directly phosphorylates BAK1 and FLS2 (Lu et al., 2010a) suggesting that transphosphorylation of FLS2/BAK1/BIK1 or EFR/BAK1/BIK1 is a key for the full activation of the receptor

super complex. In contrast to FLS2 and EFR, PEPR1 is a RD kinase with strong *in vitro* kinase activity and directly phosphorylates BIK1 *in vitro* while BIK1 also phosphorylates PEPR1. The involvement of BIK1 in both FLS2/EFR and PEPR1 indicated a convergent activation mode that transphosphorylation within receptor-co-receptor-RLCK complexes play a fundamental role in the activation of downstream signaling.

Several other subfamily VII RLCKs, including avrPphB susceptible 1 (PBS1) and PBS1-like 1 (PBL1), which share high homology with BIK1, are also phosphorylated upon flg22 treatment and play redundant roles with BIK1 in PTI responses (Lu et al., 2010b; Zhang et al., 2010). In addition, two other RLCKs BR-signaling kinase1 (BSK1) and PTI compromised RLCK1 (PCRK1) have been shown to be involved in FLS2 signaling, as both *bsk1* mutant and *pcrk1* mutant exhibit reduced flg22-triggered ROS production and increased disease susceptibility (Shi et al., 2013; Sreekanta et al., 2015). While BSK1 has been shown to interact with FLS2, whether PCRK1 directly resides in the receptor complex is still unknown. Moreover, another RLCK, PBL27, directly interacts with CERK1 in chitin-mediated signaling and CERK1 directly phosphorylates PBL27 *in vitro* (Yamada et al., 2016). Chitin-triggered downstream signaling is largely compromised in *pbl27* mutant (Shinya et al., 2014).

Notably, BIK1 and homologs PBS1/PBL1/PBL2/BSK1 can all associate with FLS2 and their interaction is largely reduced upon flg22 treatment (Lu et al., 2010a; Zhang et al., 2010). It is likely that upon activation, phosphorylated RLCKs are released from the receptor complex and interact with their substrates to further relay the signal

downstream. However, it remains elusive how BIK1 and its close family members positively regulate PTI signaling. Identification of BIK1 phosphorylation targets would fill in the missing link of BIK1 activation and downstream immune responses. Meanwhile, how redundantly they function remain unclear as single mutants of *bik1*, *bsk1*, *pcrk* show varying degree of deficiency in immunity and higher-order mutant knocking out multiple RLCKs simultaneously could provide more insights in the future.

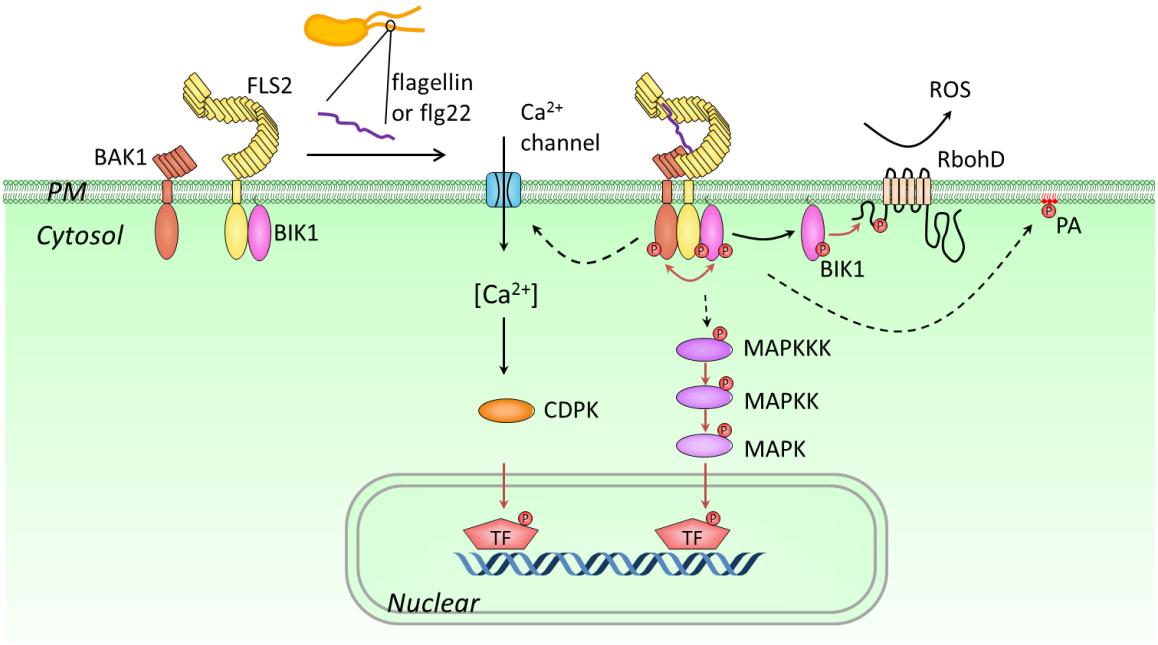

Figure 1.3 FLS2 signaling pathways. Perception of flg22 induces rapid FLS2-BAK1 complex formation and transphosphorylation with BIK1. BIK1 is released from receptor complex and phosphorylates RbohD to regulate ROS production. Downstream of receptor complex activation includes activation of MAPK cascade, Ca^{2+} influx and activation of CDPK, PA accumulation as well as transcriptome reprogramming.

1.6 Activation of MAPK cascade

Mitogen-activated protein kinase (MAPK) cascades, typically containing three sequentially activated kinases of a MAPK kinase kinase (MAPKKK or MEKK), a

MAPK kinase (MAPKK or MKK) and a MAPK (MPK), serve as convergent points downstream of multiple cell surface-resident receptors. Perception of MAMPs or DAMPs rapidly and transiently activates two major MAPK cascades: MEKK1/MEKK-MKK4/MKK5-MPK3/MPK6 and MEKK1-MKK1/MKK2-MPK4 (Meng and Zhang, 2013b). In general, MPK3 and MPK6 redundantly and positively regulate plant defense, whereas MPK4 negatively regulates it. MPK11 activity is also stimulated by flg22 treatment (Bethke et al., 2012). In chitin-mediated signaling, it has been shown PBL27 directly interacts and phosphorylates MAPKKK5 to activate the MAPKKK5-MKK4/MKK5-MPK3/MPK6 cascade (Yamada et al., 2016). However, in FLS2 or EFR signaling, it is still not clear whether BIK1 or other homologs are directly upstream or independent of the MAPK cascade. In these cases, how the receptor-co-receptor complexes activate MAPK cascades remains elusive. Additional components, such as the heterotrimeric G protein complexes and scaffold proteins, are also potential activators of MAPK cascades in diverse signaling pathways (Cheng et al., 2015).

1.7 Ca^{2+} spike and activation of CDPKs

Ca^{2+} serves as an important second messenger in various signaling pathways in mammals. In plants, different MAMP/DAMP treatment leads to rapid cytoplasmic Ca^{2+} spike within one or two minutes. Interestingly, different types of MAMPs/DAMPs mediate unique Ca^{2+} burst patterns (Seybold et al., 2014). Flg22 and eATP appear to trigger a biphasic Ca^{2+} spike, while Pep1 seems only trigger a single peak Ca^{2+} increase (Ranf et al., 2011; Tanaka et al., 2010). There are mainly two sources of Ca^{2+}

contributing to the Ca^{2+} spike: extracellular space and intracellular organelles (Seybold et al., 2014). For Pep1-mediated Ca^{2+} burst, it is believed to be an Ca^{2+} influx from the apoplastic space via membrane localized nucleotide-gated cation channel 2 (CNGC2) as a *cngc2* mutant abolishes the Pep1-triggered Ca^{2+} increase (Ma et al., 2012). For the eATP-mediated Ca^{2+} spike, a Ca^{2+} channel inhibitor mainly blocks the first peak while a PLC inhibitor suppresses the second peak (Tanaka et al., 2010). This suggests two peaks are contributed by two sources of Ca^{2+} with apoplastic Ca^{2+} contributing to the first peak while intracellular organelles supply the second peak. Contradicting evidences exist from flg22 research: PLC inhibitor didn't block Ca^{2+} increase in one report suggesting intracellular organelles are not involved, (Kwaaitaal et al., 2011) while blocking the lipid signaling downstream of the PLC pathway blocks part of the Ca^{2+} burst indicating the involvement of intracellular organelles (Ma et al., 2012). Moreover, inhibiting the activity of ionotropic glutamate receptor type Ca^{2+} channels (iGluRs) blocks flg22-triggered Ca^{2+} change while *cngc2* has no effect (Kwaaitaal et al., 2011). It is likely that flg22-triggered biphasic Ca^{2+} spike resembles the two-source model as eATP, although the involved channels might differ. To summarize, there is great diversity among signaling networks in terms of Ca^{2+} and different MAMPs/DAMPs likely induce distinct pathways to regulate Ca^{2+} via different Ca^{2+} channels.

Ca^{2+} dependent protein kinases (CDPKs) are a group of proteins each containing a kinase domain and a regulatory domain with EF-hand motifs (Schulz et al., 2013). CDPKs are Ca^{2+} sensors and flg22 treatment rapidly and transiently activate group of CDPKs including CPK4/5/6/11 (Boudsocq et al., 2010). CPKs reportedly regulate

defense gene expression with overlapping and nonoverlapping clusters regulated by MPKs. In addition, respiratory burst oxidase homolog D (RbohD), an NADPH oxidase responsible for flg22-triggered apoplastic ROS production, is directly phosphorylated by CPK5 at multiple residues (Dubiella et al., 2013). Phosphorylation of RbohD by CPK5 appears positively regulate RbohD activity as CPK5 kinase mutant rendered plant impaired ROS production upon flg22 treatment.

Recently it has been reported that another CDPK, CPK28 directly interacts with BIK1 and phosphorylates BIK1. BIK1 protein turnover seems be regulated by CPK28 and this provides another layer of negative regulation of PTI responses (Monaghan et al., 2014a).

1.8 Early defense responses lead to rapid transcriptome reprogramming

As early as fifteen to thirty minutes following PTI signaling initiation, the global transcriptome starts to be dramatically reshaped to equip plants with proper responses via sophisticated network regulations (Li et al., 2016). MAPKs directly phosphorylate certain transcription factors to direct specific gene expression. Among them, MPK3/6 directly phosphorylate WRKY33 (a WRKY family transcription factor) (Mao et al., 2011), ethylene response factor 6 (ERF6), (Meng et al., 2013) and MPK6 phosphorylates BRI1-EMS-suppressor 1 (BES1), and ERF104 to positively control MAMP-responsive genes (Bethke et al., 2009; Kang et al., 2015). In the meantime, MPK4 phosphorylates a trihelix transcription factor arabidopsis SH4-related 3 (ASR3) to negatively monitor expression of many defense genes (Li et al., 2015). In addition to function on TFs, MPK-

activated CDKCs directly phosphorylate CTD of RNA polymerase II subunit RPB1 to positively regulate defense gene expression and overall disease resistance (Li et al., 2014b).

1.9 BIK1 substrates

In order to gain more insight of the signaling downstream of BIK1, many laboratories have tried to look for BIK1 substrates using different approaches and some targets were unveiled. Two independent studies demonstrated that RbohD is a BIK1 substrate as BIK1 directly interacts and phosphorylates RbohD at multiple serine/threonine residues (Kadota et al., 2014b; Li et al., 2014f). Phosphorylation at those residues positively regulates PTI responses since alanine substitutions of these residues reduced ROS production while phosphomimetic substitutions enhanced ROS (Kadota et al., 2014b; Li et al., 2014f). Among these RbohD phosphorylation sites, some are unique to BIK1 while some are shared with CPKs, suggesting a complexed signaling network as even one RbohD residue can be phosphorylated by multiple kinases.

Another study reported heterotrimeric G proteins including XLG2 (Ga), AGB1 (Gb), and AGG1/2 (Gg) complex with FLS2 and BIK1 to regulate BIK1 stability (Liang et al., 2016). In the absence of intact G protein complex, BIK1 protein stability could not be maintained and BIK1 is degraded in the 26S proteasome. As a BIK1 substrate, XLG2 is phosphorylated at four serine residues and these phosphorylation events of XLG2 positively regulate ROS production and defense via unknown mechanism.

As mentioned above, BIK1 can phosphorylate CPK28 which in turn negatively regulates BIK1 stability (Monaghan et al., 2014a). BIK1 also interacts with a protein phosphatase PP2C38 which is responsible for BIK1 dephosphorylation (Couto et al., 2016). It was shown PP2C38 is also phosphorylated upon flg22 perception, but whether this phosphorylation is mediated by BIK1 remains unknown.

1.10 Ubiquitin and ubiquitination

Ubiquitin is a small protein involved in a wide range of cellular regulation in all eukaryotic organisms. Through a sequential three step conjugation cascade mediated by E1 ubiquitin-activating enzyme, E2 ubiquitin-conjugating enzyme, and E3 ubiquitin ligase, ubiquitin is covalently added to lysine residues of target proteins (Varshavsky, 2012) (Fig. 1.4). The human genome encodes 2 E1s, around 30 E2s and more than 600 E3 ligases. There are 2 E1s, at least 37 E2s and more than 1400 E3 in the arabidopsis genome suggesting the significance of ubiquitination to both animals and plants (Vierstra, 2009a). When the first ubiquitin is attached, all its seven lysine residues (Lys6, Lys11, Lys27, Lys29, Lys33, Lys48, Lys63) and N-terminal (Met1) are exposed and could be further targeted by other ubiquitin proteins to form different poly-ubiquitination chains (such as Lys-48 linkage or Lys-63 linkage). E1 activates ubiquitin protein for all ubiquitination events, while diverse combinations of E2 and E3 determine the specificity and chain type of substrate ubiquitination (Grabbe et al., 2011).

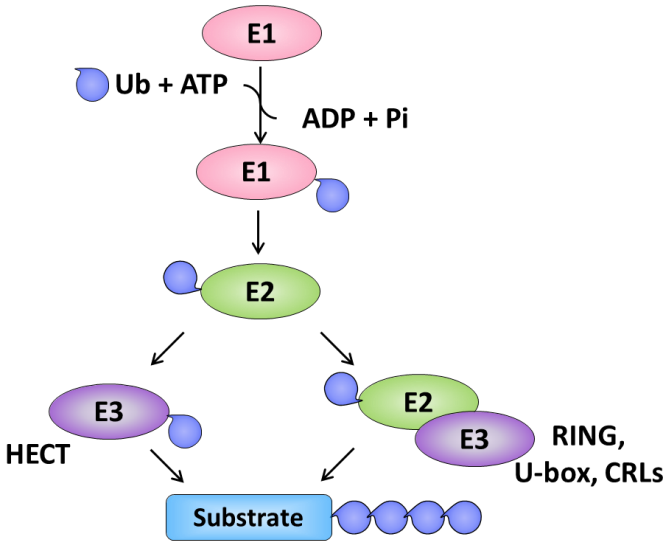

Figure 1.4 Ubiquitination cascade. E1 ubiquitin-activating enzyme activates the ubiquitin to form a thioester bond between a cysteine residue of E1 and C-terminal glycine of ubiquitin with consumption of ATP. This activated ubiquitin is then transferred to a cysteine on E2 ubiquitin-conjugating enzyme. Then the ubiquitin is covalently attached to the substrate either directly from E2 or via an E3-ubiquitin intermediate. E3-ubiquitin intermediate only happens for HECT type E3 ligase. Direct transfer from E2 to substrate is mediated by other E3 ligase including RING type, U-box type and CRLs which interact with both E2 and the specific substrate. The final covalent bond between ubiquitin and substrate is an isopeptide bond between lysine ε-amino of the substrate and C-terminal glycine of ubiquitin.

Plant E3 ligases could be classified into four main types including HECT, U-Box, RING, and cullin-RING ligases (CRLs) (Fig. 1.5). HECT type E3 ligases contain a HECT domain and form a thioester intermediate with ubiquitin when transferring it onto target. U-box, RING or CRLs transfer the ubiquitin directly from E2 to its substrate. Unlike U-box and RING E3 ligases which only contain a functional U-box or RING domain in one polypeptide, CRLs are multi-subunit E3 ligase complexes and function relies on the cooperation of each subunit (Vierstra, 2009).

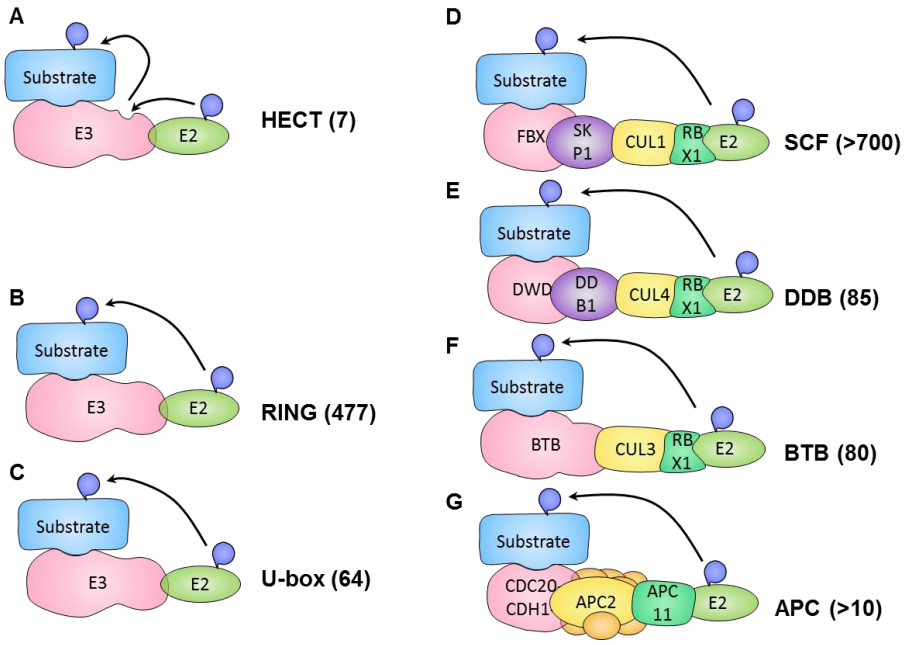

Figure 1.5 Organization and function mechanism of E3 ligases in arabidopsis. A. HECT E3 ligases are single polypeptides form a thioester intermediate with ubiquitin before transferring onto substrate. **B**. **C**. RING or U-box E3 ligases are single polypeptides interact with E2 via its RING or U-box domain and interact with substrate with other domain. Ubiquitin is directly transferred from E2 to substrate. **D** to **G**. The culllin-RING ligases (CRLs) are multisubunit complex that consist of a RING-box 1 (RBX1, E2 binding), cullin (CUL) and a variable substrate binding protein. The S phase kinase-associated protein 1 (SKP1)–cullin 1 (CUL1)–F-box (SCF) E3s contain F-box proteins (FBXs) for substrate binding which associate with CUL1 via the SKP1 (ASK1 in *Arabidopsis thaliana*); the bric-a-brac–tramtrack–broad complex (BTB) E3s use BTB proteins to bind both targets and CUL3; and the DNA damage-binding (DDB) E3s use WD40 domain-containing DWD proteins to recognize substrate and associate with CUL4 via a DDB1 protein. The anaphase-promoting complex (APC) consist of 11 or more subunits, including APC2 (similar as cullins), APC11 (similar as RBX1) and several recognition subunits (cell division cycle protein 20 (CDC20), CDC20-homology 1 (CDH1) and APC10). The numbers indicate the predicted number of genes encode the substrate binding component in each E3 type.

1.11 Function of ubiquitination

Lys-48-linked polyubiquitination is the first well studied polyubiquitination linkage type and functions by marking protein for 26S proteasome degradation

(Ciechanover, 1994). According to quantitative proteomic studies in yeast, Lys48-linked polyubiquitination is the most abundant form of polyubiquitination in cells and the majority of them mediate 26S proteasome degradation (Peng et al., 2003; Xu et al., 2009b). Besides Lys-48, polyubiquitination of Lys-11, Lys-29, Lys-63 as well as monoubiquitination in certain conditions appear to facilitate proteasome degradation of proteins (Shabek et al., 2012; Xu et al., 2009). Therefore proteolytic targeting was viewed as a classic ubiquitination function for long time. In plants, signaling initiation of several major hormones including auxin, jasmonic acid (JA) and Gibberellic acid (GA) are all tightly regulated by polyubiquitination-mediated proteasome degradation (Vierstra, 2009a). In brief, all these signaling are restrained by a potent suppressor which inhibits gene transcription in the absence of a hormone. Once the hormones are present and bind to the cognate receptor, suppressor proteins are polyubiquitinated and degraded by the proteasome, allowing for robust hormone responses.

Non-proteolytic functions of ubiquitination were largely uncovered in the past two decades and the significance of those ubiquitin linkages directing diverse outputs are now widely appreciated. Among them, monoubiquitination, or when only one ubiquitin is attached to a target protein, plays important roles in a number of biological processes (Nakagawa and Nakayama, 2015). The significance of monoubiquitination is further supported by a quantitative proteomics study which has demonstrated that monoubiquitination is the most abundant ubiquitination event in cells even when proteasome function was inhibited and other types of polyubiquitinated proteins were accumulated (Kaiser et al., 2011).

Monoubiquitination is known to regulate transcription as monoubiquitination on histone protein H2A inhibit transcription while monoubiquitination on H2B appears to positively regulate transcription (Blackledge et al., 2014; Espinosa, 2008; Nakagawa et al., 2008). Monoubiquitination is also involved in protein localization regulations. Several groups of proteins including RTKs and transporters were shown to undergo endocytosis mediated by monoubiquitination (Hislop and von Zastrow, 2011; Miranda and Sorkin, 2007). More specifically, ligand perception activates RTKs such as EGFR and activated RTKs are monoubiquitinated by the CBL RING-type E3 ligase family. When a single ubiquitin was attached to those RTKs, a ubiquitin-interacting motif (UIM) containing protein such as epsin bound the ubiquitinated receptor to form multi-protein complex including clathrin to initiate clathrin-dependent endocytosis (Haglund and Dikic, 2012). Moreover, monoubiquitination could also mediate clathrin-independent endocytosis although detailed mechanisms remains elusive. In addition, monoubiquitination could directly regulate protein shuffling in and out of the nucleus in several cases. For example, monoubiquitination of protein NEMO by E3 ligase cIAP1 mediates NEMO export from the nucleus (Jin et al., 2009b). While E3 ligase MDM2 monoubiquitinates FOXO4 which leads it import into the nucleus (Nie et al., 2007).

Furthermore, monoubiquitinaion is reportedly involved in controlling protein-protein interactions. In the Wingless-related integration site (WNT) signaling, transcription corepressor Groucho (Gro)/TLE is monoubiquitinated by E3 ligase XIAP and this monoubiquitination disrupts TLE interaction with transcription regulator TCF (Hanson et al., 2012b). In the absence of E3 ligase XIAP, the WNT signaling is inhibited.

In another case, protein proliferating cell nuclear antigen (PCNA) is monoubiquitinated by the combination of E2 Rad6 and E3 Rad18 in responses to DNA damage, which in turn recruits Y family DNA polymerases to facilitate DNA repair (Freudenthal et al., 2010; Hoege et al., 2002).

Lys63-linked polyubiquitination plays significant roles in mediating protein-protein interactions, serving as a scaffold to activate signaling as well as mediating protein endocytosis (Komander and Rape, 2012). Other than the best studied Lys48- and Lys63-linked polyubiquitination, functions of other type of polyubiquitination linkages are only beginning to be revealed. Lys6–linkages have been shown to be involved in the DNA damage response (Morris and Solomon, 2004; Wu-Baer et al., 2003). Lys11-linkages have been implicated in the membrane trafficking and TNF signaling (Dynek et al., 2010; Goto et al., 2010; Wickliffe et al., 2011). Lys27–linkages have functions during the mitochondrial damage response (Geisler et al., 2010; Glauser et al., 2011). Lys29-linkages play a role in regulating AMPK related protein kinases (Al-Hakim et al., 2008) and Lys33-linkages appear important in T-cell receptor (TCR) signaling (Huang et al., 2010).

A proteomic study in plants also demonstrated abundant ubiquitin linkages other than Lys-48 (Kim et al., 2013), but the function of specific linkages of a given protein is much less characterized than in yeast and animals.

1.12 Ubiquitination in innate immunity

In mammalian innate immunity research, numerous ubiquitination events including Lys48-, Lys63-, Met1-linked polyubiquitination of multiple proteins have been characterized in detail. For example in TLR4 signaling, ligand perception leads to the assembly of a multi-protein complex consisting of a kinase IRAK and E3 ligase TRAF6. TRAF6 is then activated in the complex and conjugates polyubiquitination via Lys63-linkage. This polyubiquitin chain serves as a scaffold to recruit TAB-TAK complex which in turn is activated and transduces signal to downstream NFkB to regulate inflammatory cytokine production.

However in plants, how ubiquitination is involved in innate immune regulation, especially PTI, is still largely unknown. It was reported that flagellin receptor FLS2 is ubiquitinated upon flg22 perception (Lu et al., 2011). Two plant U-box E3 ligases PUB12/13 mediate this polyubiquitination and promote proteasomal degradation of FLS2. Another U-Box E3 ligase PUB22 was also shown to suppress plant innate immunity by ubiquitinating Exo70B2, a subunit of the exocyst complex (Stegmann et al., 2012). Ubiquitinated Exo70B2 is turned-over by the 26S proteasome, but how Exo70B2 is involved in the early stages of PTI is still not clear. Another study showed that TF MYB30, a positive regulator of defense, is ubiquitinated by E3 ligase MIEL1 and can undergo proteasomal degradation (Marino et al., 2013). Moreover, several other E3 ligases were reported to function in innate immunity, but the substrates and mechanisms are still missing (Trujillo and Shirasu, 2010).

1.13 Overview of research focus

Research work presented in this dissertation mainly focuses on exploring plant innate immune signal transduction networks using different approaches.

In the following chapters, we first took a pharmaceutical approach to test the importance of ubiquitination in PTI responses and surprisingly we found blocking all ubiquitination events in plant cell with E1 inhibitor for 30 minutes greatly suppressed PTI responses including MAPK activation, ROS production, and BIK1 phosphorylation. We then demonstrated the inhibitor did not affect the expression of receptor and co-receptor, nor the receptor complex formation, but blocked flg22-mediated BIK1-FLS2 dissociation. To figure out how ubiquitination influences the early signaling, we tested *in vivo* ubiquitination of the proteins in the receptor complex and found BIK1 is monoubiquitinated in a ligand-dependent manner. We then examined the relationship of flg22-triggered BIK1 phosphorylation and ubiquitination and it appears phosphorylation of BIK1 precedes ubiquitination and functionally required for ubiquitination. We further tried to identify the ubiquitination sites by mutating all lysine residues individually with arginine mutations and identified one residue, Lys204, is important for ubiquitination. Moreover, this residue is indispensable for BIK1 function *in vivo* but we failed to uncouple phosphorylation and ubiquitination for this site.

The third chapter is a subsequent work following chapter two where we used a different approach to tackle how the ubiquitination regulates BIK1 function by looking for the putative E3 ligase. Using a Y2H screen to find potential BIK1-interacting proteins, we identified an E3 ligase LUCKY1 which interacts with BIK1 and

monoubiquitinates BIK1 *in vitro* at multiple sites. We further characterized the ubiquitination sites by mass spectrometry and genetically mutated all nine candidate lysine residues to eliminate ubiquitination without sacrificing BIK1 kinase activity. ROS assay and disease assay with transgenic plants expressing BIK1 with nine lysine residue mutations suggested ubiquitination of BIK1 positively regulates BIK1 function as well as PTI responses. More significantly, we found flg22-triggered ubiquitination of BIK1 didn't affect BIK1 stability but controls ligand-induced BIK1 dissociation with receptor FLS2.

In the fourth chapter, we described an unexpected discovery from our Y2H screen from chapter three. We looked at another BIK1-interacting protein DGK5 which appears to play an important role in PTI responses. The *dgk5* mutant showed reduced ROS production and enhanced disease susceptibility. We found that upon flg22 treatment, activated BIK1 phosphorylates DGK5. Mass spectrometry analysis and point mutation screen identified Ser-506 as the BIK1 phosphorylation site and phosphorylation of DGK5 at Ser-506 was found to enhance DGK5 kinase activity. Furthermore, we demonstrated another residue Thr-446, which is also phosphorylated upon flg22, is orchestrated by MPK4. Interestingly this phosphorylation negatively regulates DGK5 function. Taken together, through detailed biochemical and genetic analysis, we uncovered a previously unknown link between PTI signaling and lipid signaling.

Together, the discoveries in this dissertation focused on characterizing the unknown ubiquitin modification in plant innate immunity as well as identifying missing components in the complex PTI signaling networks.

CHAPTER II

FLAGELLIN-INDUCED MONOUBIQUITINATION OF BIK1 REGULATES ARABIDOPSIS INNATE IMMUNITY

2.1 Introduction

Lacking a circulatory system and specialized immune cells, sessile plants largely rely on the innate immune system to defend against invading pathogens. The primary immune responses are initiated by the activation of plasma membrane (PM)-resident pattern recognition receptors (PRRs) recognizing evolutionarily conserved microbial ligands, namely pathogen- or microbe-associated molecular patterns (PAMPs or MAMPs), including bacterial flagellin, lipopolysaccharide (LPS), peptidoglycan (PGN), elongation factor Tu (EF-Tu), and fungal chitin (Boller and Felix, 2009; Dodds and Rathjen, 2010; Macho and Zipfel, 2014). Activation of PRR complex upon the cognate PAMP perception induces the convergent intracellular immune signaling as exemplified by the activation of mitogen-activated protein kinase (MAPK) cascades and calcium-dependent protein kinases (CDPKs), transient production of reactive oxygen species (ROS) and defense hormone ethylene, calcium influx, stomatal closure, transcriptional reprogramming, callose deposition and production of antimicrobial compounds (Macho and Zipfel, 2014; Wu et al., 2014). PAMP-triggered immunity (PTI) generally contributes to plant basal resistance to a wide range of host-adapted pathogens and non-host resistance to non-adapted pathogens.

Bacterial flagellin or its 22-amino-acid active peptide flg22, is perceived by PM-resident leucine-rich repeat receptor-like kinase (LRR-RLK) flagellin-sensing 2 (FLS2) in arabidopsis. Upon flagellin perception, FLS2 instantaneously heterodimerizes with another LRR-RLK brassinosteroid insensitive 1 (BRI1)-associated kinase 1 (BAK1) accompanied with rapid transphosphorylation of the FLS2-BAK1 complex (Chinchilla et al., 2007a; Heese et al., 2007a; Schulze et al., 2010; Sun et al., 2013b). The PM-resident receptor-like cytoplasmic kinases (RLCKs) *Botrytis*-induced kinase 1 (BIK1) and its homolog PBL1, constitutively associate with FLS2 and BAK1 (Lin et al., 2014; Lu et al., 2010a; Zhang et al., 2010). BIK1 is rapidly phosphorylated by BAK1 at multiple serine, threonine and tyrosine residues and subsequently dissociates from the FLS2-BAK1 complex upon flagellin recognition (Lin et al., 2014). Emerging evidence indicates that BIK1 family RLCKs are essential regulators in relaying plant immune signaling via association with multiple LRR-RLK PRRs, including FLS2, and EF-Tu receptor (EFR), and damage-associated molecular pattern peptide (Pep) receptor 1 (PEPR1) (Lin et al., 2013b; Liu et al., 2013; Lu et al., 2010a; Zhang et al., 2010). Interestingly, BIK1 also associates with LRR-RLK BRI1 that perceives plant brassinosteroid (BR) hormone and negatively regulates BR signaling (Lin et al., 2013a). In addition to LRR-RLKs, CPK28 also interacts with and phosphorylates BIK1 to regulate its stability (Monaghan et al., 2014b). Downstream of PRR complex, BIK1 directly phosphorylates PM-resident NADPH oxidase family member respiratory burst oxidase homolog D (RBOHD), thereby regulating ROS production (Kadota et al., 2014a; Li et al., 2014e). Although it remains unknown how MAPKs are activated upon

PRR activation, recent study shows that MAPKs regulate immune gene transcriptional reprogramming via direct phosphorylation of cyclin-dependent kinase CDKCs, which in turn phosphorylate RNA polymerase II C-terminal domain (CTD) of the general transcription machinery (Li et al., 2014c).

Compared to the extensive studies of protein phosphoregulation in PRR complex activation and signaling relay, the involvement and regulation of protein ubiquitination in plant PTI signaling are relatively less understood (Li et al., 2014a). Three closely related plant U-box E3 ligase PUB22, PUB23 and PUB24 negatively regulate flagellin-mediated signaling via interaction and ubiquitination of Exo70B2, a subunit of the exocyst complex that is required for full activation of multiple PTI responses and resistance to different pathogens (Stegmann et al., 2012; Trujillo et al., 2008). PUB12 and PUB13 directly regulate PRR FLS2 stability and turnover via flg22-induced and BAK1-mediated interaction and ubiquitination of FLS2 to attenuate immune responses (Lu et al., 2011a). In contrast, the RING-type E3 ligase XB3 interacts with rice XA21, an LRR-RLK PRR conferring resistance to *Xanthomonas oryzae* pv. *oryzae.* XB3 positively regulates XA21 signaling likely through ubiquitination and turnover of a negative regulator in XA21 signaling (Wang et al., 2006). Apparently, the above-mentioned PUBs and XB3 lead to the polyubiquitination of targeted proteins for degradation, thereby negatively regulating the functions of targeted proteins. In addition, proteins are often subjected to monoubiquitination/multi-monoubiquitination modification, which could dictate fates of substrates distinct from protein polyubiquitination, such as nonproteolytic functions of protein kinase activation,

membrane or intracellular trafficking as well as regulating protein-protein interactions (Chen and Sun, 2009; Skaug et al., 2009; Tang et al., 2011). In this study, we demonstrate that BIK1 is monoubiquitinated upon flagellin perception. Flagellin-induced BIK1 monoubiquitination appears to follow its phosphorylation. Mutagenesis of individual lysine (K) residues to arginine (R) in BIK1 suggests that $BIK1^{K204}$ plays a crucial role in flagellin-induced BIK1 monoubiquitination and phosphorylation. Importantly, transgenic plants carrying $BIK1^{K204R}$ mutant are unable to complement the *bik1* deficiency in plant innate immunity. Our study reveals an intertwined regulation of protein phosphorylation and monoubiquitination of an essential immune regulator BIK1 associated with multiple PRR complexes in the activation of plant immune signaling.

2.2 Materials and methods

2.2.1 Plant material and growth conditions

Arabidopsis thaliana accessions Col-0, mutants *fls2*, *bak1-4*, *bik1* and transgenic *pBIK1::BIK1-HA* in the *bik1* background were described previously (Lin et al., 2014). *pBIK1::BIK1^{K204R}-HA* transgenic plants in the *bik1* background were generated in this study (see below for details). All arabidopsis plants were grown in soil (Metro Mix 366) in a growth chamber at 20-23°C, 60% relative humidity and 75 μE $m^{-2}s^{-1}$ light with a 12 hr light/12 hr dark photoperiod for four weeks before pathogen infection assay, protoplast isolation and ROS assay.

2.2.2 Plasmid construction and generation of transgenic plants

The HA or FLAG epitope-tagged FLS2, BAK1, BIK1, PBL1 and BIK1 mutant constructs used for protoplast assays were described previously (Lin et al., 2014; Lu et al., 2010a). BIK1 point mutations were generated by site-directed mutagenesis with primers listed in the Supplemental Table 1 using the pHBT-BIK1-HA construct as the template. $BIK1^{K204R}$ was further sub-cloned into the binary vector *pCB302-pBIK1::BIK1-HA* and the modified GST (pGEX4T-1, Pharmacia) vector with BamHI and StuI digestion to generate *pCB302-pBIK1::BIK1*^{K204R}*-HA* and *pGST-BIK1*^{K204R} respectively. *Agrobacterium tumefaciens*-mediated floral dip was used to transform *pCB302-pBIK1::BIK1*^{K204R}*-HA* into the *bik1* plants. The transgenic plants were selected by Glufosinate-ammonium (Basta, 50 μg/ml). Multiple transgenic lines were analyzed with Western blot (WB) for protein expression. Two lines with 3:1 segregation ratio for Basta resistance in T3 generation were selected to obtain homozygous seeds for further studies.

2.2.3 Construction of the *UBQK0* plasmid

The monomer ubiquitin of arabidopsis ubiquitin gene 10 (*UBQ10, At4g05320*) carrying lysine-to-arginine mutations at all the seven lysine residues (*UBQ K0*: 5'-ATGCAGATCTTTGTTAGGACTCTCACCGGAAGGACTATCACCCTCGAGGTGG AAAGCTCTGACACCATCGACAACGTTAGGGCCAGGATCCAGGATAGGGAAG GTATTCCTCCGGATCAGCAGAGGCTTATCTTCGCCGGAAGGCAGTTGGAGGA TGGCCGCACGTTGGCGGATTACAATATCCAGAGGGAATCCACCCTCCACTTG

GTCCTCAGGCTCCGTGGTGGTTAA-3') was synthesized and cloned into a *pUC57* vector by GenScript USA Incorporation. *UBQ K0* was then amplified by a polymerase chain reaction (PCR) with primers listed in the Supplemental Table 1 and further sub-cloned into a modified *pHBT* vector with BamHI and PstI digestions to generate *pHBT-FLAG-UBQ K0*.

2.2.4 Pathogen infection assays

Pseudomonas syringae pv. *tomato* (*Pst*) DC3000 was cultured overnight at 28°C in King's B medium supplemented with rifamycin (50 μg/ml). Bacteria were collected by centrifugation at 3500 rpm, washed and re-suspended to the density of 5 x 10^5 cfu/ml with 10 mM $MgCl_2$. Leaves from four-week-old plants were hand-inoculated with bacterial suspension using a needleless syringe. For flg22-mediated protection assay, leaves were pre-inoculated with 100 nM flg22 or H_2O as control and 24 hr later bacteria suspension was infiltrated into the same leaves. To measure *in planta* bacterial growth, three sets of two leaf discs were punched and ground in 100 μl of ddH_2O. Serial dilutions were plated on TSA plates (1% tryptone, 1% sucrose, 0.1% glutamatic acid and 1.8% agar) containing 25 μg/ml rifamycin. Plates were incubated at 28°C and bacterial colony forming units (cfu) were counted 2 days after incubation.

2.2.5 Protoplast transient expression assay and co-immunoprecipitation (co-IP) assay

Protoplast isolation and transient expression assay have been described previously (He et al., 2007). For protoplast-based co-IP assay, protoplasts were transfected with a pair of constructs (empty vector as control, 100 μg DNA for 500 μl protoplasts at the density of 2 x 10^5/ml for each sample) and incubated at room temperature for 10 hr. After treatment of flg22 with indicated concentration and time points, protoplasts were collected by centrifugation and lysed in 300 μl co-IP buffer (150 mM NaCl, 50 mM Tris-HCl, pH7.5, 5 mM EDTA, 0.5% Triton, 1 × protease inhibitor cocktail, before use, adding 2.5 μl 0.4 M DTT, 2 μl 1M NaF and 2 μl 1M Na_3VO_3 for 1 ml IP buffer) by vortexing. After centrifugation at 10,000×g for 10 min at 4°C, 30 μl of supernatant was collected for input control and 7 μl α-FLAG-agarose beads were added into the remaining supernatant and incubated at 4 °C for 1.5 hr. Beads were collected and washed three times with washing buffer (150 mM NaCl, 50 mM Tris-HCl, pH7.5, 5 mM EDTA, 0.5%Triton) and once with 50 mM Tris-HCl, pH7.5. Immunoprecipitates were analyzed by WB with indicated antibodies.

2.2.6 *In vivo* ubiquitination assay

FLAG-tagged UBQ (FLAG-UBQ) or a vector control (40 μg DNA) was cotransfected with the target gene with an HA tag (40 μg DNA) into 400 μl protoplasts at the density of 2 x 10^5/ml for each sample and protoplasts were incubated at room

temperature for 10 hr. After treatment with 100 nM flg22 at the indicated time points, protoplasts were collected for co-IP assay in co-IP buffer containing 1% triton.

2.2.7 *In vitro* ubiquitination assay

Ubiquitination assays were performed as previously described with modifications (Lu et al., 2011a; Zhou et al., 2014). Reactions containing 1 μg of MBP-FLS2CD-HA, 1 μg of HIS_6-E1 (AtUBA1), 1 μg of HIS_6-E2 (AtUBC8), 1 μg of GST-E3 (AtPUB13), 1 μg of HIS_6-ubiquitin (Boston Biochem) in the ubiquitination buffer (20 mM Tris-HCl, pH 7.5, 5 mM MgCl2, 0.5 mM DTT, 2 mM ATP) with or without PYR-41 were incubated at 30°C for 3 hr. The ubiquitinated FLS2 proteins were detected by WB using α-HA antibody.

2.2.8 MAPK assay

Protoplasts from four-week-old Col-0 plants were incubated 3 hr at room temperature before flg22 treatment. Protoplasts were collected and lysed in 100 μl co-IP buffer. Protein samples with 1 X SDS buffer were separated in 10% SDS-PAGE gel to detect pMPK3, pMPK6 and pMPK4 by WB with α-pERK1/2 antibody (Cell Signaling, #9101).

2.2.9 Detection of ROS production

Leaves from 4 to 5-week-old soil-grown arabidopsis plants were punched into leaf discs with the diameter of 5 mm and then cut three times with a razor blade into leaf

strips. Leaf strips were incubated in 100 µl ddH_2O overnight with gentle shaking to eliminate the wounding effect. Then, water was replaced with 100 µl reaction solution containing 50 µM luminol, 10 µg/ml horseradish peroxidase (Sigma-Aldrich) supplemented with or without 100 nM flg22. Luminescence was measured with a luminometer (Perkin Elmer, 2030 Multilabel Reader, Victor X3) with a setting of 1 min as the interval for a period of 40 min. Detected values of ROS production were indicated as means of Relative Light Units (RLU).

2.2.10 Recombinant protein isolation and *in vitro* kinase assays

Fusion proteins were produced from *E. coli* BL21 strain at 16°C using LB medium with 0.25 mM isopropyl β-D-1-thiogalactopyranoside (IPTG). Glutathione S-transferase (GST) fusion proteins were purified with Pierce glutathione agarose (Thermo Scientific), and maltose binding protein (MBP) fusion proteins were purified using amylose resin (New England Biolabs) according to the standard protocol from companies. The *in vitro* kinase assays were performed with 0.5 µg of kinase proteins and 5 µg of substrate proteins in 30 µl kinase reaction buffer (10 mM Tris-HCl, pH7.5, 5 mM $MgCl_2$, 2.5 mM EDTA, 50 mM NaCl, 0.5 mM DTT, 50 µM ATP and 1 µCi [γ-^{32}P]ATP). After gentle shaking at room temperature for 2 hr, samples were denatured with 4 x SDS loading buffer and separated by 10% SDS-PAGE gel. Phosphorylation was analyzed by autoradiography.

2.3 Results

2.3.1 Ubiquitination inhibitor PYR-41 blocks flg22-triggered early immune responses.

To determine whether and how protein ubiquitination involves in plant PTI responses, we tested the effect of an ubiquitination inhibitor PYR-41 on flg22-triggered signaling. PYR-41 is a cell-permeable pyrazone compound, which irreversibly inhibits E1 activity (Yang et al., 2007). We first examined the effectiveness and specificity of PYR-41 inhibitor on protein ubiquitination. PUB13 is able to ubiquitinate FLS2 *in vivo* and *in vitro* to promote FLS2 degradation (Lu et al., 2011a). PUB13-mediated FLS2 ubiquitination was largely blocked by PYR-41 treatment (Fig. 2.1A). However, PYR-41 did not affect the autophosphorylation and transphosphorylation activity of BAK1 and BIK1 with an *in vitro* kinase assay (Fig. 2.1B). The data support that PYR-41 is an effective protein ubiquitination inhibitor.

Activation of MAP kinases is one of the robust early signaling events following MAMP recognition. We examined the effect of PYR-41 on flg22-induced MAP kinase activation with α-pERK antibody that cross-reacts with phosphorylated arabidopsis MPK3, MPK4 and MPK6. As shown in Fig. 2.2A, MPK3, MPK4 and MPK6 were activated 10 min after flg22 treatment, whereas pre-treatment with 50 μM of PYR-41 completely suppressed flg22-induced MAP kinase activation (Fig. 2.2A). PAMP perception triggers a rapid and transient burst of ROS. Pre-treatment of PYR-41

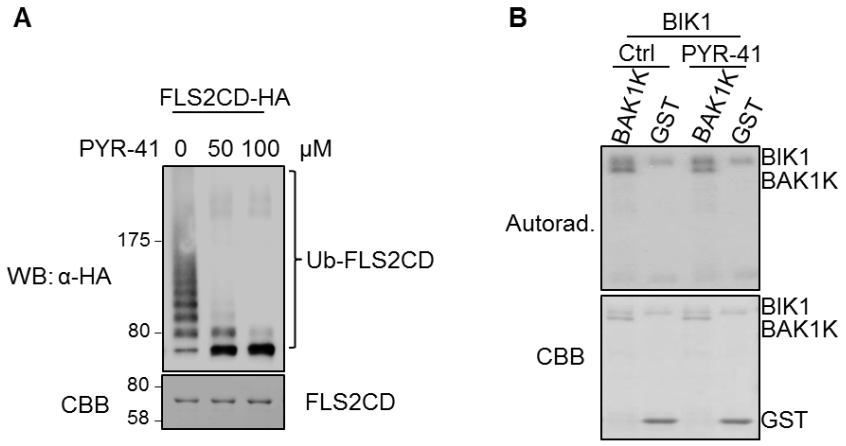

Figure 2.1 PYR-41 is an efficient ubiquitination inhibitor. A. PYR-41 blocks ubiquitination *in vitro*. An *in vitro* ubiquitination assay was performed with E1, E2, ubiquitin and purified GST-PUB13, MBP-FLS2CD-HA in the ubiquitination assay buffer. PYR-41 was added at 50 or 100 μM. Proteins were separated with SDS-PAGE and the ubiquitinated FLS2 proteins were analyzed by WB using an α-HA antibody (WB: α-HA). The protein loading of FLS2 is shown by CBB staining at the bottom panel. **B**. PYR-41 does not affect kinase activity. An *in vitro* kinase assay was performed by using GST-BIK1 as kinase and GST or GST-BAK1K as substrate. PYR-41 was added at 50 μM. Phosphorylation is shown with Autorad (top panel) and protein loading is shown by CBB staining (bottom panel).

largely reduced flg22-induced ROS production (Fig. 2.2B). The data suggest that blocking ubiquitination likely impedes flg22-triggered signaling and certain protein ubiquitination event(s) could play a positive role in flg22-triggered signaling. The result is rather surprising since several E3 ligases have been shown to negatively regulate flg22-triggered responses.

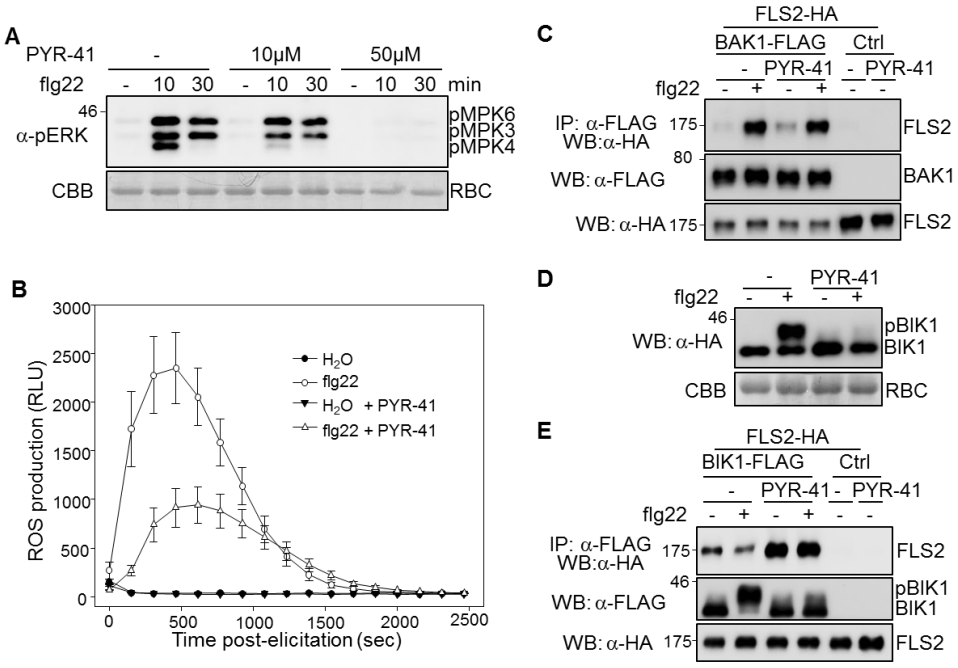

Figure 2.2 Ubiquitination inhibitor PYR-41 blocks flg22 signaling. **A.** PYR-41 treatment blocks flg22-induced MAPK activation. Protoplasts from wild-type (WT) Col-0 plants were treated with or without 10 or 50 μM PYR-41 for 30 min and followed by 100 nM flg22 treatment for 10 or 30 min. MAPK activation was analyzed with an α-pERK antibody (top panel), and protein loading was shown by Coomassie Brilliant Blue (CBB) staining for RuBisCO (RBC) (bottom panel). **B**. PYR-41 treatment compromises flg22-induced ROS production. Leaf discs were pre-treated with or without 200 μM PYR-41 for 30 min and followed by H_2O or 100 nM flg22 treatment. ROS production was measured as relative luminescence units (RLU) by a luminometer. The data are shown as means ± standard errors from 12 leaf discs for H_2O and 36 leaf discs for flg22 treatment. **C.** PYR-41 treatment does not affect flg22-induced FLS2 and BAK1 complex formation. Protoplasts from WT Col-0 plants were co-expressed with FLS2-HA and BAK1-FLAG or a control vector. After pretreatment with 50 μM PYR-41 for 30 min, protoplasts were stimulated with 100 nM flg22 for 15 min. Co-IP was carried out with an α-FLAG-agarose (IP: α-FLAG), and proteins were analyzed using Western blot with an α-HA antibody (WB: α-HA) (top panel). The middle and bottom panels show the expression of BAK1 and FLS2 proteins respectively. **D.** PYR-41 treatment diminishes flg22-induced BIK1 phosphorylation. Protoplasts expressing BIK1-HA were pretreated with or without 50 μM PYR-41 for 30 min and further stimulated by 100 nM flg22 for 30 min. Samples were immuno-blotted with an α-HA antibody (top panel) and protein loading was shown by CBB staining for RBC (bottom panel). **E**. PYR-41 treatment impairs flg22-induced BIK1 dissociation from the FLS2 complex. Protoplasts from WT Col-0 plants were co-expressed with FLS2-HA and BIK1-FLAG or a control vector. After pretreatment with 50 μM PYR-41 for 30 min, protoplasts were stimulated with 100 nM flg22 for 15 min. Co-IP and WB were performed as in C.

We further dissected which step(s) of flg22 signaling pathway is impeded by PYR-41. Flg22 perception triggers rapid heterodimerization of FLS2 and BAK1 (Chinchilla et al., 2007a; Heese et al., 2007a). As shown in Fig. 2.2C, FLAG epitope-tagged BAK1 co-immunoprecipitated HA epitope-tagged FLS2 in protoplasts upon flg22 treatment. Pre-treatment of PYR-41 did not interfere with flg22-induced FLS2 and BAK1 complex formation (Fig. 2.2C), suggesting that protein ubiquitination may not be required for flg22 perception by the FLS2-BAK1 complex. Interestingly, pre-treatment of PYR-41 blocked flg22-triggered BIK1 phosphorylation as indicated by a protein mobility shift of BIK1 on the immunoblot (Fig. 2.2D). BIK1 constitutively associates with FLS2 in the absence of flg22 treatment, and dissociates from the FLS2-BAK1 complex upon flg22 perception (Lu et al., 2010a; Zhang et al., 2010). It appears that BIK1 and FLS2 interaction was enhanced in the presence of PYR-41 before flg22 treatment (Fig. 2.2E). Furthermore, flg22-induced BIK1 dissociation from FLS2 was inhibited by PYR-41 treatment (Fig. 2.2E). Notably, this difference was unlikely caused by the level or stability of FLS2 and BIK1 proteins as we did not observe any demonstrable changes of FLS2 and BIK1 proteins in the presence or absence of PYR-41 (Fig. 2.2E). Taken together, the results indicate that protein ubiquitination regulates flg22 signaling activation at a step between FLS2-BAK1 complex formation and BIK1 phosphorylation and subsequent dissociation from the FLS2-BAK1 complex.

2.3.2 Flg22 perception induces BIK1 monoubiquitination.

We hypothesize that ubiquitination of FLS2, BAK1 and/or BIK1 may play a role in flg22 signaling activation. We have shown that upon prolonged flg22 stimulation, FLS2 is polyubiquitinated by PUB13 and PUB12, thereby down-regulating flg22 signaling (Fig. 2.3A) (Lu et al., 2011a). We thus determined the potential ubiquitination of BAK1 and BIK1 with an *in vivo* ubiquitination assay in protoplasts co-expressing FLAG epitope-tagged ubiquitin (FLAG-UBQ) and HA epitope-tagged target genes. The ubiquitinated target proteins were detected with an α-HA immunoblot upon immunoprecipitation with α-FLAG antibody. As shown in Fig. 2.4A, in the presence of FLAG-UBQ, immunoprecipitated BAK1 proteins were detected as a ladder-like smear

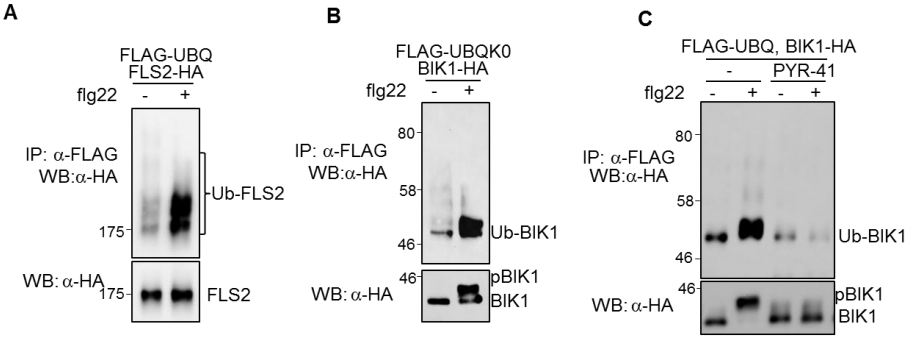

Figure 2.3 FLS2 and BIK1 *in vivo* ubiquitination. A. flg22 induces polyubiquitination of FLS2. Protoplasts from WT Col-0 plants were transfected with FLS2-HA, FLAG-UBQ and incubated for 10 hrs. After treatment with 100 nM flg22 for 30 min, IP was carried out with α-FLAG-agarose (IP: α-FLAG). The ubiquitinated FLS2 (Ub-FLS2) proteins were detected as a smear with α-HA WB (WB: α-HA) (Top panel). The bottom panel shows the expression of FLS2-HA protein. **B.** Monoubiquitination of BIK1 with UBQ K0. Protoplasts isolated from *35S::BIK1-HA* transgenic plants were transfected with FLAG-UBQK0 and followed by 100 nM flg22 treatment for 30 min. After IP with α-FLAG-agarose, ubiquitinated BIK1 was detected by WB with α-HA antibody (WB: α-HA) (top panel). The bottom panel shows the expression of BIK1-HA. **C.** PYR-41 blocks flg22-induced BIK1 monoubiquitination. The BIK1 ubiquitination assay was carried out similarly with the above assays. The 50 μM PYR-41 was added 30 min prior to flg22 treatment.

Figure 2.4 PAMP perception induces BIK1 monoubiquitination. A. BAK1 is constitutively polyubiquitinated *in vivo*. Protoplasts from WT Col-0 plants were transfected with BAK1-HA and FLAG-ubiquitin (FLAG-UBQ) or a control vector (Ctrl), and followed by the treatment with 100 nM flg22 for 30 min. Co-IP was carried out with α-FLAG-agarose (IP: α-FLAG). The ubiquitinated BAK1 (Ub-BAK1) proteins were detected as a smear with α-HA WB (WB: α-HA) (Top panel). The middle panel shows the expression of BAK1-HA proteins and the bottom panel is CBB staining for RBC. **B.** flg22 treatment induces monoubiquitination of BIK1. Protoplasts were transfected with BIK1-HA and FLAG-UBQ or a control vector, and followed by the treatment with 100 nM flg22 for 30 min. After a co-IP with α-FLAG-agarose, ubiquitinated BIK1 was detected by WB using α-HA antibody (WB: α-HA) (top panel). The middle panel shows the expression of BIK1-HA proteins and the bottom panel shows CBB staining for RBC. **C.** flg22 treatment induces BIK1 monoubiquitination in *pBIK1::BIK1-HA* transgenic plants. Protoplasts isolated from *pBIK1::BIK1-HA* transgenic plants in the *bik1* mutant background were transfected with FLAG-UBQ and followed by 100 nM flg22 treatment for 30 min. After IP with α-FLAG-agarose, ubiquitinated BIK1 was detected by WB with α-HA antibody (WB: α-HA) (top panel). The bottom panel shows the expression of BIK1-HA. **D.** Monoubiquitination of BIK1 with UBQ K0. Protoplasts isolated from *pBIK1::BIK1-HA* transgenic plants were transfected with FLAG-UBQK0 and followed by 100 nM flg22 treatment for 30 min. After IP with α-FLAG-agarose, ubiquitinated BIK1 was detected by WB with α-HA antibody (WB: α-HA) (top panel). The bottom panel shows the expression of BIK1-HA. The mutations of lysine to arginine in UBQ K0 are shown on the top with the positions of amino-acid labeled. **E.** The flg22-induced BIK1 monoubiquitination depends on the FLS2 and BAK1 receptor complex. Protoplasts were isolated from WT Col-0, *fls2* and *bak1-4* plants for BIK1 ubiquitination assay. **F.** The elf18 treatment induces BIK1 monoubiquitination in *pBIK1::BIK1-HA* transgenic plants. The *in vivo* ubiquitination assay was carried out similarly as in 2C. The 1μM elf18 was added for 30 min. **G**. BIK1 homolog PBL1 is monoubiquitinated upon flg22 treatment. PBL1-HA and FLAG-UBQ were expressed in protoplasts. Co-IP and WB were performed as in 2A.
The above experiments were repeated three times with similar results.

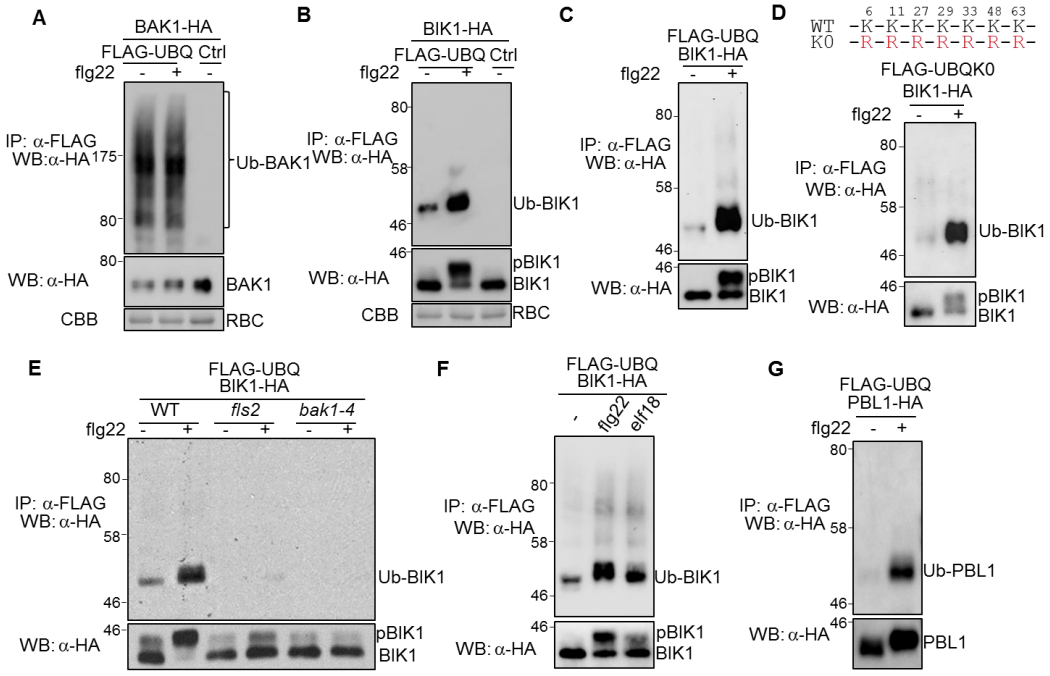

migrating above its predicated molecular weight (MW, 70.6 kDa with 2HA tag) before and after flg22 treatment (Fig. 2.4A), suggesting that BAK1 is constitutively polyubiquitinated in the cells. In contrast, a strong and discrete band with a MW of approximately 52 kDa was detected in protoplasts co-expressing BIK1-HA and FLAG-UBQ but not when expressing BIK1-HA alone (Fig. 2.4B). Importantly, the band intensity was significantly enhanced upon flg22 treatment (Fig. 2.4B), suggesting that flg22 treatment induces BIK1 ubiquitination. The flg22-induced BIK1 ubiquitination was further confirmed with transgenic plants carrying HA epitope-tagged BIK1 under the control of its native promoter (*pBIK1::BIK1-HA*). Similar with transiently expressed BIK1 in protoplasts, BIK1 expressed in transgenic plants also showed flg22-induced ubiquitination (Fig. 2.4C). Notably, we observed that the basal ubiquitination of BIK1 in the absence of flg22 treatment was almost undetectable in the *pBIK1::BIK1-HA* plants

(Fig. 2.4C). The MW of ubiquitinated BIK1 (~52 kDa) is about 8 kDa bigger than the predicated BIK1 MW (44 kDa), suggesting the attachment of a single ubiquitin (8.5 kDa) to BIK1 protein. To further support flg22-induced BIK1 monoubiquitination, we expressed BIK1-HA with FLAG epitope-tagged UBQ K0 variant, in which all 7 lysine (K) residues in UBQ were changed to arginine (R), thus preventing the polyubiquitination chain formation. A similar ubiquitination pattern of BIK1 as using WT UBQ was observed upon immunoprecipitation of UBQ K0 when BIK1 was expressed under either native promoter in *pBIK1::BIK1-HA* transgenic plants (Fig. 2.4D) or *35S* promoter in *35S::BIK1-HA* transgenic plants (Fig. 2.3B), supporting that flg22 induces BIK1 monoubiquitination. Notably, flg22-induced BIK1 ubiquitination was blocked by PYR-41 treatment (Fig. 2.3C). Initiation of flg22 signaling depends on the FLS2-BAK1 receptor complex. Consistently, the flg22-induced BIK1 monoubiquitination was not observed in *fls2* and *bak1-4* mutant protoplasts (Fig. 2.4E). In addition to flg22, elf18 also induced monoubiquitination of BIK1 (Fig. 2.4F). PBL1, the closest homolog of BIK1, was also monoubiquitinated after flg22 treatment (Fig. 2.4G). The data support that MAMP perception induces monoubiquitination of BIK1 family RLCKs.

2.3.3 Flg22-induced BIK1 phosphorylation occurs temporally prior to ubiquitination

Upon flg22 perception, BIK1 is rapidly phosphorylated as detected by a mobility shift in immunoblot within 1 min after treatment and reaching a plateau around 10 min

(Fig. 2.5A & 2.5B). Interestingly, flg22-induced BIK1 ubiquitination became apparent only at 10 min after treatment and reached a plateau around 30 min (Fig. 2.5A & 2.5B). Apparently, flg22-induced BIK1 ubiquitination mainly occurs after its phosphorylation. However, ubiquitination appears to be required for flg22-induced BIK1 phosphorylation (Fig. 2.2D). It is likely that phosphorylation and ubiquitination of BIK1 are two intertwined events and mutually required to mediate signaling activation. To further reveal the relationship between flg22-induced BIK1 phosphorylation and ubiquitination, we tested the ubiquitination of several BIK1 phosphorylation deficient mutants, including BIK1 kinase inactive mutant (BIK1Km, carrying a mutation in the ATP binding site), and BAK1 phosphorylation site mutants ($BIK1^{T237A}$ and $BIK1^{Y250A}$). As shown in Fig. 2.5C, these mutants are deficient in flg22-induced phosphorylation. Interestingly, flg22-induced ubiquitination was also largely compromised in these mutants, further substantiating that flg22-induced BIK1 phosphorylation is a prerequisite step for its subsequent ubiquitination. Consistently, the kinase inhibitor K252a also blocked flg22-induced BIK1 ubiquitination (Fig. 2.5D). BIK1 localizes to the plasma membrane and the N-terminal putative myristoylation motif is required for its function in plant defense (Abuqamar et al., 2008). The myristoylation motif mutant $BIK1^{G2A}$ was unable to be ubiquitinated upon flg22 treatment (Fig. 2.5E), suggesting that BIK1 plasma membrane localization might be required for its ubiquitination. Taken together, the data suggest that flg22-induced BIK1 ubiquitination occurs after its phosphorylation modification at the plasma membrane.

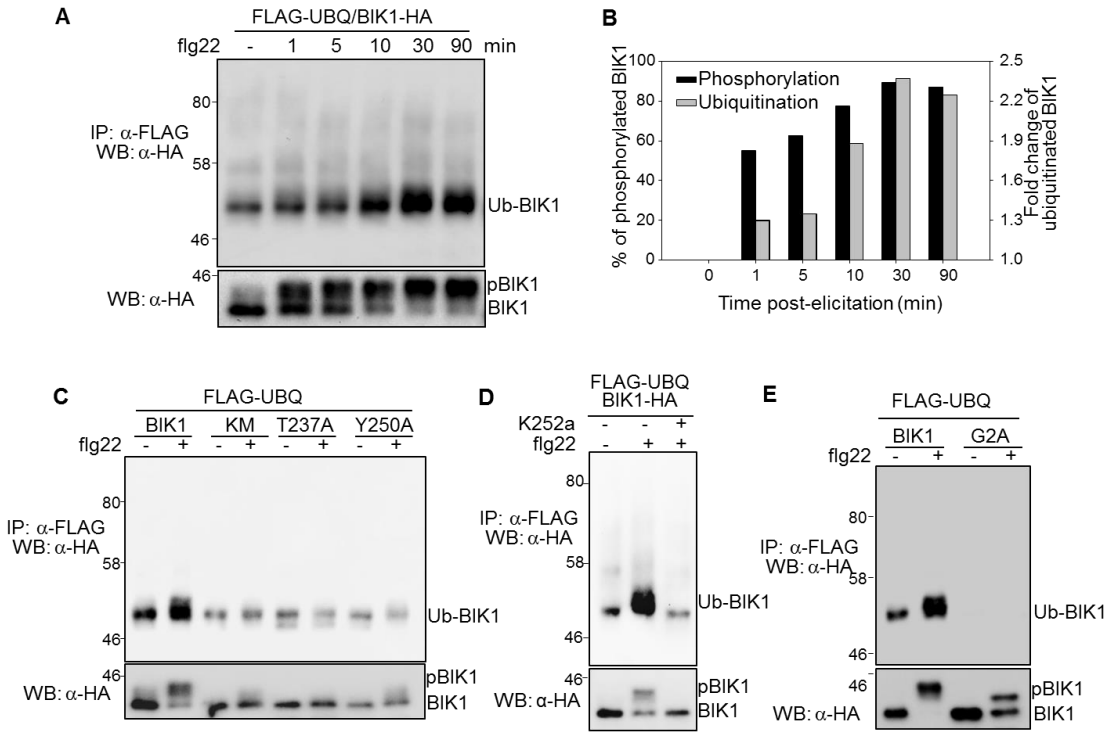

Figure 2.5 Flg22-induced BIK1 phosphorylation precedes its ubiquitination. A. The time course of flg22-induced BIK1 phosphorylation and ubiquitination. Protoplasts were co-transfected with FLAG-UBQ and BIK1-HA, and stimulated with 100 nM flg22 for the indicated time. BIK1 ubiquitination and phosphorylation were detected as in 2B. **B.** Quantification of BIK1 ubiquitination and phosphorylation. Intensity of BIK1 bands was quantified with Image Lab (Bio-Rad) from the gel in Fig. 3A. The percentage of BIK1 phosphorylation is the ratio of intensity of the shifted upper band (pBIK1) to the total BIK1 bands (pBIK1+BIK1) from the bottom panel WB. The amount of BIK1 ubiquitination is the relative intensity of Ub-BIK1 band (set no treatment as 1.0). **C.** The BIK1 variants with impaired phosphorylation compromise flg22-induced ubiquitination. HA-tagged WT BIK1 or BIK1 mutants (KM: kinase-inactive mutant with a mutation of KK105106AA) was co-transfected with FLAG-UBQ in protoplasts. Ubiquitination of BIK1 variants was detected as in 2B. **D.** The general kinase inhibitor K252a blocks flg22-induced BIK1 ubiquitination. The protoplasts transfected with FLAG-UBQ and BIK1-HA were treated with 1 μM K252a 30 min prior to 100 nM flg22 treatment. **E.** The putative myristoylation site is required for flg22-induced BIK1 monoubiquitination. HA-tagged WT BIK1 or BIK1G2A mutant was co-expressed in protoplasts with FLAG-UBQ. Ubiquitination of BIK1 was detected as in 2B.The above experiments were repeated three times with similar results.

2.3.4 BIK1^{K204} is important in flg22-induced BIK1 ubiquitination and phosphorylation.

Identification of ubiquitination sites by mass spectrometry (MS) analysis requires relatively high quality and quantity of ubiquitinated proteins. Likely due to the low abundance of ubiquitinated BIK1 proteins *in vivo* expressed in transgenic plants or protoplasts, we were unable to get enough ubiquitinated BIK1 for MS assay. We performed arginine scanning to investigate which lysine residue is a potential ubiquitination site. There are 30 lysine residues in BIK1 including K105/K106 residing in the ATP binding pocket required for its kinase activity. We individually mutated 28 lysine residues to arginine and screened for its flg22-induced ubiquitination with an *in vivo* ubiquitination assay. Significantly, BIK1^{K204R} mutant, but not the others, largely compromised flg22-induced BIK1 monoubiquitination (Fig. 2.6 and 2.7A). BIK1^{K204} is an invariant residue in the subdomain VI b of the kinase and is conserved between BIK1 and PBL1. The corresponding residue in PBL1, PBL1^{K199}, is also indispensable for flg22-induced monoubiquitination (Fig. 2.7B). Notably, it appears that BIK1^{K204R} exhibited altered flg22-induced phosphorylation as indicated by the reduced mobility shift in Western blot (Fig. 2.7A).

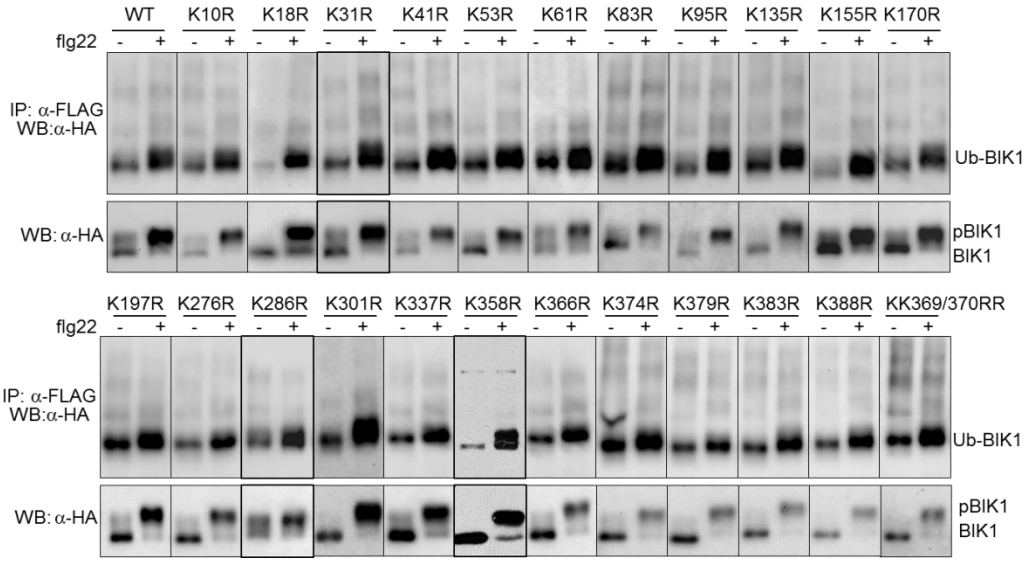

Figure 2.6 BIK1 ubiquitination site screen. The BIK1 mutants do not affect flg22-induced BIK1 ubiquitination. HA-tagged WT BIK1 or BIK1 mutants was co-transfected with FLAG-UBQ in protoplasts. Ubiquitination of BIK1 variants was detected as in 2B.

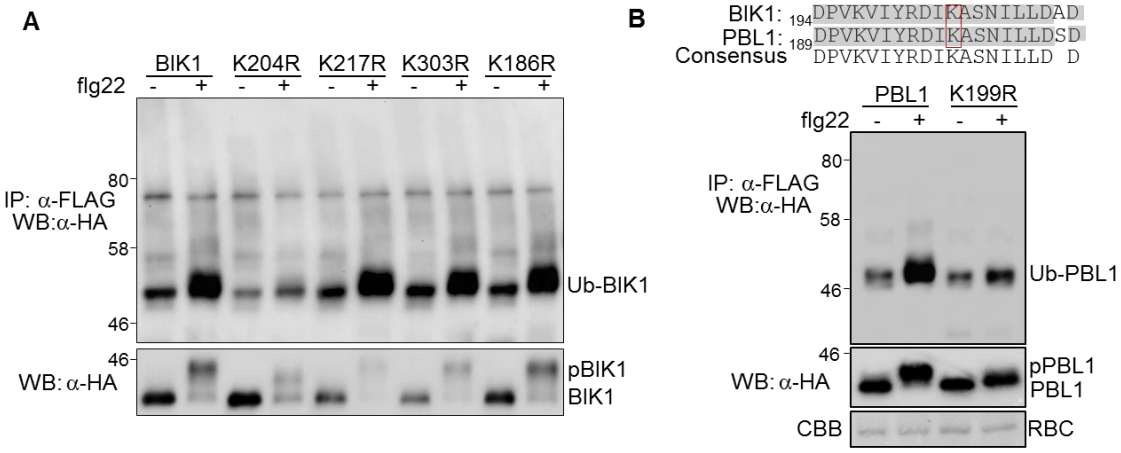

Figure 2.7 BIK1^{K204} is required for flg22-induced BIK1 ubiquitination. A. BIK1^{K204R} mutant blocks the flg22-induced BIK1 ubiquitination. WT or different variants of BIK-HA was co-expressed with FLAG-UBQ in protoplasts. Ubiquitination of BIK1 was detected as in 2B. **B.** PBL1^{K199} plays an important role in flg22-induced PBL1 ubiquitination. PBL1-HA or PBL1^{K199R}-HA was co-expressed with FLAG-UBQ in protoplasts. Ubiquitination of PBL1 was detected similarly as in 2B. The amino-acid sequence alignment of BIK1 and PBL1 surrounding BIK1^{K204} residue is shown on the top. The number indicates the position of the first amino-acid. BIK1^{K204} and PBL1^{K199} are boxed in red.
The above experiments were repeated three times with similar results.

We further tested BIK1^{K204R} autophosphorylation and transphosphorylation activity with an *in vitro* kinase assay. The cytosolic domain of BAK1 (BAK1CD), including the intracellular kinase domain and juxtamembrane domain, exhibits kinase activity whereas the BAK1 kinase domain alone (BAK1K) does not have kinase activity but could be phosphorylated by BIK1 (Lu et al., 2010a) (Fig. 2.8A and 2.8B). We isolated BAK1CD, BAK1K and BIK1 as maltose binding protein (MBP) or glutathione S-transferase (GST) fusion proteins from *Escherichia coli*. As shown in Fig. 2.8A, an *in vitro* kinase assay using BIK1 as the kinase and BAK1K as the substrate indicates that

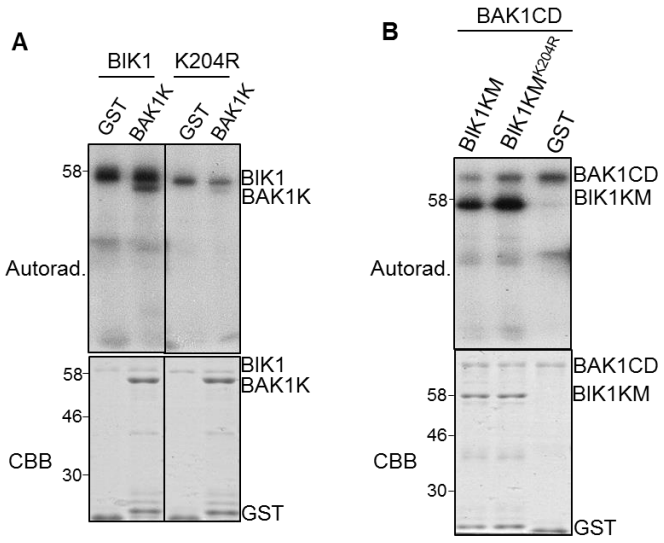

Figure 2.8 BIK1^{K204} has impaired kinase activity. A. BIK1^{K204R} exhibits reduced autophosphorylation and phosphorylation activity on BAK1. An *in vitro* kinase assay was performed by using GST-BIK1 or GST-BIK1^{K204R} as kinase and GST or GST-BAK1K as substrate in the kinase buffer containing [γ-^{32}P] *ATP*. Proteins were separated with SDS-PAGE and analyzed by autoradiography (Autorad.) (top panel). Protein loading control is shown by CBB staining (bottom panel). **B**. BIK1^{K204} is not required for BAK1-mediated phosphorylation on BIK1. An *in vitro* kinase assay was performed by using MBP-BAK1CD as kinase and GST, GST-BIK1KM or GST-BIK1KM^{K204R} as substrate. Phosphorylation is shown in Autorad. (top panel) and protein loading is shown by CBB staining (bottom panel).

BIK1^{K204R} had reduced autophosphorylation activity and transphosphorylation activity towards BAK1K. We further introduced BIK1^{K204R} mutation into BIK1Km to eliminate autophosphorylation activity and used GST-BIK1Km^{K204R} as the substrate for an *in vitro* kinase assay with MBP-BAK1CD as the kinase. Interestingly, BIK1^{K204R} mutation did not affect BAK1-mediated transphosphorylation on BIK1 as BAK1CD phosphorylated BIK1Km^{K204R} and BIK1Km to a similar extent (Fig. 2.8B).

2.3.5 BIK1^{K204} positively regulates BIK1-mediated plant immune responses

To elucidate the importance of BIK1^{K204} in relaying PTI responses, we transformed HA-tagged BIK^{K204R} under the control of its native promoter (*pBIK1::BIK1^{K204R}-HA*) into the *bik1* mutant. Multiple transgenic lines with detectable protein expression were obtained and two homozygous lines (line 1 and 2) were further characterized for PTI responses assays. The *bik1* mutant is deficient in flg22-induced ROS burst, *pBIK1::BIK1-HA* transgenic plants restored the *bik1* mutant ROS production to WT type level (Fig 2.9A and Fig 2.9B). The *pBIK1::BIK1^{K204R}-HA* transgenic plants exhibited similar ROS burst as the *bik1* mutant (Fig. 2.9A), suggesting that BIK1^{K204} is indispensable for BIK1 function in regulating flg22-triggered ROS production.

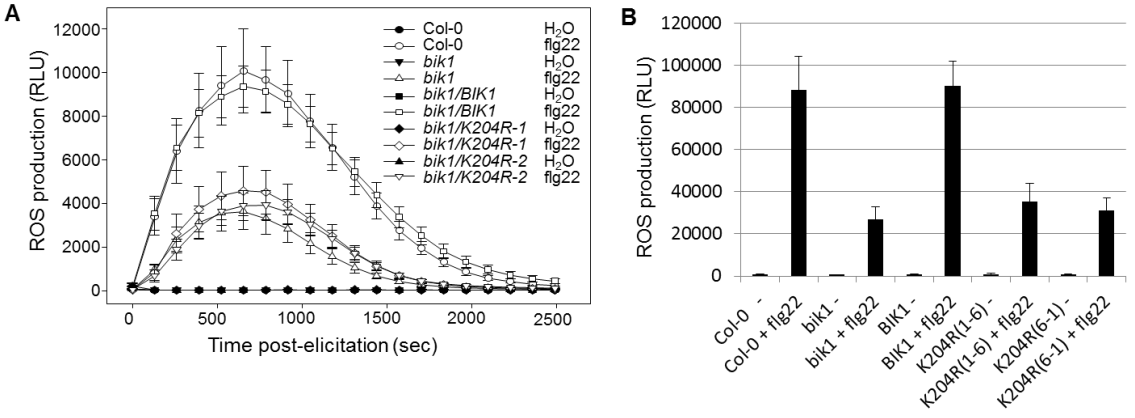

Figure 2.9 BIK1^{K204} plays an essential role in BIK1-mediated immune responses. A. BIK1^{K204} is required for BIK1-mediated flg22-induced ROS production. Leaf discs were treated with H_2O (Ctrl) or 100 nM flg22, and the ROS production was measured with a plate reader over 40 min. The data are shown as means ± standard errors from 4 leaf discs for control and 12 leaf discs for flg22 treatment. **B**. Quantification of total ROS production from transgenic plants. Total photon count was summed from the result of panel A. The data are shown as means ± standard errors.
The above experiments were repeated three times with similar results.

2.4 Discussion

Similar to protein phosphorylation, protein ubiquitination is a fundamental regulatory post-translational modification controlling various intracellular signaling events. However, compared to the well-studied phosphorylation system, many key regulatory mechanisms controlled by protein ubiquitination are much less understood. This is in large part due to the vastly more complex features of the ubiquitination system compared with phosphorylation (Komander, 2009). The nature of ubiquitination, includes monoubiquitination and polyubiquitination, dictates distinct fates of substrates, such as proteasome-mediated protein degradation or nonproteolytic functions of protein kinase activation or membrane trafficking (Chen and Sun, 2009; Skaug et al., 2009). Using an *in vivo* ubiquitination assay coupled with ubiquitination chemical inhibitor, we

show here that FLS2-BAK1 complex activation upon microbial ligand perception induces BIK1 monoubiquitination, likely occurring after rapid BIK1 phosphorylation. Arginine scanning revealed that $BIK1^{K204}$ is an important residue required for flg22-induced BIK1 monoubiquitination. Importantly, the $BIK1^{K204R}$ variant could not complement the *bik1* mutant plants, indicating that $BIK1^{K204}$ is indispensable for BIK1-mediated plant immunity. Consistently, treatment of ubiquitination inhibitor PYR-41 blocked flg22-triggered early immune responses. Thus, the data suggest that ligand-induced monoubiquitination of a convergent immune regulator BIK1 in multiple PRR complexes is essential to relay plant immune signaling.

Protein phosphorylation and ubiquitination are often intertwined, act either positively or negatively in both directions and reconcile the conflicting signaling outputs as intracellular constraints to balance physiological responses (Hunter, 2007). The BIK1 phosphorylation occurs within 2~3 min after flagellin treatment (Lu et al., 2010a), whereas BIK1 ubiquitination was detected 10 min later (Fig. 2.5A). Apparently, BIK1 phosphorylation temporally precedes its ubiquitination. In line with this observation, the BIK1 phosphorylation deficient mutant variants were no longer to be ubiquitinated. However, the $BIK1^{K204R}$ variant, which has compromised flg22-induced ubiquitination, also displays altered kinase activity. Notably, mutation of $BIK1^{K204R}$ did not appear to alter BIK1 protein stability. In addition, $BIK1^{K204R}$ still could be phosphorylated by BAK1 to a similar extent as WT BIK1. Sequence analysis according to the known kinase structure revealed that $BIK1^{K204}$ is located at a conserved motif RDLKxxN in the catalytic loop in subdomain VIb and likely mediates a direct contact with γ phosphate

from ATP during catalysis. Despite an extensive mutational screen, we were unable to identify a BIK1 mutant variant that only affects its ubiquitination, but not kinase activity and vice versa. It is possible that the initial BIK1 ubiquitination requires BIK1 basal kinase activity, and the ubiquitinated BIK1 is able to further enhance its phosphorylation activity, for instance via an allosteric regulation. This is supported by that the K163R variant in IKKβ completely abolished its monoubiquitination but selectively affected phosphorylation of certain serine residues. It was proposed that monoubiquitination of K163 occurs after phosphorylation of S177 and S181, which in turn regulates the phosphorylation of other serine and threonine residues. Therefore, monoubiquitination acts as a positive feedback to enhance IKKβ phosphorylation (Carter et al., 2005).

K48-linked polyubiquitination of proteins usually leads to 26S proteasome-mediated degradation, which serves as one of the mechanisms to control the abundance of key regulatory proteins (Vierstra, 2009b). In contrast, monoubiquitination often triggers target proteins endocytic trafficking and activates the signaling (Chen and Sun, 2009; Komander, 2009). Plasma membrane-resident auxin transporter PIN2 and brassinosteroid receptor BRI1 are constitutively polyubiquitinated via K63 polyubiquitin chains, which are required for their internalization and vacuolar targeting (Leitner et al., 2012; Martins et al., 2015). In contrast, the high-affinity iron transporter IRT1 has been shown to be monoubiquitinated *in vivo* (Barberon et al., 2011). Interestingly, IRT1 appears to be monoubiquitinated at multiple lysine residues based on the ubiquitination pattern and mutational analysis. Ubiquitinated BIK1 was detected primarily as a strong and discrete band and mutational analysis of individual lysine residues revealed that one

site is indispensable for flg22-induced BIK1 ubiquitination, suggesting that BIK1 is largely monoubiquitinated. Like many PM-resident proteins, IRT1 constitutively cycles between early endosomal compartments and the PM and traffics to the vacuole for degradation, which requires monoubiquitination of IRT1 (Barberon et al., 2011). It appears that iron deficiency or sufficiency did not affect IRT1 ubiquitination and endocytosis. We have shown that monoubiquitination of BIK1 is ligand-induced, which likely plays a positive role in flg22 signaling activation. In addition, we did not observe a demonstrable flg22-induced BIK1 degradation, suggesting that BIK1 monoubiquitination may not be associated with protein turnover. It has been shown recently that BIK1 is constitutively turned over in a 26S proteasome dependent-manner in the absence of MAMP treatment, and phosphorylation by CPK28 may contribute to BIK1 turnover (Monaghan et al., 2014b). We propose that different E3 ubiquitin ligases regulate ligand-independent BIK1 polyubiquitination for 26S proteasome-dependent degradation and ligand-dependent monoubiquitination for signaling activation. The studies elucidate a complex regulatory mechanism by protein ubiquitination to balance the activation and attenuation of plant immune signaling.

CHAPTER III

MONOUBIQUITINATION OF BIK1 BY A RING-TYPE E3 LIGASE LUCKY1 MEDIATES BIK1 FUNCTION IN PLANT IMMUNITY

3.1 Introduction

Being possibly the most abundant ubiquitination event in cells, monoubiquitination is involved in numerous processes including regulating transcription, mediating protein localization, and directly modulating activity of proteins (Kaiser et al., 2011). (Nakagawa and Nakayama, 2015). Along with the discoveries about the significance of monoubiquitination functions, corresponding E3 ligases which determine the types of ubiquitination and substrate specificity were demonstrated.

The more than 600 E3 ligases in human and more than 1400 E3 ligases in arabidopsis fall into two major E3 ligase families: HECT type and RING type. With only 28 members in human and 7 members in arabidopsis, HECT type E3 ligases comprise a small portion of the large number of E3s (Rotin and Kumar, 2009; Vierstra, 2009a). The rest of E3s belong to either single chain RING type E3s or RING-like multi-protein E3 complexes. HECT E3 ligases form an intermediate ubiquitin binding state before transferring the ubiquitin to the lysine residue of the substrate. In contrast, RING type E3 ligases serve as a bridge between E2 and the substrate while ubiquitin is directly transferred from E2 to the substrate. Interestingly, members from both HECT type and RING type E3s have been shown to mediate monoubiquitination at least in human (Nakagawa and Nakayama, 2015). One of the HECT type E3 ligase, Smurf2, is the

cognate E3 ligase for SMAD3 and mediates monoubiquitination of SMAD3 at three lysines: K33, K53 and K81. Both in *in vivo* and *in vitro* experiments support that Smurf2 indeed is the designated E3 ligase with monoubiquitination activity (Tang et al., 2011). Another HECT type E3 ligase, NEDD4, mediates monoubiquitination of target protein PTEN at K289 and induces its nuclear translocation (Trotman et al., 2007). From the seven HECT type E3 ligases in arabidopsis, no common protein domain is shared between Smurf2/NEDD4 and arabidopsis HECT E3s other than the HECT domain (Downes et al., 2003). Only few studies are available describing plant HECT E3s and their mechanisms. One example is UPL5 polyubiquitinates a TF WRKY53 for protein degradation (Miao and Zentgraf, 2010). To date, it is unknown if any plant HECT E3 ligase possesses monoubiquitination activity.

RING type E3 ligases are more abundant than HECT E3s and, in human, many mediate monoubiquitination (Nakagawa and Nakayama, 2015). Several RING type E3 ligases, including RNF2 and TRIM37, have been shown to monoubiquitinate histone protein H2A at K119 to inhibit transcription (Bhatnagar et al., 2014; Wang et al., 2004). E3 ligase MDM2 monoubiquitinates TF FOXO4 at K199 and K211 to regulate nuclear import (Brenkman et al., 2008; van der Horst et al., 2006) while monoubiquitination of NEMO by E3 ligase cIAP1 at K277 and K309 regulates nuclear export (Jin et al., 2009a). In the WNT (Wingless-related integration site) signaling, transcription corepressor Groucho (Gro)/TLE is monoubiquitinated by E3 ligase XIAP and this monoubiquitination disrupts TLE interaction with transcription regulator TCF (Hanson et al., 2012a). Another RING type E3 ligase Rad18 monoubiquitinates PCNA at K164

during DNA damage responses (Bergink and Jentsch, 2009). In plants, there are a large number of RING type E3 ligases but research about RING type E3 mediating monoubiquitination is very limited. One report shows E2 AtUBC2 alone is enough to mediate monoubiquitination of AtPCNA at the conserved K164, similar to other eukaryotes, and suggested E3 ligase AtRAD5a is involved in this process (Strzalka et al., 2013). Unfortunately, this research failed to include proper controls to conclude that AtRAD5a is required for this process. Another report suggested the involvement of CUL3-RING E3 ligase $CRL3^{NPH3}$ in monoubiquitination of Phototropin 1 (Phot1) (Roberts et al., 2011). In this paper, they detected the ubiquitination of Phot1 using anti-Ubiquitin antibody and failed to observe signal from antibody FK1, an antibody only recognizing polyubiquitinated proteins. They concluded that Phot 1 is monoubiquitinated without further supporting evidence. Considering the poor detection from antibody FK1, this conclusion is not very solid. To our knowledge, there are no additional protein monoubiquitination findings and yet a clear E3 ligase identified in plants.

In this study, we have identified a putative E3 ligase LUCKY which interacts with BIK1 and monoubiquitinates BIK1 *in vitro* at multiple sites. Combining *in vitro* ubiquitination- mass spectrometry and mutational analysis, we characterized a $BIK1^{9KR}$ mutant that abrogates most flg22-triggered monoubiquitination without compromising BIK1 kinase activity. Transgenic plants carrying $BIK1^{9KR}$ mutant were unable to restore the *bik1* deficiency in plant innate immunity, suggesting a positive regulation of PTI by BIK1 monoubiquitination. More significantly, we found flg22-triggered ubiquitination

of BIK1 did not affect BIK1 stability but rather controls ligand-induced BIK1 dissociation with receptor FLS2, providing a mechanistic insight for this monoubiquitination.

3.2 Materials and methods

3.2.1 Plant material and growth conditions

Arabidopsis thaliana accessions Col-0 and transgenic *pBIK1::BIK1-HA* in the *bik1* background were generated as previously described (Lin et al., 2014). *pBIK1::BIK1^{9KR}-HA* transgenic plants in the *bik1* background and *35S::BIK1-HA*, *35S::BIK1^{9KR}-HA* transgenic plants in the Col-0 background were generated in this study (see below for details). All arabidopsis plants were grown in soil (Metro Mix 366/ Sunshine LC1) in a growth chamber at 20-23°C, 60% relative humidity and 75 μE $m^{-2}s^{-1}$ light with a 12 hr light/12 hr dark photoperiod for four weeks before pathogen infection assay, protoplast isolation, and ROS assay.

3.2.2 Plasmid construction and generation of transgenic plants

The HA or FLAG epitope-tagged FLS2, BAK1, BIK1 constructs used for protoplast assays were generated as described previously (Lin et al., 2014; Lu et al., 2010a). BIK1 point mutations were generated by site-directed mutagenesis with primers listed in the Supplemental Table 1 using the pHBT-BIK1-HA construct as the template. BIK1^{9KR} was further sub-cloned into a binary vector *pCB302-pBIK1::BIK1-HA*,

pCB302-35S::BIK1-HA and the modified GST (pGEX4T-1, Pharmacia) vector with BamHI and StuI digestion to generate *pCB302-pBIK1::BIK1*^{9KR}*-HA* , *pCB302-35S::BIK1*^{9KR}*-HA* and *pGST-BIK1*^{K204R} respectively. *Agrobacterium tumefaciens*-mediated floral dipping was used to transform above binary vectors into the *bik1* plants and Col-0 plants. The transgenic plants were selected by Glufosinate-ammonium (Basta, 50 μg/ml). Multiple transgenic lines were analyzed with Western blot (WB) for protein expression. Two lines with 3:1 segregation ratio for Basta resistance in T3 generation were selected to obtain homozygous seeds for further studies.

The *LUCKY1* gene (AT2G17450) was cloned by PCR amplification from Col-0 cDNA with primers containing BamHI site at the 5' end and StuI site at the 3' end, followed by BamHI and StuI digestion and ligation into plant expression vector pHBT with HA or FLAG tag at the C-terminus. The *LUCKY2* gene (AT4G35480) was cloned similarly as *LUCKY1* with BamHI and SmaI sites-containing primers. *LUCKY1* was sub-cloned into a modified GST (pGEX4T-1, Pharmacia) vector and a modified MBP (pMAL-c2, NEB) vector with BamHI and StuI for *E. coli* fusion protein isolation. For Y2H assay, *LUCKY1* was sub-cloned into a modified pGBKT7 vector and a modified pGADT7 vector (Clontech) with same restriction enzymes. Promoter of *LUCKY1* and *LUCKY2* gene was PCR amplified from genomic DNA of Col-0 with primers containing SacI and BamHI. The promoter was then introduced to pHBT vector and then pLUCKY1::LUCKY1-FLAG was digested and ligated into pCAMBIA2300 vector. *Agrobacterium tumefaciens*-mediated floral dipping was used to transform

pCAMBIA2300-pLUCKY1::LUCKY1-FLAG into transgenic plant expressing *pBIK1::BIK1-HA*.

Artificial mircoRNA (amiRNA) was constructed as previously described (Li et al., 2014d). In brief, amiRNA candidates were obtained from the website http://wmd3.weigelworld.org/cgi-bin/webapp.cgi by typing in AGI number. Then three candidates were chosen for each gene. For LUCKY1, amiRNA480: TTTTGTCAATACACTCCACGG; amiRNA211: TCAACGCAGATAAGAGCGCTA; amiRNA109: TCAAGTAATCTTGACGGTCGT. For LUCKY2, amiRNA444: TTATGCATATTGCACACTCCG; amiRNA113: TAATCTAGAGGAGCGAGTCAG; amiRNA214: TCTACGCATACGAGAGCGCAT. Primers for cloning amiRNAs were generated with wmd3 website (http://wmd3.weigelworld.org/cgi-bin/webapp.cgi) and cloning was done with pHBT-amiRNA-ICE1 as template as previously described (Li et al., 2014d). Final constructs were sequenced via Sanger sequencing.

3.2.3 Yeast two-hybrid screen

The cDNA library constructed in a modified pGADT7 vector (Clontech) as previously described (Lu et al., 2011b). The BIK-G2A was cloned into a DNA-binding domain fusion vector pBridge (Clontech) and transformed into yeast first. The cDNA library was then transformed into the yeast containing pBridge-BIK1-G2A and transformants were screened in the synthetic defined media (SD) without Trp, Leu, His, Ade (SD-T-L-H-A) and SD-T-L-H + 1 mM 3-Amino-1,2,4-triazole (3AT). No colonies grew in the medium SD-T-L-H-A and the biggest colonies in SD-T-L-H+3AT were

further confirmed in SD-T-L-H+3AT medium and subjected to plasmid isolation and sequencing.

3.2.4 Pathogen infection assays

Pseudomonas syringae pv. *tomato* (*Pst*) DC3000 was cultured for overnight at 28°C in the King's B medium supplemented with rifamycin (50 μg/ml). Bacteria were collected by centrifugation at 3500 rpm, washed and re-suspended to the density of 5 x 10^5 cfu/ml with 10 mM $MgCl_2$. Leaves from four-week-old plants were hand-inoculated with bacterial suspension using a needleless syringe. For flg22-mediated protection assay, leaves were pre-inoculated with 100 nM flg22 or H_2O as control and 24 hr later bacteria suspension was infiltrated into the same leaves. To measure *in planta* bacterial growth, three sets of two leaf discs were punched and ground in 100 μl of ddH_2O. Serial dilutions were plated on TSA plates (1% tryptone, 1% sucrose, 0.1% glutamatic acid and 1.8% agar) containing 25 μg/ml rifamycin. Plates were incubated at 28°C and bacterial colony forming units (cfu) were counted 2 days after incubation.

3.2.5 Protoplast transient expression assay and co-immunoprecipitation (co-IP) assay

Protoplast isolation and transient expression assay were performed as previously described (He et al., 2007). For protoplast-based co-IP assay, protoplasts were transfected with a pair of constructs (empty vector as control, 100 μg DNA for 500 μl protoplasts at the density of 2 x 10^5/ml for each sample) and incubated at room

temperature for 6-10 hr. After treatment of flg22 with indicated concentration and time points, protoplasts were collected by centrifugation and lysed in 300 μl co-IP buffer (150 mM NaCl, 50 mM Tris-HCl, pH7.5, 5 mM EDTA, 0.5% Triton, 1 × protease inhibitor cocktail, before use, adding 2.5 μl 0.4 M DTT, 2 μl 1M NaF and 2 μl 1M Na_3VO_3 for 1 ml IP buffer) by vortexing. After centrifugation at 10,000×g for 10 min at 4°C, 30 μl of supernatant was collected for input control and 7 μl α-FLAG-agarose beads were added into the remaining supernatant and incubated at 4 °C for 1.5 hr. Beads were collected and washed three times with washing buffer (150 mM NaCl, 50 mM Tris-HCl, pH7.5, 5 mM EDTA, 0.5%Triton) and once with 50 mM Tris-HCl, pH7.5. Immunoprecipitates were analyzed by WB with indicated antibodies. The amiRNA candidates screen were performed as previously described (Li et al., 2014d).

3.2.6 *In vivo* ubiquitination assay

FLAG-tagged UBQ (FLAG-UBQ) or a vector control (40 μg DNA) was cotransfected with the target gene with an HA tag (40 μg DNA) into 400 μl protoplasts at the density of 2 x 10^5/ml for each sample and protoplasts were incubated at room temperature for 10 hr. After treatment with 100 nM flg22 at the indicated time points, protoplasts were collected for co-IP assay in co-IP buffer containing 1% triton.

3.2.7 *In vitro* ubiquitination assay

Ubiquitination assays were performed as previously described with modifications (Lu et al., 2011a; Zhou et al., 2014). Reactions containing 1 μg of substrate, 1 μg of

HIS_6-E1 (AtUBA1), 1 μg of HIS_6-E2 (AtUBC8), 1 μg of GST-E3, 1 μg of HIS_6-ubiquitin (Boston Biochem) in the ubiquitination buffer (20 mM Tris-HCl, pH 7.5, 5 mM MgCl2, 0.5 mM DTT, 2 mM ATP) were incubated at 30°C for 3 hr. The ubiquitinated substrate proteins were detected by WB.

3.2.8 *In vitro* GST pull-down assay

MBP fusion protein isolation was described in previous chapters. For GST-agarose beads, GST-BIK1 or GST protein isolation was performed as described before and the agarose beads were obtained after elution and washed with PBS for three times. MBP-LUCKY1CD or MBP protein (2 μg) were pre-incubated with 10 μl prewashed glutathione agarose in 300 μl pull-down incubation buffer (20 mM Tris-HCl, pH 7.5, 100 mM NaCl, 0.1mM EDTA, and 0.2% Triton X-100) for 30 min at 4°C. 5 μl GST or GST-BIK1 agarose beads were pre-incubated with 20 μg BSA in 300 μl incubation buffer for 30 min at 4°C. Then the supernatant containing MBP-LUCKY1/MBP was mixed with the pre-incubated GST/GST-BIK1 agarose beads for 1hr at 4°C. The agarose beads were precipitated and washed three times in pull-down washing buffer (20 mM Tris-HCl, pH 7.5, 300 mM NaCl, 0.1 mM EDTA, and 0.5% Triton X-100). The pull-down proteins were analyzed by WB with an α-HA antibody.

3.2.9 Mass spectrometry analysis of ubiquitination sites

The *in vitro* ubiquitination with GST-LUCKY1CD and GST-BIK1/GST-$BIK1^{K204R}$ were performed as mentioned above with overnight incubation to maximize

ubiquitination. Reactions were loaded in an SDS-PAGE gel (7.5%) and ran for a short time till the ubiquitinated bands can be separated from the original GST-BIK1 (band of GST-BIK1 travel less than 0.5 cm in separating gel). Ubiquitinated bands were sliced, trypsin digested before LC-MS/MS analysis on an LTQ-Orbitrap hybrid mass spectrometer (Thermo Fisher) as previously described (Boname et al., 2010). The MS/MS spectra were analyzed with PEAKS and SEQUEST software and images are exported from PEAKS.

3.3 Results

3.3.1 Y2H screen identified a putative E3 ligase for BIK1 ubiquitination

In order to study the function of BIK1 monoubiquitination, blocking the ubiquitination by mutating the putative ubiquitination site(s) or knocking out the putative E3 ligases are feasible approaches. In chapter 2, we screened all lysine residues and ubiquitination of BIK1 was only blocked in the $BIK1^{K204R}$ mutant. Considering phosphorylation of BIK1 is a prerequisite of monoubiquitination and $BIK1^{K204R}$ possesses reduced activity, it is expected that monoubiquitination will be compromised in $BIK1^{K204R}$ and Lysine-204 might not be the putative ubiquitination site. Since there is no single K-to-R mutation that could block BIK1 monoubiquitination without affecting the kinase activity, alternatively we tried to look for the cognate E3 ligase. A Yeast-two-hybrid (Y2H) screen was carried out to identify BIK1-interacting proteins. Considering the putative myristoylation might perturb BIK1 localization in yeast nucleus, we used

BIK1-G2A as the bait for the screen. Clones from 196 strongest interacting colonies out of ~120,000 transformants were sequenced and 84 of them aligned to 35 genes that were in-frame and unique in BIK1 screen (Supplemental Table 2). Among them, there is only one gene encoding an E3 ligase, which we named ***L****ooking for* ***U****biquitin E3 ligase* ***C****orrelate with BI****K1*** (*LUCKY1*). With 185 amino acids, LUCKY1 consists of one putative transmembrane domain and a catalytic RING domain (Fig 3.1A). The sequence from the positive-interaction yeast colony (LUCKY1-Y2H) matches amino acid 71-185 of LUCKY1 C-terminus (Fig 3.1A). We first confirmed the interaction of BIK1-G2A with LUCKY1-Y2H in yeast (Fig 3.1B). The full length LUCKY1 and cytosolic domain (LUCKY1-CD) did not interact with BIK1 as strongly as LUCKY1-Y2H, which suggests that specific portion of the N-terminus is hindering its interaction in yeast. Next we tested BIK1-LUCKY1 interaction in plant by a co-immunoprecipitation assay after co-expressing BIK1-FLAG and LUCKY1-HA in arabidopsis protoplasts. Indeed, BIK1 associates with LUCKY1 in protoplasts as shown in Fig 3.1C and the interaction was confirmed in transgenic plants expressing both proteins driven by their own promoters (Fig 3.1D). In line with this observation, *in vitro* GST-pull-down assay showed recombinant GST-BIK1 directly pulled down MBP-LUCKY1CD (Fig 3.1E). Taken together, BIK1 interacts with LUCKY1 and likely the C-terminus mediates this direct interaction.

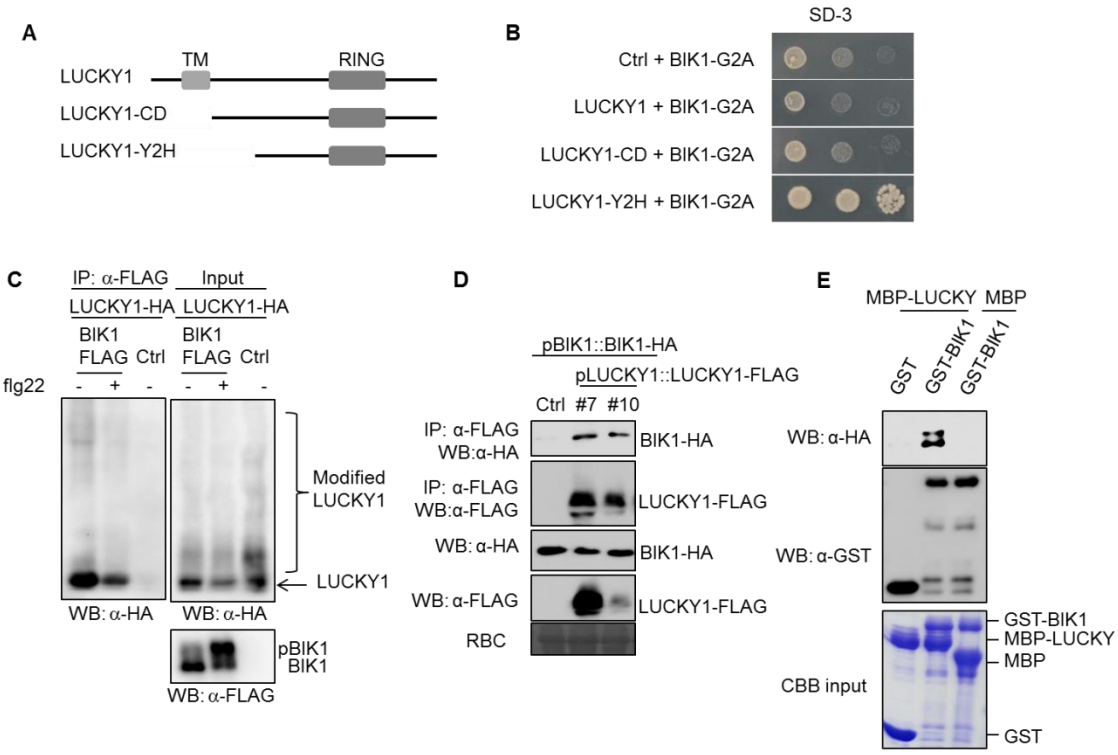

Figure 3.1 BIK1 interacts with a novel E3 ligase LUCKY1. A. Domain organization of LUCKY1. TM: Transmembrane domain; RING: E3 catalytic domain; CD: cytoplasmic domain; Y2H: truncation from yeast two-hybrid screen. **B**. LUCKY1-Y2H interacts with BIK1-G2A in yeast two-hybrid assay. pBK-BIK1-G2A and different construct in pAD vectors were co-transformed into yeast. Transformants grown on SD-L-T plate were tested on SD-L-T-H plate with series dilutions. **C**. BIK1 interacts with LUCKY1 in Co-IP assay. Protoplasts were co-expressed with LUCKY1-HA and BIK1-FLAG or Ctrl. The Co-IP assay was carried out with α-FLAG-Agarose and interacting proteins were examed by WB with α-HA. **D**. BIK1 interacts with LUCKY1 in transgenic plants. Transgenic plants expressing pBIK1::BIK1-HA and pLUCKY1::LUCKY1-FLAG were used for CoIP assay. The Co-IP assay was carried out with α-FLAG-Agarose and interacting proteins were examed by WB with α-HA. **E**. BIK1 interacts with LUCKY1 by in vitro pull-down assay. GST or GST-BIK1 immobilized on glutathione sepharose beads was incubated with MBP or MBP-LUCKY1 proteins. Washed beads were subjected to WB with α-HA or α-GST (top two panels). Input proteins were shown by CBB (bottom panel).

3.3.2. BIK1 phosphorylates LUCKY1 *in vitro*

BIK1 is a protein kinase, which prompted us to test if BIK1 could directly phosphorylate this interacting E3 ligase. We isolated GST tagged BIK1 or LUCKY1-CD and performed an *in vitro* kinase assay. As shown in Fig 3.2, BIK1 phosphorylated LUCKY1CD as strongly as BIK1 phosphorylated BAK1K which served as a positive control. This indicates BIK1 not only interacts with LUCKY1, but it also might regulate LUCKY1 by directly phosphorylating it.

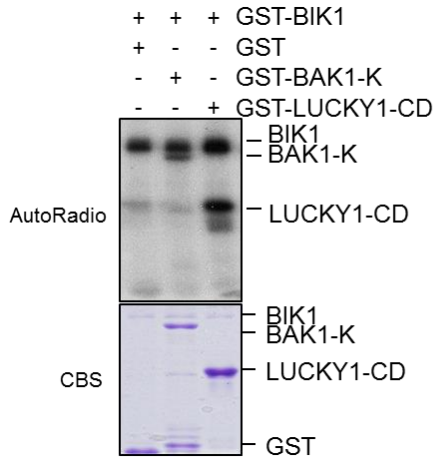

Figure 3.2 BIK1 phosphorylates LUCKY1 *in vitro*. BIK1 phosphorylates LUCKY1 *in vitro*. *In vitro* kinase assay was performed by incubating GST-BIK1 fusion protein with GST, GST-BAK1 or GST-LUCKY1 in kinase buffer. Phosphorylation was detected by autoradiography (top panel). Protein loading control was shown by CBB (bottom panel).

3.3.3. LUCKY1 monoubiquitinates BIK1

To understand if LUCKY1 is the cognate E3 ligase that ubiquitinates BIK1, we performed an *in vitro* ubiquitination assay by incubating purified E1, E2, GST-LUCKY1CD and GST-BIK1 together in a reaction buffer and followed by a WB detecting the ubiquitinated BIK1 protein. Without ubiquitination reaction, GST-BIK1 is

a single band (Fig 3.3A, lane 1). After *in vitro* ubiquitination reaction, mobility of a portion of GST-BIK1 got reduced in SDS-PAGE gel and multiple bands were observed (Fig 3.3A lane 2). The molecular weight differences between those bands are around 8 kD which equals the molecular weight of one ubiquitin protein suggesting ubiquitination modifications. There are at least three additional upper bands of GST-BIK1 compared to its original size, suggesting one, two, or three ubiquitin proteins are attached (Fig 3.3A lane 2). Those higher molecular weight bands could be derived from monoubiquitination at multiple sites (multimonoubiquitination) or di-, tri- and polyubiquitination of BIK1 at one site. To understand the type of ubiquitination, we performed an *in vitro* ubiquitination assay with an ubiquitin mutant (UBQ-noK) which has all lysine residues mutated. Since no available lysine residues for further ubiquitin attachment, di-, tri- or

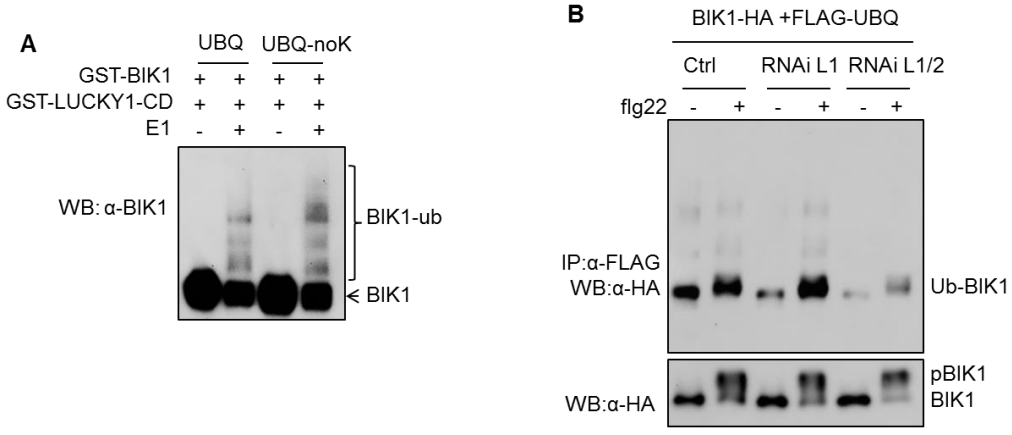

Figure 3.3 LUCKY1 monoubiquitinates BIK1 *in vitro* and *in vivo*. A. LUCKY1 monoubiquitinates BIK1 *in vitro*. *In vitro* ubiquitination assay was performed by incubating GST-LUCKY1-CD fusion protein with GST-BIK1 in ubiquitination buffer containing E1 and E2. Ubiquitin (UBQ) or ubiquitin mutant UBQ^{noK} (all lysine mutated to arginine) were used in the *in vitro* reaction. BIK1 ubiquitination was detected by WB with α-BIK1 antibody. **B.** LUCKY1 monoubiquitinates BIK1 in vivo. In vivo BIK1 ubiquitination assay was carried out similarly as previous with co-expressing control or 35s::amiRNALUCKY1(L1) or together with 35S::amiRNALUCKY2 (L2).

polyubiquitination will be blocked while multimonoubiquitination remains unaffected. We observed the same pattern of ubiquitination as WT ubiquitin when UBQ-noK was used (Fig 3.3A lane 4), suggesting LUCKY1 monoubiquitinates BIK1 *in vitro* at multiple residues.

To determine if LUCKY1 is the cognate E3 ligase for BIK1, an *in vivo* BIK1 ubiquitination assay in *lucky1* knock-out would provide direct genetic evidence. Unfortunately, there is no T-DNA insertion knock-out available for both *LUCKY1* and its closest homolog *LUCKY2*. Alternatively, we used an artificial microRNA (amiRNA) silencing approach to test our hypothesis (Li et al., 2014d). More specifically, we cloned three amiRNA constructs to target three sequences of LUCKY1 and three amiRNA constructs to target LUCKY2. We then compared the silencing efficiency of each construct on LUCKY1 or LUCKY2 by co-expressing the candidate amiRNA and the corresponding LUCKY gene in protoplasts. Based on a Western Blot analysis, we decided to use amiRNA480 for LUCKY1 and amiRNA444 for LUCKY2 (Fig 3.4). Next we tried co-expressing LUCKY1 amiRNA480 together with BIK1 and UBQ for *in vivo* BIK1 ubiquitination assay but it did not affect BIK1 monoubiquitination (Fig 3.3B lane 1-4). When we co-expressed LUCKY1 amiRNA480 and LUCKY2 amiRNA444 together in an *in vivo* ubiquitination assay, monoubiquitination of BIK1 was greatly suppressed (Fig 3.3B lane 5,6). This suggests LUCKY1 and LUCKY2 potentially play redundant roles in mediating BIK1 monoubiquitination *in vivo*. Together with the *in vitro* data, we conclude that LUCKY1 and LUCKY2 are the cognate E3 ligases mediate BIK1 monoubiquitination.

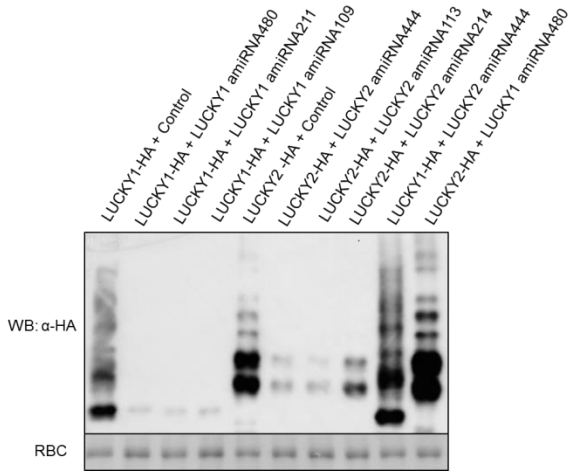

Figure 3.4 WB screen of amiRNA for LUCKY1/2. LUCKY1/2-HA were co-expressed with amiRNAs for 12 hrs with DNA ratio 1:3 (LUCKY:amiRNA). Expression of LUCKY1/2 was detected by WB with anti-HA antibody.

3.3.4. LUCKY1 is able to ubiquitinate BIK1 at multiple sites

Based on the observation that LUCKY1 monoubiquitinates BIK1 *in vitro* at multiple sites, we hypothesized that if we identified all BIK1 lysine residues ubiquitinated by LUCKY1 *in vitro* and mutate all of them simultaneously, we might be able to block BIK1 ubiquitination and further investigate the function of ubiquitination in plants. To identify the putative ubiquitination sites, we performed an *in vitro* BIK1 ubiquitination reaction and subjected the ubiquitinated BIK1 for MS/MS analysis. We were able to identify 10 lysine residues (Fig 3.5A, B). With the exception of lysine-105, which resides right in the ATP binding pocket and blocked BIK1 kinase activity when mutated, K-to-R mutation for all other 9 residues did not appear to affect BIK1 ubiquitination *in vivo*. Therefore, we further constructed a quintuple N-terminus K-to-R mutant (N5KR), a quadruple C-terminus K-to-R mutant (C4KR), as well as the nonuple

mutant (9KR) mutating all 9 lysines except K105. When BIK1 *in vivo* ubiquitination was examined with all those mutants, we found that N5KR and C4KR partially suppressed BIK1 ubiquitination while 9KR almost completely blocked BIK1 monoubiquitination (Fig 3.5 C,D). More importantly, blocking BIK1 ubiquitination by 9KR was not due to affected BIK1 kinase activity, as BIK1^{9KR} possessed similar kinase activity as BIK1 WT from both *in vitro* kinase assay (Fig 3.6) and *in vivo* flg22-triggered BIK1 band shift (Fig 3.5C). These data support the idea that LUCKY1 can

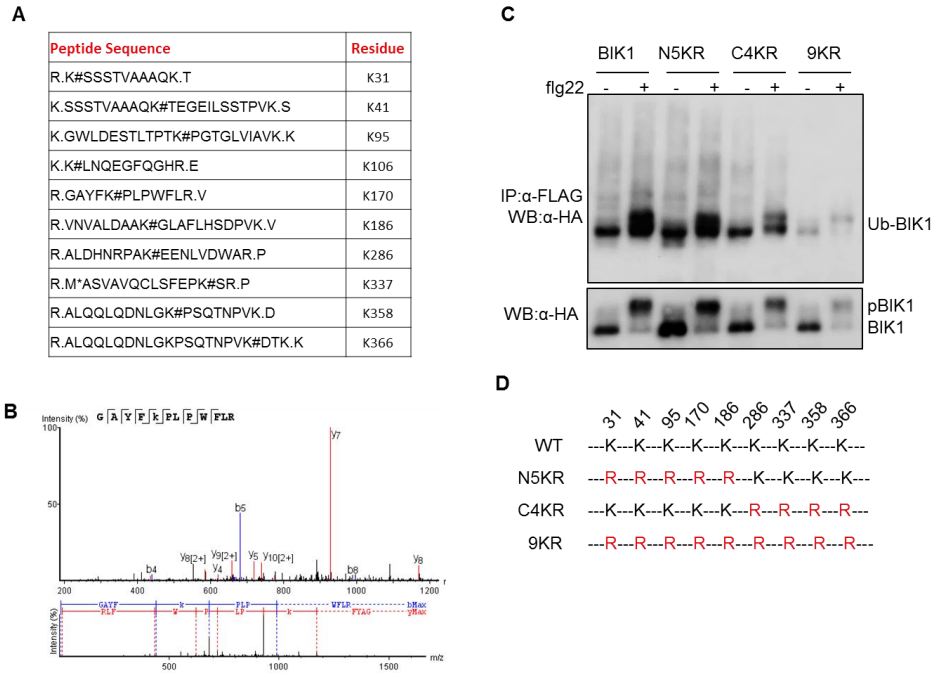

Figure 3.5 LUCKY1 ubiquitinates BIK1 at multiple sites *in vitro* and BIK1^{9KR} blocks monoubquitination. A. BIK1 is ubiquitinated by LUCKY1 at multiple residues. In vitro ubiquitinated GST-BIK1 was subjected to trypsin digestion and followed LC-MS/MS to identify ubiquitination site. Ions detected containing diglycine remnant on lysine residue were shown. **B**. MS/MS spectrum of peptide containing K170 is shown. **C. D.** 9KR mutation blocks BIK1 ubiquitination. Protoplasts were co-expressed with FLAG-UBQ and different BIK1 mutant tagged with HA. In vivo BIK1 ubiquitination assay were performed as before. Detailed mutations for N-terminus 5KR (N5KR), C-terminus 4KR (C4KR) and 9KR are shown in D.

monoubiquitinate BIK1 at alternative sites when the preferred sites are not available both *in vivo* and *in vitro*. In contrast with BIK1^{K204R} which failed to uncouple BIK1 phosphorylation and ubiquitination, BIK1^{9KR} enables us to test the function of BIK1 monoubiquitination without hindering the kinase activity.

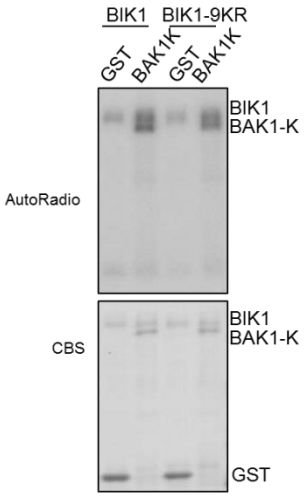

Figure 3.6 BIK1^{9KR} has normal kinase activity. *In vitro* kinase assay was performed by incubating GST-BIK1/GST-BIK19KR fusion protein with GST or GST-BAK1 in kinase buffer. Phosphorylation was detected by autoradiography (top panel). Protein loading control was shown by CBB (bottom panel).

3.3.5. Monoubiquitination is required for BIK1 function in innate immunity

Since BIK1^{9KR} lost *in vivo* monoubiquitination, we transformed BIK1^{9KR} driven by its own promoter into the *bik1* mutant and constructed homozygous transgenic plants. When plants were challenged with flg22, the *bik1* mutant plants exhibited reduced ROS burst while WT BIK1-HA complemented the ROS to similar level as Col-0 (Fig 3.7A). However, two lines of BIK1^{9KR} transgenic plants failed to complement *bik1* ROS level, while one line showed a slight partial complementation (Fig 3.7A). Though the kinase activity of BIK1^{9KR} was unaffected and *in vivo* phosphorylation remained normal,

BIK1^{9KR} was unable to function as BIK1, suggesting that the monoubiquitination of BIK1 is required for BIK1 function in regulating ROS production. Moreover, transgenic plants with overexpression of BIK1^{9KR} were more susceptible to the bacterial pathogen *Pst* DC3000 compared to Col-0 or BIK1 overexpression transgenic plants (Fig 3.7B). This indicates BIK1^{9KR} plays negative role in plant defense responses and monoubiquitination of BIK1 is required and plays a positive role in regulating plant immunity.

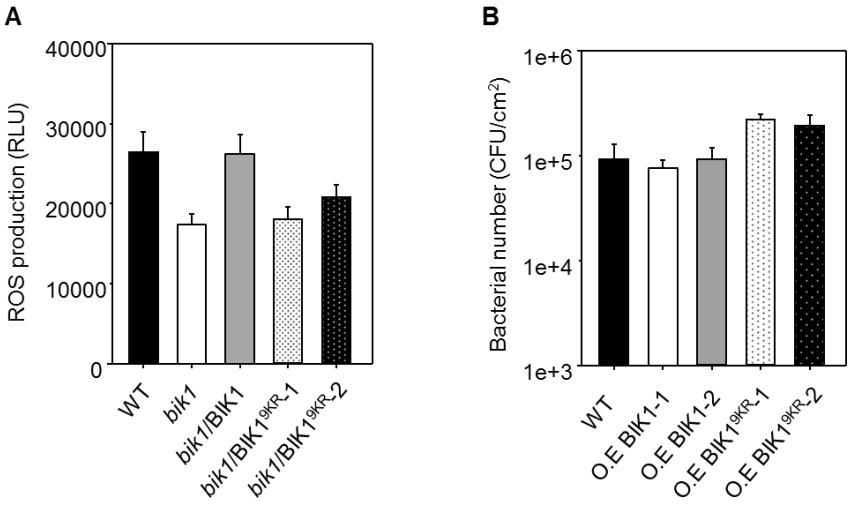

Figure 3.7 Monoubiquitination is required for BIK1 function in innate immunity. **A**. Monoubiquitination positively regulate BIK1 function in flg22-induced ROS production. Leaf discs from indicated genetic background were treated with flg22, and the ROS production was measured over 60 min. **B**. Monoubiquitination positively regulate BIK1 function in disease resistance to *Pst* DC3000 infection. WT, overexpression (O.E) BIK1-HA or BIK1^{9KR}-HA transgenic plants (two independent lines for each transgene) were hand-inoculated with *Pst* DC3000 at 5×10^5cfu/ml. The *in planta* bacterial growth was measured at 2 days-post inoculation.

3.3.6. Monoubiquitination mediates BIK1 dissociation from FLS2

It is challenging to understand how monoubiquitination of BIK1 positively regulates BIK1 function as well as innate immune responses, considering the function of

monoubiquitination is largely unknown in plants. Because BIK1 monoubiquitination happens very rapidly and regulates early responses such as ROS, we hypothesized that BIK1 monoubiquitination controls a very early molecular event in the receptor complex. Moreover, it has been shown monoubiquitination regulates protein-protein interactions and that flg22 treatment leads to BIK1 dissociation with FLS2. Therefore, we decided to test if BIK1 monoubiquitination is involved in interaction dynamics. We expressed FLS2 and BIK1 or BIK1^{9KR} in protoplasts and performed a CoIP assay to test FLS2-BIK1 interaction dynamics upon flg22 perception. Consistent with a previous report, FLS2 associated with BIK1 and this interaction was weakened upon flg22, suggesting a ligand-mediated dissociation (Fig 3.8A lane 1,2). Surprisingly, when we tested BIK1^{9KR}

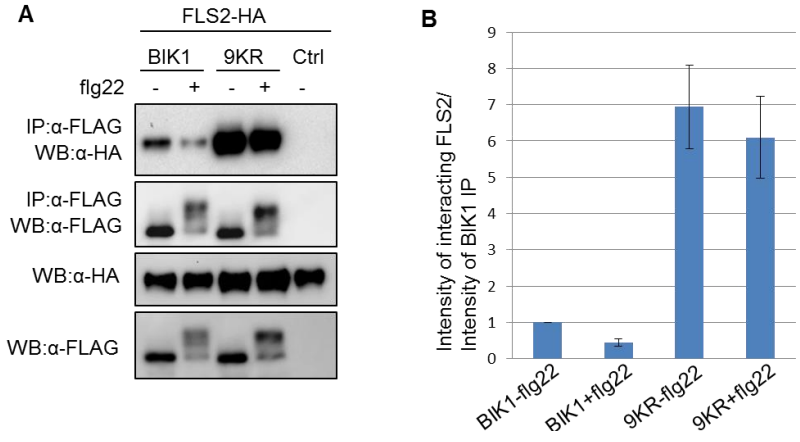

Figure 3.8 Monoubiquitination mediates BIK1 dissociation from FLS2 upon flg22 perception. A. Blocking ubiquitination suppresses BIK1 dissociation from the FLS2 complex. Protoplasts were co-expressed with FLS2-HA and BIK1-FLAG, BIK1^{9KR}-FLAG or Ctrl. After flg22 treatment, cell lysate was subjected to CoIP with α-FLAG-agarose, and proteins were analyzed using WB. **B.** Quantification of BIK1 dissociation from FLS2. Band intensity from IP: α-FLAG, WB:α-HA was used to divide band intensity from IP: α-FLAG, WB:α-FLAG. Data from 3 repeat and error bar represent the standard error.

interaction with FLS2, we observed a relatively stronger (7 fold higher) interaction of FLS2-BIK1^{9KR} (Fig 3.8A lane 3,4, Fig 3.8B). In addition, flg22-triggered FLS2-BIK1^{9KR} dissociation was greatly blocked and a large portion of interaction remained upon flg22 treatment. This result suggests that multimonoubiquitination of BIK1 positively regulates flg22-triggered BIK1-FLS2 dissociation and this dissociation plays an indispensable role of BIK1 function.

3.4 Discussion

Being a fundamental post-translational modification, protein ubiquitination is involved in almost every aspect of intracellular biology including transcription, trafficking, protein degradation, and signal transduction. Structurally diverse ubiquitination modifications exist, including monoubiquitination with only one ubiquitin being attached to the target protein or polyubiquitination when the primary ubiquitin was further modified by additional ubiquitin(s). Monoubiquitination appears to be the most abundant ubiquitination event in cells (Kaiser et al., 2011) as it orchestrates various molecular processes including transcriptional regulation, DNA damage response, protein trafficking, protein activity regulation, as well as protein-protein interactions (Nakagawa and Nakayama, 2015). As the enzyme catalyzing the last step of ubiquitination, E3 ligases primarily determine the type and specificity of ubiquitination. Large amount of research from yeast to human has demonstrated E3 ligases, from both HECT type and RING type, could mediate protein monoubiquitination. In plants, the functions of protein monoubiquitination are largely unknown and the underline E3 ligases remain elusive. In

order to gain more mechanistic insight of BIK1 monoubiquitination, we undertook a Y2H screen to look for the cognate E3 ligase and identified a RING type E3 LUCKY1. Combining biochemical and genetic analysis, we found LUCKY1 monoubiquitinates BIK1 at multiple lysine residues (Fig 3.3, 3.5). This provides one of the first evidence that some RING type E3 ligases in plants possess monoubiquitination activity both *in vivo* and *in vitro*. There are more than 400 RING type single-peptide E3 ligases in the arabidopsis genome and some of them have been shown to mediate protein polyubiquitination (Bueso et al., 2014; Zhang et al., 2015; Zhang et al., 2005). How many of these RING E3s can direct monoubiquitination and whether other type of E3 ligases including HECT type or U-box type are involved in monoubiquitination will be interesting questions to address in the future.

An Y2H interaction assay as well as an *in vitro* pull-down assay suggested BIK1 directly interacts with LUCKY1, likely via C-terminus. No protein domain other than the RING domain has been annotated in the C-terminus of LUCKY1. It remains unknown which part of LUCKY interacts with BIK1. Future structural studies could provide more insight of the interaction interface between BIK1 and LUCKY1. Additionally, LUCKY1 also consists of a putative transmembrane domain and a relatively short N-terminus. Software prediction (SUBA3) indicates a high probability LUCKY1 is localized on the plasma membrane, which is consistent with our observation that LUCKY1 interacts with BIK1 *in vivo* (Fig 3.1). It is still difficult to assess the function of the N-terminus as well as the transmembrane domain due to the lack of a *lucky1* knock-out mutant, but future functional analysis will be important with a generated CRISPR-CAS9 *lucky1* mutant.

When full length HA-tagged LUCKY1 was expressed in protoplasts (Fig 3.1C), we observed a major polypeptide band matching the calculated molecular weight of LUCKY1-HA (20kDa) and several less intense upper bands. These polypeptides are likely post-translationally modified LUCKY1 through phosphorylation and/or ubiquitination. Consistent with this hypothesis, LUCKY1 was phosphorylated by BIK1 *in vitro* (Fig 3.2). While the impact of BIK1 phosphorylation on LUCKY1 remains unclear, we speculate this phosphorylation might be involved in LUCKY1 stability control as LUCKY1 protein level is reduced upon flg22 treatment when co-expressing BIK1 (Fig 3.1C).

In vitro and *in vivo* ubiquitination together indicated that LUCKY1 is likely the cognate E3 ligase mediating BIK1 monoubiquitination (Fig 3.3). We used an amiRNA approach to test the *in vivo* BIK1 ubiquitination by overexpressing the amiRNAs to silence LUCKY1 and its closest homolog LUCKY2 in protoplasts and found that BIK1 monoubiquitination was diminished. *In vivo* BIK1 monoubiquitination assay in stable transgenic plants expressing the amiRNA to silence LUCKYs will provide more solid genetic evidence and we are currently generating the transgenic plants. If BIK1 monoubiquitination is abrogated in LUCKY-silencing plants, we can conclude LUCKYs are the cognate E3 ligases.

The WB pattern of BIK1 monoubiquitination upon flg22 *in vivo* (Fig 2.2B, C) is consistent with BIK1 modified by a single ubiquitin. Meanwhile in the *in vitro* BIK1 ubiquitination assay (Fig 3.3A), we observe at least three bands with similar intensity suggesting one, two and three ubiquitin attached covalently. Comparing the *in vitro*

ubiquitination result with WT ubiquitin and ubiquitin^{noK}, we concluded BIK1 was multimonoubiquitinated by LUCKY1 *in vitro*. Based on those seemingly inconsistent *in vivo* and *in vitro* ubiquitination data, we hypothesize that multiple potential monoubiquitination sites exist on BIK1 and alternative sites could be ubiquitinated when the preferred site(s) is inaccessible. In the protoplasts, the most preferred site is available on WT BIK1, so flg22-triggered monoubiquitination on this site and monoubiquitinated BIK1 may no longer be accessible to LUCKY1 considering potential interaction dynamic or localization change. In the *in vitro* reaction, monoubiquitinated BIK1 still kept contacting with LUCKY1, therefore alternative sites were ubiquitinated with time. Consistent with this hypothesis, single K-to-R mutation from the putative 9 lysine residues failed to block BIK1 monoubiquitination because alternative sites are accessible for ubiquitination (Fig 2.6). Therefore, higher order mutants blocking all the alternative lysine residues are expected to completely disrupt BIK1 monoubiquitination *in vivo*.

Mass spectrometry analysis of *in vitro* ubiquitinated BIK1 sample together with a detailed mutagenesis study allowed us to locate most if not all the putative ubiquitination sites (Fig 3.5). When all nine candidate ubiquitination sites were mutated simultaneously, monoubiquitination of BIK1 dramatically reduced while BIK1 kinase activity and flg22-triggered phosphorylation remained unaffected. More significantly, BIK1^{9KR} had normal kinase activity yet failed to possess similar function as WT BIK1 in regulating ROS production and plant disease resistance (Fig 3.6, 3.7). This supports the assertion that monoubiquitination positively regulates BIK1 involvement in plant innate immunity. Moreover, we found BIK1^{9KR} exhibited much stronger interaction with FLS2 and flg22-

triggered FLS2-BIK1^{9KR} dissociation is largely abolished compared to FLS2-BIK1 (Fig 3.8). This observation suggests monoubiquitination of BIK1 is required for FLS2-BIK1 dissociation and is also consistent with a previous report that monoubiquitination could disrupt protein-protein interaction (Hanson et al., 2012b). Our study is the first study in plants demonstrating that monoubiquitination directly regulates protein interaction dynamics.

Monoubiquitination is known to direct membrane protein trafficking and the receptor FLS2, which interacts with BIK1, undergoes rapid endocytosis upon flg22 perception (Robatzek et al., 2006). Whether flg22 triggers BIK1 endocytosis and if monoubiquitination plays a role in this process remain unknown. It is possible that upon dissociation with FLS2, BIK1 remains on the plasma membrane and this localization needs monoubiquitination. Confocal microscopy analysis with double transgenic plant expressing different fluorescent protein tagged FLS2 and BIK1 could potentially provide more detailed insight of the membrane PRR and interacting RLCK localization and interaction dynamics. Together, our study identified a novel RING type E3 ligase regulating BIK1 monoubiquitination and this post-translational modification of BIK1 mediates dissociation with FLS2 to positively regulate plant innate immunity.

CHAPTER IV

DIFFERENTIAL PHOSPHORYLATION OF DIACYLGLYCEROL KINASE DGK5 REGULATES PLANT INNATE IMMUNITY AND CONCLUSIONS

4.1 Introduction

As in mammals, plants largely rely on innate immunity to mount the immediate counter-pathogen defenses. The first line of plant immune responses is initiated upon the detection of non-self molecular signatures, namely microbe- or pathogen-associated molecular patterns (MAMPs or DAMPs) such as bacterial flagellin, lipopolysaccharide (LPS), elongation factor Tu (EF-Tu), or fungal chitin by plasma membrane localized pattern recognition receptors (PRRs) (Ausubel, 2005; Boller and Felix, 2009). Direct recognition of a ligand by a cognate PRR leads to rapid signal transduction, triggering production of anti-microbial molecules such as reactive oxygen species (ROS), reprogramming of transcription-translation, shaping hormone equilibrium, and cell wall re-composition (Xu et al., 2017; Yu et al., 2017).

Bacterial flagellin is recognized by two leucine-rich repeat receptor-like kinases (LRR-RLKs): receptor flagellin-sensing 2 (FLS2) and co-receptor brassinosteroid insensitive 1 (BRI1)-associated kinase 1 (BAK1) (Chinchilla et al., 2007a; Felix et al., 1999; Gomez-Gomez and Boller, 2000; Heese et al., 2007a). Binding of flagellin or the conserved 22-amino-acid of the N-terminus (flg22) by FLS2 triggers instant heterodimerization with BAK1 following rapid transphosphorylation of FLS2/BAK1

and a cytoplasmic kinase Botrytis-induced kinase 1 (BIK1) in the complex (Chinchilla et al., 2007a; Lu et al., 2010a; Zhang et al., 2010). As a group of receptor-like cytoplasmic kinases (RLCKs), BIK1 family proteins are emerging as a signaling hub immediately downstream of multiple PRR complexes including FLS2, EFR, chitin receptor CERK1 (OsCERK1 in rice), and damage-associated molecular pattern peptide Pep1 receptor PEPR1 (Liu et al., 2013; Lu et al., 2010a; Zhang et al., 2010). Phosphorylation-activated BIK1 can directly phosphorylate NADPH oxidase RBOHD to promote ROS production; however, how BIK1 family protein regulating other downstream signaling pathways remains largely unknown (Kadota et al., 2014b; Li et al., 2014f).

As a conserved signaling module consisting of three sequentially activated kinases, mitogen-activated protein kinase (MAPK) cascades play important roles in innate immunity and are activated by multiple PRR signals (Meng and Zhang, 2013a). It comprises of at least two MAPK cascades downstream of FLS2 signaling: MEKK1/MEKK-MKK4/MKK5-MPK3/MPK6 which positively regulate immune responses and MEKK1-MKK1/MKK2-MPK4 which play a negative role. Activated MPKs exert their function via phosphorylation of substrate proteins including transcription factors/transcription repressors, protein kinases, or hormone biosynthesis enzymes (Yu et al., 2017).

Lipid signaling plays critical roles in diverse biological responses. For example, in mammals, G-protein coupled receptor (GPCR) activation leads to hydrolysis of phosphatidylinositol 4,5-bisphosphate (PIP2) by phospholipase C to produce inositol 1,4,5-trisphosphate (IP3) and diacylglycerol (DAG). IP3 molecule regulates Ca^{2+} release

from the ER into cytoplasm while DAG in the plasma membrane recruits and activates critical protein kinase C (PKC) family proteins. Many components in lipid signaling including PIP2, DAG, IP3 are evolutionally conserved from human to plants, however plants heavily rely on the phosphorylated derivative of DAG – phosphatidic acid (PA) – instead of DAG to monitor complex physiology (Munnik and Testerink, 2009). This is likely due to the high abundance of DAG as well as the absence of PKC in plants.

Increasing studies reveal the importance of PA function in plant response to environmental cues. The level of PA is influenced by abiotic stresses including cold, osmotic stress, wounding as well as biotic stresses (Testerink and Munnik, 2011). More specifically, PAMPs such as flagellin, xylanase, and chitosan have been reported to boost plant cellular PA content while PA has also been proposed to be involved in hypersensitive response (HR) (den Hartog et al., 2003; van der Luit et al., 2000). Different stimuli induce PA production through two distinct biochemical pathways. One is the PLC-diacylglycerol kinase (DGK) pathway: DGK phosphorylates PLC-generated DAG to form PA and it is believed to be responsible for PAMP-elicited and Avr4-induced PA spikes (de Jong et al., 2004; van der Luit et al., 2000). Another is the phospholipase D (PLD) pathway: PLD hydrolyses phosphatidylcholine (PC) and phosphatidylethanolamine (PE) into PA and likely this contributes to wound-triggered PA as well as effector-triggered PA in HR (Andersson et al., 2006; Wang et al., 2000).

How PA exerts its function in the plant biotic stress response is still largely unknown. Interestingly, incubation of plant leaves in PA solution directly induces plant defense gene expression and causes HR (Andersson et al., 2006). Although the

underlying mechanism remains elusive, a few PA targets have been reported including PDK1 (3-phosphinositide-dependent protein kinase 1), RbohD (respiratory burst oxidase homolog D), CTR1 (constitutive triple response 1) and MPK6. PA was found to directly bind to the PDK1 PH domain and exogenous application of PA promotes PDK1 kinase activity (Anthony et al., 2004). Direct binding of PA to four arginines of RbohD stimulates the function of this NADPH oxidase (Zhang et al., 2009). CTR1 binds PA at its kinase domain and this binding inhibits CTR1 kinase activity *in vitro* (Testerink et al., 2007). PA can also directly bind to MPK6 and blocking the PLD-generated PA leads to reduced MPK6 kinase activity (Yu et al., 2010).

It has been known that PA functions in plant defense, how PA is produced in this circumstance and how PA generated through the PLC-DGK pathway affects plant innate immunity are still largely unknown. One genetic study has shown that over-expression of rice OsBIDK1 (a DGK) in tobacco confers resistance to tobacco mosaic virus and *Phytophthora parasiticai* (Zhang et al., 2008). However, how PAMP treatment leads to accumulation of PA is unknown. Our work first reports that AtDGK5 interacts with a key PTI signaling transducer BIK1. PAMPs induce phosphorylation of DGK5 at Ser-506 by BIK1. We further found that MPK4 can phosphorylate DGK5 at Thr-446. More importantly, phosphorylation of DGK5 at Ser-506 by BIK1 enhances DGK5 activity, therefore promoting PA production and positively regulating plant immunity. Conversely, Thr-446 phosphorylation by MPK4 suppresses DGK5 activity and negatively regulates immune responses. Our study reveals a direct link between PRR-

activated protein kinases and PA signaling and provides novel insight of the activation of signal messengers in plant innate immunity.

4.2 Materials and methods

4.2.1 Plant material and growth conditions

Arabidopsis thaliana accessions Col-0, *Ler* and mutants *fls2* (SALK_141277), *bak1-4* (SALK_116202), *bik1* were described before. The *dgk5-1(*SAIL-1212-E10*)*, *dgk5-2* (SAIL_127_B03, in Col-3 background), *mpk4* (CS5205, in *Ler* background) were obtained from the ABRC. The *mpk6/MPK3RNAi* was described previously (Li et al., 2015). *pDGK5::DGK5-HA, pDGK5::DGK5T446A-HA, pDGK5::DGK5S506A-HA* transgenic plants in the *dgk5-1* background were generated in this study (see below for details). All arabidopsis plants were grown in soil (Metro Mix 366) in a growth chamber at 20-23°C, 60% relative humidity and 75 μE $m^{-2}s^{-1}$ light with a 12 hr light/12 hr dark photoperiod for four weeks before pathogen infection assay, protoplast isolation and ROS assay. For MAPK assay and CoIP assay for transgenic plants, 10-14-days-old seedlings were germinated on ½ MS plate containing 1% sucrose and 0.5% agar under similar growth condition as described above. Seedlings were transferred to water for overnight and treated as described in the figure.

4.2.2 Plasmid construction and generation of transgenic plants

The HA or FLAG epitope-tagged BIK1, FLS2, MPK3, MPK4, MPK6 and BIK1-km (kinase mutant) constructs used for protoplast assays were described previously (Li et al., 2015; Lu et al., 2010a). The *DGK5* gene was PCR amplified from Col-0 cDNA with primers containing BamHI at 5' end and StuI at 3' end and introduced into a plant expression vector pHBT with encoding an HA or FLAG epitope-tag at the C-terminus. Two variants of clones with different molecular weights of DGK5 were obtained during the cloning. The clone with sequence matching DGK5β was used as DGK5β. The clone with sequence matching DGK5α contains one extra intron bearing an early stop codon. It was further subjected to site-directed mutagenesis with primers listed in the supplemental table to get rid of the stop codon and extra un-translating sequences including part of the extra intron and last exon. The clone with sequence matching DGK5α CDS was used as DGK5α. Truncations of DGK5 were PCR amplified with primers containing BamHI or StuI sites similar as above mentioned. The promoter of *DGK5* was PCR amplified from genomic DNA of Col-0 with primers containing SacI and BamHI. The promoter was then introduced to pHBT vector and then pDGK5::DGK5-HA was digested and ligated into pCAMBIA1300 vector. DGK5 point mutations were generated by site-directed mutagenesis with primers listed in the Supplemental Table 1 using the pHBT-DGK5-HA or pHBT-DGK5-FLAG construct as the template. DGK5β, DGK5^{T446A} and DGK5^{S506A} were further sub-cloned into the binary vector *pCAMBIA1300-pDGK5::DGK5-HA* and the modified GST (pGEX4T-1, Pharmacia) vector with BamHI and StuI digestion to generate WT and mutant version of

pCAMBIA1300-pDGK5::DGK5-HA and *pGST-DGK5* respectively. *Agrobacterium tumefaciens*-mediated floral dip was used to transform WT and mutant version of *pCAMBIA1300-pDGK5::DGK5-HA* into the *dgk5-1* plants. The transgenic plants were selected by hygromycin. Multiple transgenic lines were analyzed with Western blot (WB) for protein expression. Two lines with 3:1 segregation ratio for Basta resistance in T3 generation were selected to obtain homozygous seeds for further studies.

4.2.3 Pathogen infection assays

Pseudomonas syringae pv. *tomato* (*Pst*) DC3000 was cultured for overnight at 28°C in King's B medium supplemented with rifamycin (50 μg/ml). Bacteria were collected by centrifugation at 3500 rpm, washed and re-suspended to the density of 5 x 10^5 cfu/ml with 10 mM $MgCl_2$. Leaves from four-week-old plants were hand-inoculated with bacterial suspension using a needleless syringe. For flg22-mediated protection assays, leaves were pre-inoculated with 100 nM flg22 or H_2O as control and 24 hr later bacteria suspensions were infiltrated into the same leaves. To measure *in planta* bacterial growth, three sets of two leaf discs were punched and ground in 100 μl of ddH_2O. Serial dilutions were plated on TSA plates (1% tryptone, 1% sucrose, 0.1% glutamatic acid and 1.8% agar) containing 25 μg/ml rifamycin. Plates were incubated at 28°C and bacterial colony forming units (cfu) were counted 2 days after incubation.

4.2.4 Protoplast transient expression assay and co-immunoprecipitation (co-IP) assay

Protoplast isolation and transient expression assay have been described previously (He et al., 2007). For protoplast-based co-IP assay, protoplasts were transfected with a pair of constructs (empty vector as control, 100 μg DNA for 500 μl protoplasts at the density of 2 x 10^5/ml for each sample) and incubated at room temperature for 10 hr. After treatment of flg22 with indicated concentration and time points, protoplasts were collected by centrifugation and lysed in 300 μl co-IP buffer (150 mM NaCl, 50 mM Tris-HCl, pH7.5, 5 mM EDTA, 0.5% Triton, 1 × protease inhibitor cocktail, before use, adding 2.5 μl 0.4 M DTT, 2 μl 1M NaF and 2 μl 1M Na_3VO_3 for 1 ml IP buffer) by vortexing. After centrifugation at 10,000×g for 10 min at 4°C, 30 μl of supernatant was collected for input control and 7 μl α-FLAG-agarose beads were added into the remaining supernatant and incubated at 4 °C for 1.5 hr. Beads were collected and washed three times with washing buffer (150 mM NaCl, 50 mM Tris-HCl, pH7.5, 5 mM EDTA, 0.5%Triton) and once with 50 mM Tris-HCl, pH7.5. Immunoprecipitates were analyzed by WB with indicated antibodies.

4.2.5 MAPK assay

Ten days old seedlings grown vertically on 1/2MS plates were transferred into water for overnight before 100 nM flg22 treatment. Seedlings after treatment were frozen in liquid nitrogen and ground in 100 ul IP buffer. Protein samples with 1 X SDS

buffer were separated in 10% SDS-PAGE gel to detect pMPK3, pMPK6 and pMPK4 by WB with α-pERK1/2 antibody (Cell Signaling, #9101).

4.2.6 Detection of ROS production

Leaves from 4 to 5-week-old soil-grown arabidopsis plants were punched into leaf discs with the diameter of 5 mm. Leaf discs were incubated in 100 µl ddH_2O overnight with gentle shaking to eliminate the wounding effect. Then, water was replaced with 100 µl reaction solution containing 50 µM luminol, 10 µg/ml horseradish peroxidase (Sigma-Aldrich) supplemented with or without 100 nM flg22. Luminescence was measured with a luminometer (Perkin Elmer, 2030 Multilabel Reader, Victor X3) with a setting of 1 min as the interval for a period of 40 min. Detected values of ROS production were indicated as means of Relative Light Units (RLU).

4.2.7 Recombinant protein isolation and *in vitro* kinase assays

Fusion proteins were produced from *E. coli* BL21 strain at 16°C using LB medium with 0.25 mM isopropyl β-D-1-thiogalactopyranoside (IPTG). Glutathione S-transferase (GST) fusion proteins were purified with Pierce glutathione agarose (Thermo Scientific), and maltose binding protein (MBP) fusion proteins were purified using amylose resin (New England Biolabs) according to the standard protocol from companies. The *in vitro* kinase assays were performed with 0.5 µg of kinase proteins and 5 µg of substrate proteins in 30 µl kinase reaction buffer (10 mM Tris-HCl, pH7.5, 5 mM $MgCl_2$, 2.5 mM EDTA, 50 mM NaCl, 0.5 mM DTT, 50 µM ATP and 1 µCi [γ -

^{32}P]ATP). After gentle shaking at room temperature for 2 hr, samples were denatured with 4 x SDS loading buffer and separated by 10% SDS-PAGE gel. Phosphorylation was analyzed by autoradiography.

4.2.8 Yeast two-hybrid screen

The cDNA library constructed in a modified pGADT7 vector (Clontech) was described before (Lu et al., 2011b). The BIK-G2A was cloned into a DNA-binding domain fusion vector pBridge (Clontech) and transformed into yeast first. The cDNA library was then transformed into the yeast containing pBridge-BIK1-G2A and transformants were screened in the synthetic defined media (SD) without Trp, Leu, His, Ade (SD-T-L-H-A) and SD-T-L-H + 1 mM 3-Amino-1,2,4-triazole (3AT). No colonies grew in the medium SD-T-L-H-A and the biggest colonies in SD-T-L-H+3AT were further confirmed in SD-T-L-H+3AT medium and subjected to plasmid isolation and sequencing.

4.2.9 *In vitro* GST pull-down assay

MBP fusion protein isolation was described in previous chapters. For GST-agarose beads, GST-DGK5 or GST protein isolation was performed as described before and the agarose beads were obtained after elution and washed with PBS for three times. MBP-BIK1 or MBP protein (2 μg) were pre-incubated with 10ul prewashed glutathione agarose in 300ul pull-down incubation buffer (20 mM Tris-HCl, pH 7.5, 100 mM NaCl, 0.1mM EDTA, and 0.2% Triton X-100) for 30 min at 4°C. 5ul GST or GST-BIK1

agarose beads were pre-incubated with 20 μg BSA in 300ul incubation buffer for 30 min at 4 °C. Then the supernatant containing MBP-BIK1/MBP was mixed with the pre-incubated GST/GST-DGK5 agarose beads for 1hr at 4°C. The agarose beads were precipitated and washed three times in pull-down washing buffer (20 mM Tris-HCl, pH 7.5, 300 mM NaCl, 0.1 mM EDTA, and 0.5% Triton X-100). The pull-down proteins were analyzed by WB with an α-HA antibody.

4.2.10 Mass spectrometry analysis of phosphorylation sites

FLAG-tagged DGK5 was expressed in Co-0 protoplasts for 12 h and treated with or without flg22 for 10 min. Protoplasts were then lysed with lysis buffer (20 mM Tris-HCl, pH 7.5,100 mM NaCl, 10% glycerol, 1% Triton X-100, and protease inhibitor cocktail) and immunoprecipitated with α-FLAG-Agarose (Sigma-Aldrich). The IP product was analyzed in 10% SDS-PAGE gel followed silver staining. The band of DGK5 was sliced, trypsin digested and phospho-peptides were enriched before LC-MS/MS analysis using a LTQ Orbitrap XL LC-MS/MS system (Thermo Scientific) as previously described (Gao et al., 2013). The MS spectra were analyzed with Mascot (Matrix Science; version 2.2.2).

4.2.11 *In vitro* DGK activity assay

In vitro DGK5 activity assay was performed based on the protocol described previously but with some modifications (Munnik and Zarza, 2013). Briefly, reaction was initiated by adding 2μg of purified protein (GST-DGK5 or GST-mutant) in a 200-μL

total reaction volume containing 10mM $MgCl_2$, 1mM EGTA, 1mM DTT, 50mM Tris-HCl (pH 7.4), 0.1% Triton X-100, 500µM 1-2-dioleoyl-*sn*-glycerol and 500µM [γ-^{32}P]-ATP (5 µCi; specific activity= 0.05 Ci/mmol). The specific activity of hot ATP was adjusted by adding cold ATP substrate. The assay was incubated for 30 min at 30°C followed by termination of reaction by addition of 750µL of chloroform:methanol(1:2) and 200µL 0.9% NaCl. Reaction products were extracted by vortexing and then centrifuged at 10,000 x *g* for 2 min to separate the two phases. The lower organic phase was transferred to a new tube containing 750µL of chloroform: methanol:1M HCl (3:48:47), vortexed vigorously and centrifuged at 10,000 x *g* for 2 min. The lower organic phase containing the reaction products was transferred into a new tube, solvent dried using speed vacuum and resuspended with chloroform in a final volume of 30 µL. The reaction products were then analyzed using activated Silica Gel 60 TLC plate, developed using chloroform: methanol: 25% NH_4OH:H_2O (90:70:4:16) as the mobile phase, and the plates visualized using iodine vapor. The iodine spot corresponding to authentic standard of phosphatidic acid was scrapped and the γ-^{32}P incorporation into phospatidic acid was determined by using liquid scintillation counter.

4.3 Results

4.3.1 Identification of DGK5 as a novel BIK1 interacting protein

In order to gain insight of PAMP-triggered immune signaling network immediately downstream of PRR complex activation, we carried out a Yeast-two-hybrid

(Y2H) screen to identify BIK1 interacting proteins. Considering the putative myristoylation (site Glysine-2) may perturb BIK1 localization in yeast nucleus, we used BIK1-G2A which theoretically abolished myristoylation as the bait for the screen. Clones from 196 of strong interacting colonies out of around 120,000 transformants were sequenced and 84 of them align to 35 genes which are in-frame and unique in BIK1 screen (Supplemental Table 2). Among them, 14 clones aligned to AtDGK5 (Fig 4.1A, DGK5-T1/Y2H).

There are seven DGKs belonging to three clusters in *Arabidopsis thaliana* genome. Cluster I members DGK1 and DGK2 are structurally similar to mammalian DGKε and consists of catalytic DGK kinase domain and two DAG binding C1-type domain (Cysteine rich) (Arisz et al., 2009). Distinct from DGK1/2, all other five DGKs from cluster II and III only possess DGK kinase domain while the C1-type domain is absent. Two splicing variant of DGK5 exist in arabidopsis: DGK5β contains an extra C-terminal domain (CTD) making it 509 amino acids; DGK5α doesn't splice out the last intron and stops early at 491 amino acids (Fig 4.1A). DGK5-Y2H matches amino acids 317-509 from DGK5β C-terminus. We first tested BIK1-G2A interaction with DGK5β and DGK5α in yeast. DGK5β weakly interacts with BIK1, while almost no interaction was observed for DGK5α (Fig 4.1B). It appears the CTD is required for BIK1-DGK5 interaction as DGK5-T2 which truncated CTD lost the ability to interact with BIK1. In line with this observation, *in vitro* GST pull-down assay showed recombinant GST-DGK5β directly pulled down MBP-BIK1 while GST-DGK5α only weakly interacted with MBP-BIK1 (Fig 4.1C). To confirm BIK1-DGK5 interaction in plant, we performed

Figure 4.1 BIK1 interacts with a positive defense regulator DGK5. A. Domain organization of DGK5β, DGK5α and truncations. DGKc: Diacylglycerol kinase (DGK) catalytic domain; DGKa: DGK accessory domain; CTD: carboxy terminal domain. The number above each domain indicates position of amino acid in the protein. **B.** BIK1 interacts with DGK5 in yeast two-hybrid assay. DGK5β, DGK5α, DGK5 T1, T2, T3 (truncations as shown in A.) interactions with BIK1 were tested in yeast. Control plates (SD-L-T, Left panel) contain histidine and test plates (SD-L-T-H, Right panel) contain 1mM 3-aminotrizole (3-AT) without histidine. 10 fold serial dilutions of cells are shown. **C**. BIK1 interacts with DGK5 with in vitro pull-down assay. GST, GST-DGK5β or GST-DGK5α immobilized on glutathione sepharose beads was incubated with MBP or MBP-BIK1 proteins. Washed beads were subjected to Western blotting (WB) with an α-HA antibody. Input proteins were shown by Coomassie bright blue staining (CBB). **D**. BIK1 interacts with DGK5 in co-immunoprecipitation (Co-IP) assay. Protoplasts were co-expressed with BIK1-FLAG and DGK5-HA or a control vector. The Co-IP assay was carried out with α-FLAG-Agarose and interacting proteins were analyzed by WB with α-HA antibody. **E**. BIK1 associates with DGK5 in transgenic plants. Total proteins from plant leaves carrying *35S::BIK1-GFP/pDGK5::DGK5-HA* or *pDGK5::DGK5-HA* alone were immunoprecipitated with an α-GFP antibody and analyzed by WB with α-HA. The expression of BIK1-GFP and DGK5-HA are shown in the bottom panels. **F**. DGK5 is required for disease resistance to *Pst* DC3000*ΔAvrPto/AvrPtoB* infection. Four-week-old plants were hand-inoculated with *Pst* DC3000*ΔAvrPto/AvrPtoB* at 5×10^5 cfu/ml. The *in planta* bacterial growth was measured at 0 and 4 days-post inoculation (dpi). The data are shown as means ± standard errors. **G**. DGK5 is required for flg22-triggered ROS production. Leaf discs from WT or *dgk5* were treated with 100 nM flg22, and the ROS production was measured with a plate reader over 40 min (2400 seconds). The data are shown as means ± standard errors from 20 leaf discs for flg22 treatment.
The above experiments were repeated as least two times with similar results.

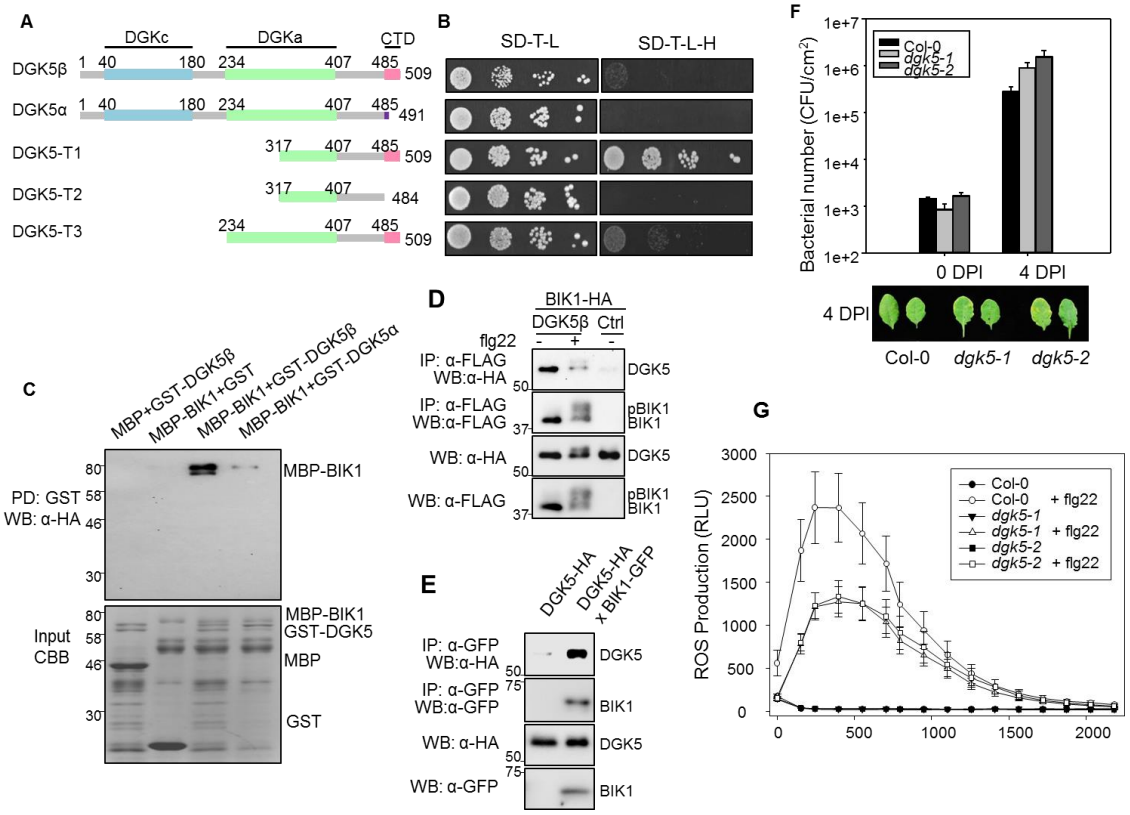

a CoIP assay and found that BIK1 associated with both DGK5β and DGK5α *in vivo* (Fig 4.1D, E). We examined BIK1-DGK5 interactions further using a bimolecular fluorescence complementation (BiFC) assay and it suggests BIK1 interacts strongly with DGK5β and weakly with DGK5α (Fig 4.2B). Taken together, BIK1 interacts with DGK5β and the DGK5β CTD is indispensable for this direct interaction.

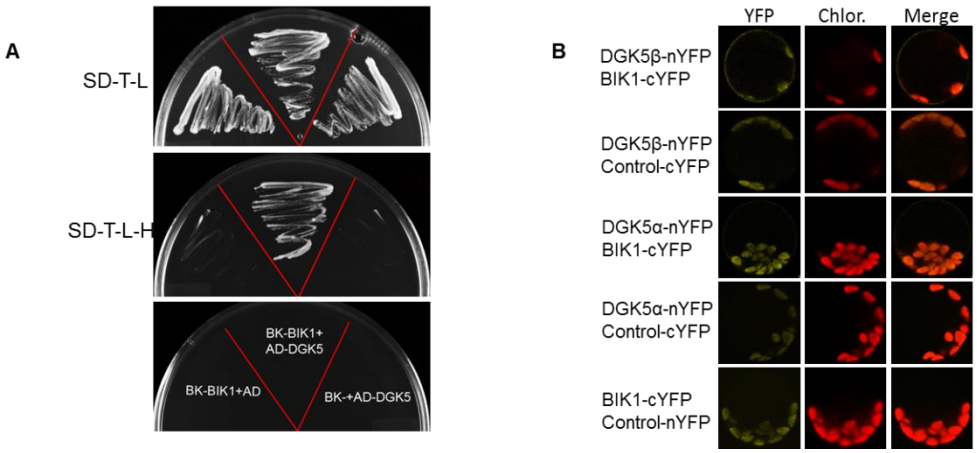

Figure 4.2 BIK1 interacts with DGK5. A. BIK1 interacts with DGK5 in yeast two-hybrid screen. DGK5-Y2H (truncations as shown in 1A.) interaction with BIK1 was tested in yeast. Control plates (SD-L-T, Upper panel) contain histidine and test plates (SD-L-T-H, Middle panel) without histidine. **B.** BIK1 interacts with DGK5 in Bimolecular fluorescence complementation (BiFC) assay. Indicated constructs were co-transformed into arabidopsis protoplasts and cells were examined with confocal microscopy for YFP fluorescence. Clear YFP signal at periphery of the plasma membrane was only observed when DGK5α/β and BIK1 both present.

4.3.2 DGK5 is a positive regulator of plant immunity

To address the involvement of DGK5 in defense against bacterial pathogens, we challenged two T-DNA knock-out lines of DGK5, *dgk5-1* and *dgk5-2*, with *Pseudomonas syringae* pv. *tomato(Pst)* DC3000 and both lines showed increased disease susceptibility (Fig 4.1F). In addition, the *dgk5-1* mutant was also more susceptible to *P. s.* pv. *maculicola* ES4326 (Psm), the less virulent strain *Pst* DC3000 *ΔAvrPto/AvrPtoB*, and the nonpathogenic strain *Pst* DC3000 *hrcC* (Fig 4.3). Next, we determined the requirement for DGK5 in flg22-triggered immunity. When wild type Col-0 was pre-inoculated with 200 nM flg22 for 24 hours before *Pst* infection, bacterial growth in plant

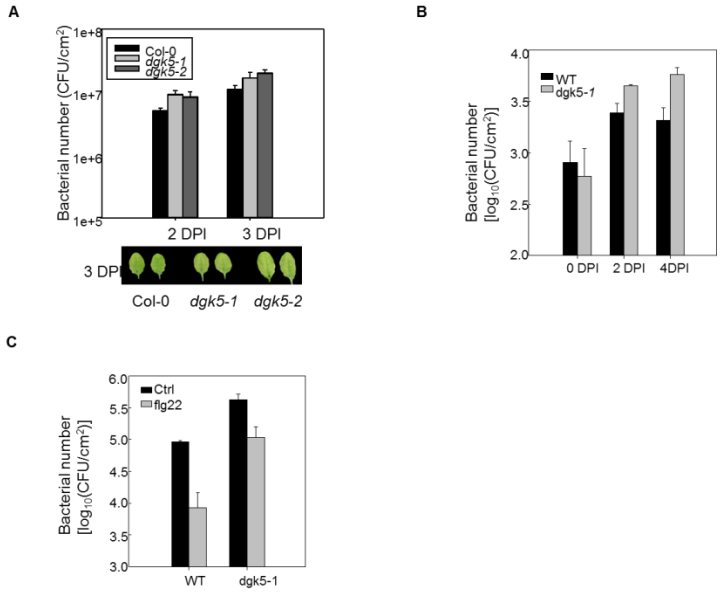

Figure 4.3 DGK5 plays a positive role in defense against bacterial infection. A. DGK5 is required for disease resistance to *Pst* DC3000 infection. Four-week-old plants were hand-inoculated with *Pst* DC3000 at 5×10^5 cfu/ml. The *in planta* bacterial growth was measured at 2 or 3 days-post inoculation (dpi). The data are shown as means ± standard errors. **B.** DGK5 is required for disease resistance to *Pst* DC3000 *hrcC* infection. Four-week-old plants were hand-inoculated with *Pst* DC3000 *hrcC* at 5×10^5 cfu/ml. The *in planta* bacterial growth was measured at 0, 2 and 4 days-post inoculation (dpi). The data are shown as means ± standard errors. **C.** DGK5 is required for flg22-mediated protection against *Pst* DC3000 infection. Four-week-old plants were hand-inoculated with H_2O or 200 nM flg22 24 hours before inoculation of *Pst* DC3000 at 5×10^5 cfu/ml. The *in planta* bacterial growth was measured at 2 days-post inoculation (dpi). The data are shown as means ± standard errors.

decreased for more than ten fold. The *dgk5* mutant is more susceptible to *Pst* infection in the control group and flg22-mediated protection is compromised to only 4 fold (Fig 4.3). These results suggest DGK5 plays a positive role in plant immunity and is involved in FLS2 signaling.

Previous reports have shown PAMPs trigger PA production in plants via PLC/DGK pathway. PA is believed to be a potent secondary messenger in plant signaling, but how DGK-generated PA contributes to plant immunity is still unknown. It has been shown PA can directly bind to RbohD to regulate ROS production in ABA signaling, so we investigated if DGK5 is involved in flg22-triggered ROS production. Two *dgk5* mutants exhibited clearly lower ROS production compared to WT (Fig 4.1G). A previous study also suggested PA could directly bind to MPK6 to regulate its protein kinase activity upon salt stress (Yu et al., 2010). It is well known that FLS2 signaling leads to activation of three major MAP kinases: MPK3, MPK4 and MPK6, so we tested the potential role of DGK5 in flg22-triggered MAPK activation. We first examined phosphorylation of MPK3/4/6 upon flg22 treatment with anti-p44/42 immuno-blotting. However, we did not observe any differences in Col-0 and *dgk5* mutants (Fig 4.4A). We further tested MPK3/4/6 kinase activity towards substrate MBP upon flg22 perception and no obvious differences were detected from WT and *dgk5* (Fig 4.4B-D). In summary, DGK5 positively regulated PTI responses at minimally through promotion of ROS production.

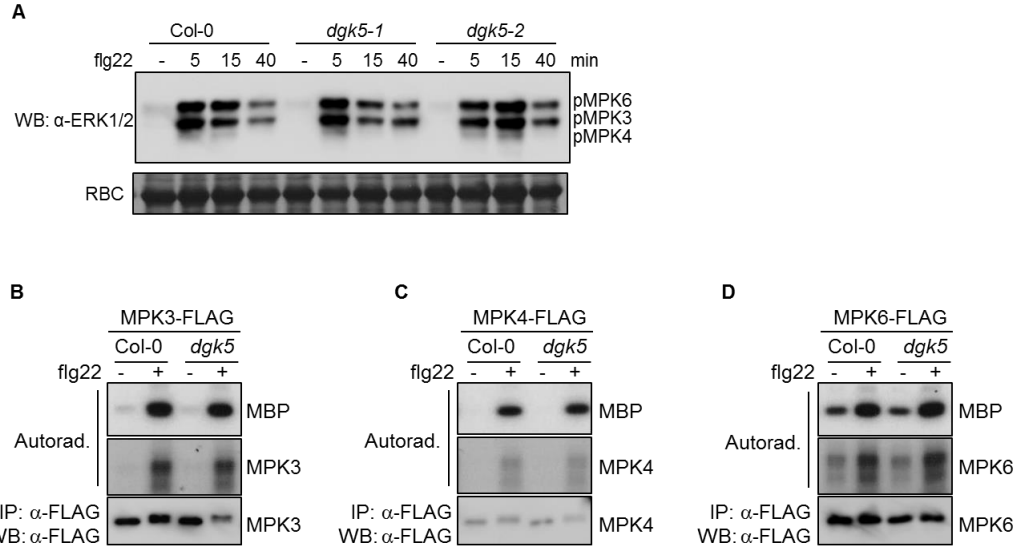

Figure 4.4 Flg22-triggered MAPK activation is not altered in *dgk5*. A. flg22-induced phosphorylation of MPK3/4/6 is not changed in *dgk5*. 10-days-old seedling from wild-type (WT) Col-0 or *dgk5* plants were treated with or without 100 nM flg22 treatment for indicated time points. MAPK activation was analyzed with an α-pERK antibody (top panel), and protein loading was shown by Coomassie Brilliant Blue (CBB) staining for RuBisCO (RBC) (bottom panel). **B**. flg22-activated MPK3/4/6 kinase activity remains similar in *dgk5*. FLAG-tagged MPK3, MPK4 or MPK6 were expressed in protoplast and activated by 10 min flg22 (100nM) treatment. FLAG-tagged MPKs were isolated by IP and washed beads were incubated with MBP protein for 30 minutes in kinase assay buffer. Reactions were stopped by SDS buffer and phosphorylation was detected by autoradiography (top panel). Part of the IP product was subjected to WB with anti-FLAG antibody.

4.3.3 PAMPs induce rapid phosphorylation of DGK5

When carefully analyzing the immuno-blotting pattern of DGK5β-HA in protoplasts (Fig 4.1D), we noticed the flg22 treatment caused a mobility band shift of DGK5. To determine the temporal order of this modification, we performed a time course and found the mobility shift was observable as fast as one minute after flg22 treatment (Fig 4.5A), with a gradual increase to a peak around five-to-ten minutes before completely diminishing by thirty minutes. Considering DGK5 interacts with the protein

kinase BIK1, we speculated this band shift is likely due to phosphorylation. Consistently, treatment of a general kinase inhibitor K252a completely blocked this band shift (Fig 4.5C). In order to obtain better separation and confirm the mobility change was due to phosphorylation, we repeated flg22-triggered DGK5 band shift assay with phos-tag gel which incorporates polyacrylamide-bound di-nuclear Mn^{2+} complex to bind phosphorylated protein to enhance mobility shifts. Surprisingly, when the membrane was exposed for longer time, we observed additional, lower mobility bands (higher bands, DGK5-H) only in the phos-tag gel, suggesting multiple phosphorylation events of DGK5 (Fig 4.5B). To exclude the possibility that K252a blocked phosphorylation in the FLS2-BAK1-BIK1 receptor complex upstream of DGK5 instead of blocking DGK5 phosphorylation, we further treated the flg22-induced cell lysate with Lambda Protein Phosphatase (λ-PP). As a protein phosphatase with activity towards phosphorylated serine, threonine and tyrosine, λ-PP treatment removed the DGK5 band shift indicating that DGK5 was phosphorylated upon PAMP perception (Fig 4.5D). More significantly, the lower mobility bands could also be removed by λ-PP treatment, supporting the idea of multiple phosphorylation events on DGK5. In addition, both phosphorylation bands exhibited similar temporal dynamics and responded to flg22 similarly (Fig 4.5E). Other PAMPs such as elf18, chitin and damage-associated molecular pattern (DAMP) pep1 could trigger DGK5 phosphorylation as well (Fig 4.5F). Taken together, PAMP recognition by PRRs could lead to a few rapid phosphorylation events of DGK5 which is easily visualized by a mobility band shift.

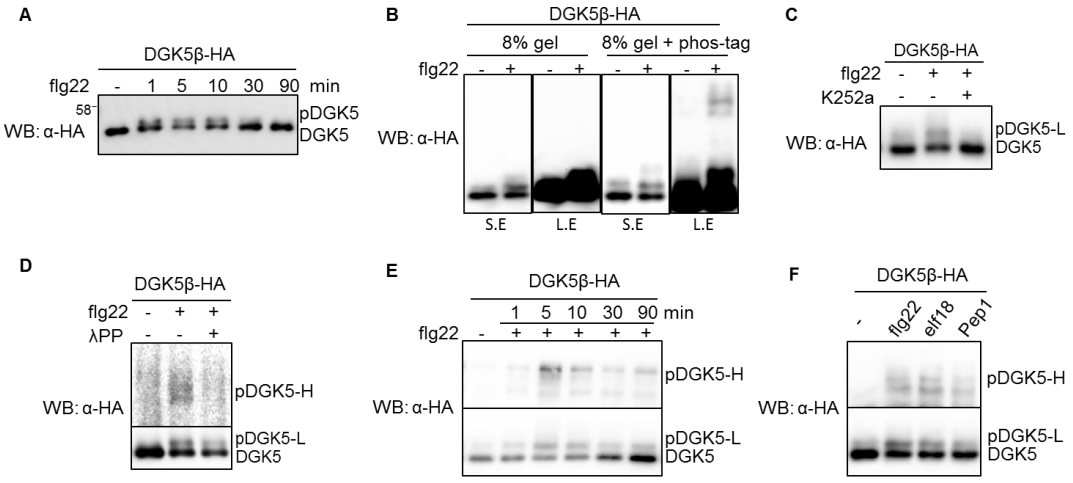

Figure 4.5 Flg22 induces phosphorylation of DGK5. A. flg22 induces a rapid and transit mobility band shift of DGK5β. DGK5β-HA was expressed in arabidopsis protoplasts and flg22 (100 nM) was added at indicated time points (minutes) for treatment. Cell lysate were examined by WB with α-HA antibody. **B**. flg22-triggered DGK5 band shift show multiple bands with phospho-tag gel. Protoplasts expressing DGK5β-HA were treated with flg22 for 10 minutes. Same sample was loaded in regular 8% SDS-PAGE gel or 8% SDS-PAGE gel containing phospho-tag. From left to right: first panel shows short exposure of PVDF membrane from 8% gel, second panel shows longer exposure for the same membrane as first panel, third panel shows short exposure of PVDF membrane from phospho-tag gel and forth panel shows longer exposure for the same membrane as third panel. **C**. General kinase inhibitor K252a blocks DGK5 band shift. DGK5 band shift was tested same as in A. K252a (1 uM) was added 30 minutes before flg22 treatment. **D.** λ phosphatase removes flg22-induced DGK5 band shift. Protoplasts expressing DGK5β-HA were treated with flg22 (100 nM) for 10 minutes. Cells lysate were incubated in buffer containing λ phosphatase and then examined by WB with α-HA antibody in 8% gel containing phospho-tag. Lower panel shows shorter exposure for the lower part of membrane and upper panel shows longer exposure for the upper part of same membrane. **E**. Time course of flg22-triggered DGK5 band shift dissected with phospho-tag gel. DGK5 band shift assay was carried out same as in A but examined with 8% gel containing phospho-tag. Lower panel shows shorter exposure for the lower part of membrane and upper panel shows longer exposure for the upper part of same membrane. **F**. Different PAMPs and DAMP trigger DGK5 band shift with phospho-tag gel. DGK5β-HA was expressed in protoplasts and flg22 (100 nM), elf18 (1 uM), pep1 (100 nM) were added for 10 minutes. Cell lysate were analyzed by WB with α-HA antibody in 8% gel containing phospho-tag. Lower panel shows shorter exposure for the lower part of membrane and upper panel shows longer exposure for the upper part of same membrane.
The above experiments were repeated as least two times with similar results.

4.3.4 BIK1 phosphorylates DGK5 at Ser-506

Direct interaction detected between DGK5-BIK1 and flg22-mediated DGK5 phosphorylation promoted us to test whether BIK1 directly phosphorylates DGK5. When BIK1 or BIK1 kinase mutant were over-expressed together with DGK5, the lower band phosphorylation event remained similar, while co-expressing BIK1 dramatically increased higher band phosphorylation. In contrast, co-expressing BIK1 kinase mutant completely abolished the higher band phosphorylation (Fig 4.6A). This indicates that among the different sets of phosphorylation events of DGK5, BIK1 regulates one of them and possesses the most dramatic mobility shift via phos-tag gel. Consistently, only the higher band DGK5 phosphorylation is reduced in *bik1* while the lower band phosphorylation remains unaltered (Fig 4.6B). To distinguish whether BIK1 directly phosphorylates or functions upstream of DGK5, recombinant proteins were isolated to perform *in vitro* kinase assay. Clearly, BIK1 showed similar level of *in vitro* kinase activity towards DGK5β compared to BAK1K serving as a known BIK1 substrate (Fig 4.6C, lane 1-3). DGK5α could not be phosphorylated by BIK1 *in vitro* (Fig 4.6C, lane 4). The direct phosphorylation of DGK5β requires BIK1 kinase activity as the kinase mutant lost phosphorylation and other kinases such as BAK1 could not phosphorylate DGK5β, supporting the specificity by BIK1 (Fig 4.6C). There are two possibilities to explain the distinct phosphorylation of DGK5β and DGK5α: BIK1 directly phosphorylates DGK5β at the CTD so DGK5α could not be phosphorylated due to lacking the phosphorylation site, or BIK1 does not interact with DGK5α resulting in an

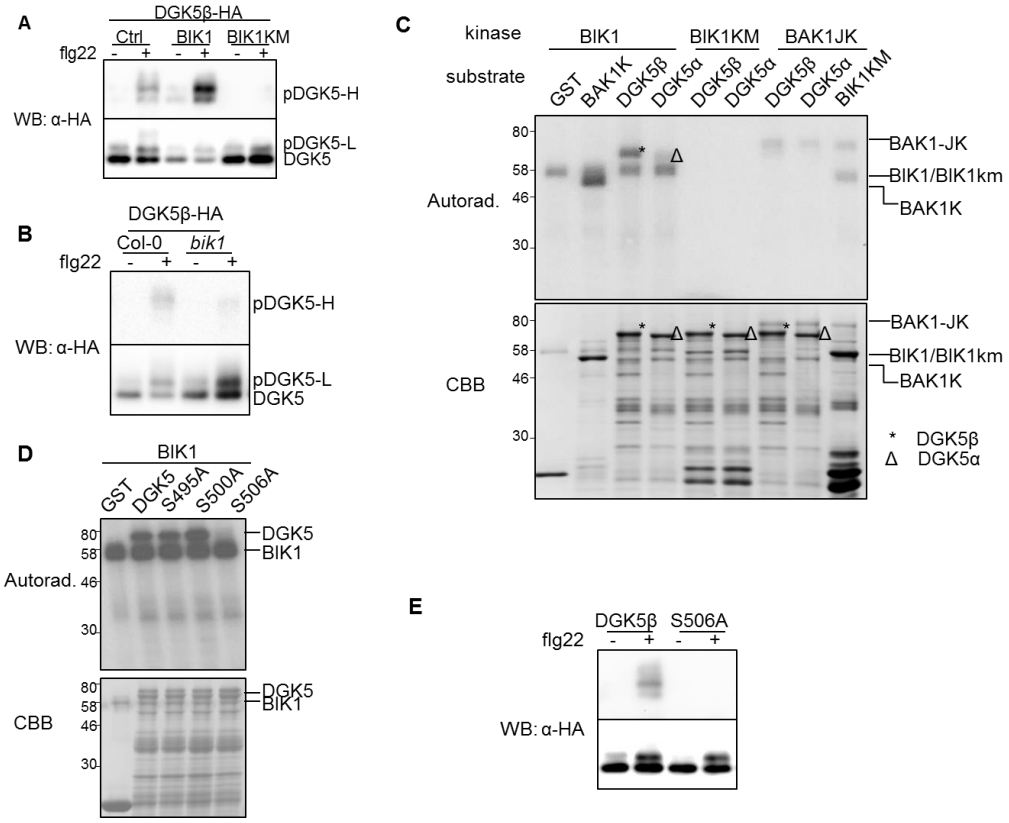

Figure 4.6 BIK1 phosphorylates DGK5 at Ser-506. A. BIK1 phosphorylates DGK5 *in vivo*. DGK5β-HA was co-expressed with control/ BIK1-FLAG/BIK1-km-FLAG in protoplasts and treated with flg22. Cell lysate were analyzed by WB with anti-HA antibody. **B**. flg22-induced DGK5 phosphorylation requires BIK1. Protoplasts were isolated from Col-0 or *bik1* plant, transformed with DGK5β-HA and treated with flg22 for 10 minutes. Cell lysate were examined by anti-HA WB with 8% SDS-PAGE gel containing phospho-tag. Lower panel shows shorter exposure for the lower part of membrane and upper panel shows longer exposure for the upper part of same membrane. **C**. BIK1 directly phosphorylates DGK5 in vitro. In vitro kinase assay was performed by incubating GST-BIK1/GST-BIK1-km/MBP-BAK1-JK fusion protein with GST, GST-DGK5β or GST-DGK5α in kinase buffer. Phosphorylation was detected by autoradiography (top panel). Protein loading control was shown by Coomassie blue staining (bottom panel). **D**. BIK1 phosphorylates DGK5 in vitro at Ser-506. In vitro kinase assay was performed by incubating GST-BIK1 fusion protein with GST, GST-DGK5β or indicated S to A mutants in kinase buffer. Phosphorylation was detected by autoradiography (top panel). Protein loading control was shown by Coomassie blue staining (bottom panel). **E**. Ser-506 is an in vivo phosphorylation site of DGK5. Flg22-mediated WT DGK5β and S506A phosphorylation were tested by anti-HA WB with 8% SDS-PAGE gel containing phospho-tag. Lower panel shows shorter exposure for the lower part of membrane and upper panel shows longer exposure for the upper part of same membrane.

absence of phosphorylation. To determine if the CTD harbors the phosphorylation site(s), we individually mutated all potential Serine/Threonine/Tyrosine phosphorylation sites in the CTD, Ser-495, Ser-500, Ser-506, and performed an *in vitro* phosphorylation assay. Out of all the mutations, S506A alone completely blocked DGK5β phosphorylation by BIK1 suggesting Ser-506 is the major phosphorylation site (Fig 4.6D). Moreover, DGK5-S506A lost the flg22-triggered higher band phosphorylation in protoplasts and transgenic plants supporting the idea that BIK1 phosphorylates DGK5 at Ser-506 (Fig 4.6E).

4.3.5 MPK4 phosphorylates DGK5 at Thr-446

The above data suggest BIK1 is responsible for one set of flg22-mediated DGK5 phosphorylation. It remains unclear what is the other phosphorylation event as shown by the lower band shift. To gain more understanding of DGK5 phosphorylation, we expressed DGK5β tagged with FLAG and immunoprecipitated DGK5 for phosphorylation site identification by mass spectrometry. Several potential phosphorylation sites were identified and four of them were the most abundant: Thr-446, Ser-463, Thr-478 and Ser-488 (Fig 4.7A). We did alanine substitution individually and found T446A alone could disrupt flg22-induced band shift in regular gel (Fig 4.7B). With phos-tag gel, T446A mainly blocked the lower band shift with almost no effect on the higher band shift (Fig 4.7C). It appears that there are at least two phosphorylation events of DGK5β that are activated upon flg22 treatment: Thr-446 and Ser-506, and likely they are independent.

Figure 4.7 MPK4 phosphorylates DGK5 at Thr-446. A. Most abundant DGK5 phosphorylation sites identified by MS. Protoplasts expressing DGK5β-FLAG were treated with flg22 for 10 minutes. Immunoprecipitation was carried out for the cell lysate with anti-FLAG and then analyzed with SDS-PAGE following Commassie blue staining. Target band was subjected to LC-MS/MS to identify phosphorylation site. Ions detected more than 3 times were shown in table. **B**. T446A blocks flg22-triggered DGK5 band shift in vivo. DGK5β-HA or indicated alanine substitution mutants were expressed in protoplasts and treated with flg22 (100 nM) for 10 minutes. Cell lysate were analyzed by WB with α-HA antibody. **C**. flg22 induces two uncoupled phosphorylation events of DGK5 at Ser-506 and Thr-446. DGK5β or indicated mutants were expressed in protoplast and treated with flg22 for 10 minutes. Cell lysate were examined by anti-HA WB with 8% SDS-PAGE gel containing phospho-tag. Lower panel shows shorter exposure for the lower part of membrane and upper panel shows longer exposure for the upper part of same membrane. **D**. flg22-induced DGK5 phosphorylation is reduced in *mpk4*. Protoplasts were isolated from Ler-0 or *mpk4* plant, DGK5β-HA was expressed and detected by anti-HA WB with 8% SDS-PAGE gel containing phospho-tag. Lower panel shows shorter exposure for the lower part of membrane and upper panel shows longer exposure for the upper part of same membrane. **E**. DGK5 interacts with MPK4 in co-immunoprecipitation assay. Protoplasts were co-expressed with DGK5-FLAG and MPK4-HA. The Co-IP assay was carried out with α-FLAG and interacting proteins were detected by WB with α-HA. **F**. MPK4 directly phosphorylates DGK5 at Thr-446. MPK4-FLAG was expressed in protoplasts and activated by 10 minutes flg22 treatment. Cell lysate was subjected to immunoprecipitation with anti-FLAG-Agarose and protein on the agarose beads were incubated with GST-DGK5 in vitro in a kinase reaction buffer containing [γ-^{32}P] ATP. Proteins were separated with SDS-PAGE and analyzed by autoradiography (Autorad.) (top panel). Protein loading control is shown by WB with anti-GST or anti-FLAG (bottom panels).

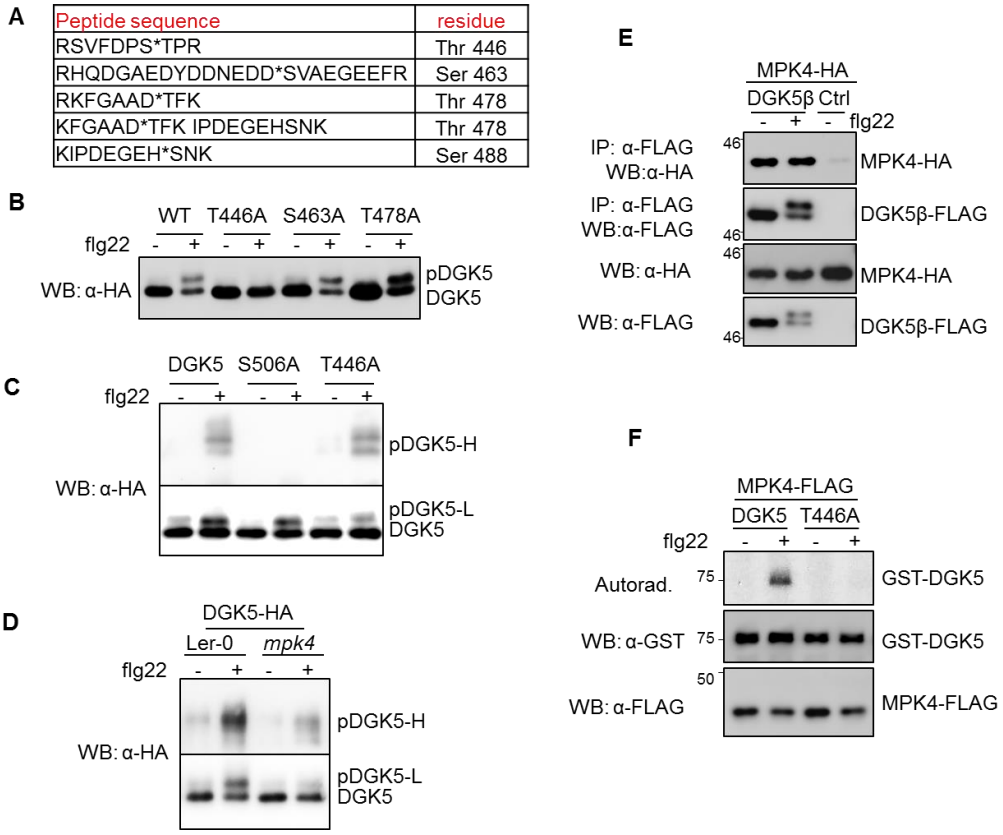

We then investigated which kinase phosphorylates Thr-446. Interestingly when we looked at Thr-446 carefully, the surrounding sequences PST^{446}P matches the consensus extracellular signal-regulated kinase (ERK) type MAPK phosphorylation site PxT/SP. As flg22-activated MAPKs are most similar to ERK type MAPK, we hypothesized that certain MAPK could phosphorylate Thr-446 when triggered by flg22. To demonstrate this possibility, we took two different approaches. The first approach involved co-expressing phosphatase MKP to de-phosphorylate MAPKs. The second approach involved blocking phosphorylation of MAPKs by inhibitor PD184161. Both approaches were able to suppress DGK5 Thr-446 phosphorylation (Fig 4.8A, B).

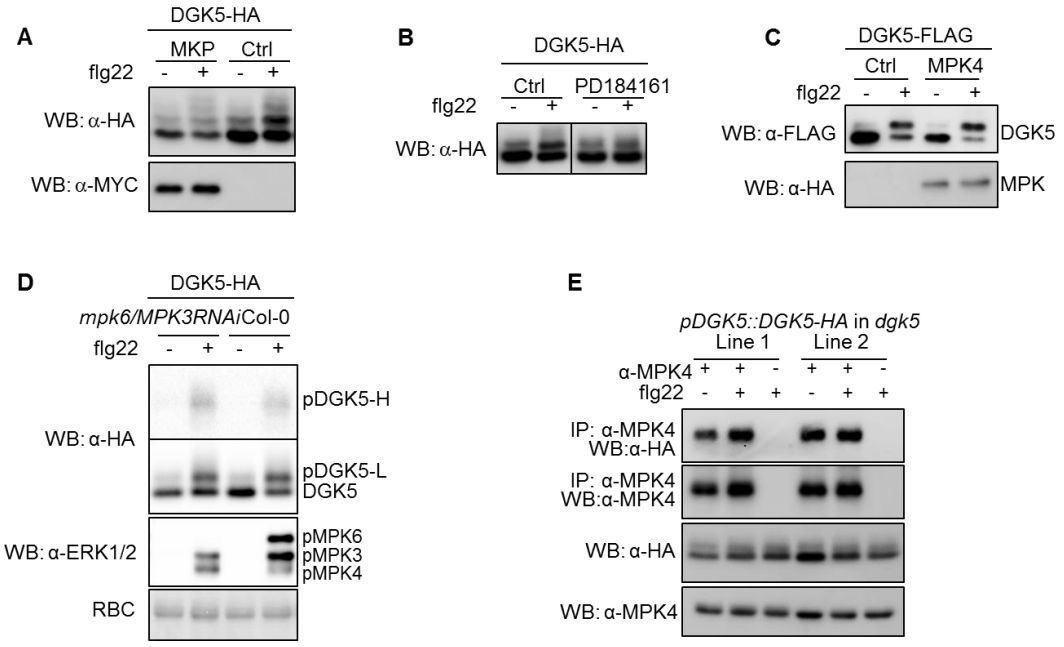

Figure 4.8 MPK4 phosphorylates DGK5 and interacts with DGK5 *in vivo*. A. MKP suppresses DGK5 Thr-446 phosphorylation. DGK5β-HA was co-expressed with control/ MKP-MYC in protoplasts and treated with flg22. Cell lysate were analyzed by WB with anti-HA antibody in phos-tag-containing gel. **B**. MAPK inhibitor PD184161 inhibits DGK5 Thr-446 phosphorylation. DGK5β-HA was expressed in protoplasts and treated with inhibitor PD184161 at 5 uM for 30min before adding 100 nM flg22 for 10 minutes. Cell lysate were analyzed by WB with anti-HA antibody in phos-tag-containing gel. **C**. MPK4 phosphorylates DGK5 *in vivo*. DGK5β-FLAG was co-expressed with control/ MPK4-HA in protoplasts and treated with flg22. Cell lysate were analyzed by WB with anti-HA antibody. **D**. flg22-induced DGK5 phosphorylation remains unchanged in *mpk6/MPK3RNAi*. Protoplasts were isolated from *mpk6/MPK3RNAi* plant or Col-0 pre-sprayed with 10 uM Dex. DGK5β-HA was expressed and detected by anti-HA WB with 8% SDS-PAGE gel containing phospho-tag. Lower panel shows shorter exposure for the lower part of membrane and upper panel shows longer exposure for the upper part of same membrane. **E**. DGK5 interacts with MPK4 in transgenic plants. Total proteins from plant leaves carrying *pDGK5::DGK5-HA* were immunoprecipitated with or without an α-MPK4 antibody and analyzed by WB with α-HA. The expression of MPK4 and DGK5-HA are shown in the bottom panels.

Upon flg22 perception, at least two MAPK cascades are activated including MEKK1-MKK1/2-MPK4 and MEKK?-MKK4/5-MPK3/6. In order to determine if one of the pathways is responsible for Thr-446 phosphorylation, we examined the DGK5

band shift in an *mpk4* knock-out (Fig 4.7D) and *mpk6/MPK3RNAi* mutant plants (Fig 4.8D). DGK5 Thr-446 phosphorylation was almost completely lost in *mpk4* compared to WT control, while remained unaffected in *mpk6/MPK3RNAi* suggesting MPK4 is the major MAPK phosphorylating DGK5. In line with this result, we found DGK5 associated with MPK4 in protoplasts and in transgenic plants expressing DGK5-HA by CoIP assay (Fig 4.7E). More importantly, flg22-activated MPK4 could directly phosphorylate GST-DGK5 at Thr-446 in an *in vitro* kinase assay (Fig 4.7F).

4.3.6 DGK5 is an active diacylglycerol kinase and phosphorylation of DGK5 at Ser-506 and Thr-446 oppositely regulate DGK5 activity

How post-translational modification regulates DGK activity remains largely unknown in plants. Study in human has suggested phosphorylation of DGK could directly regulate DGK activation and function. To understand how two different phosphorylation events of DGK5 by BIK1 and MPK4 regulate its activity, we isolated recombinant GST-DGK5 protein to test its kinase activity against DAG. Indeed, GST-DGK5 is an active kinase catalyzing phosphorylation of DAG to generate PA (Fig. 4.9A). We further tested two phosphomimetic mutant forms of DGK5, $DGK5^{T446D}$ and $DGK5^{S506D}$, for its activity. The S506D substitution clearly enhanced DGK5 kinase activity while the T446D only slightly reduced the activity (Fig 4.9A). This result suggests two phosphorylation events regulate DGK5 activity in an opposing manner with BIK1 phosphorylation promoting activity, while MPK4 phosphorylation suppressing it.

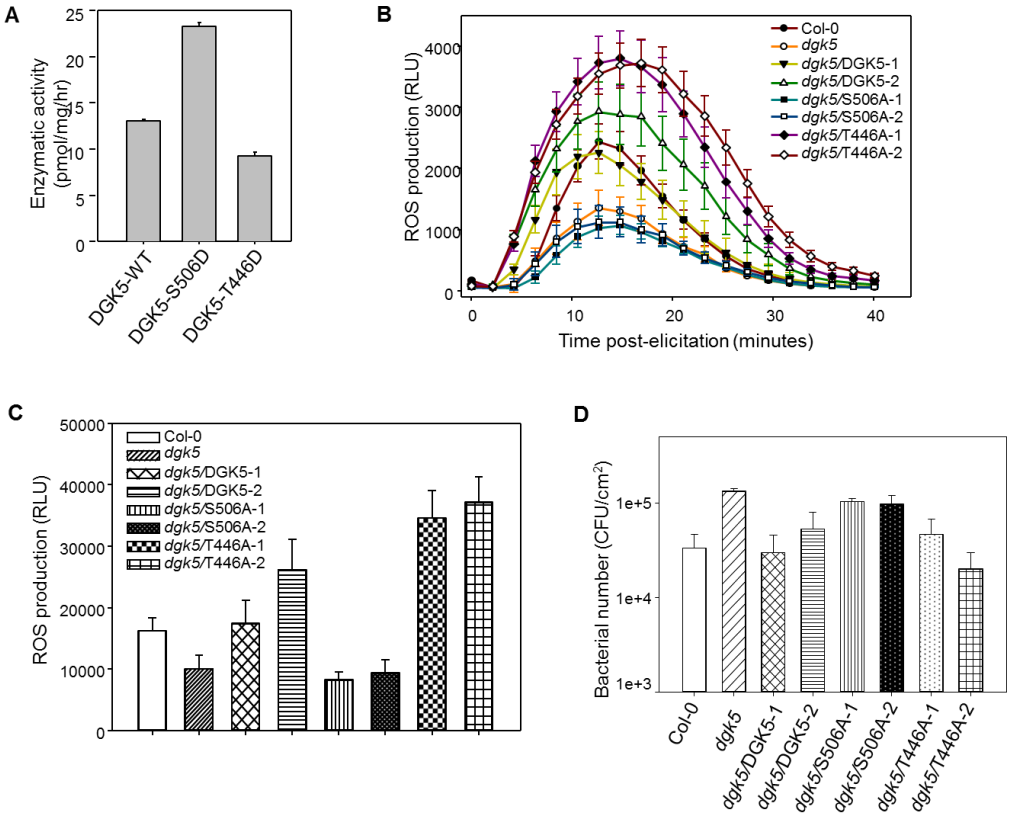

Figure 4.9 Phosphorylation at Ser-506 and Thr-446 oppositely regulates DGK5 function in ROS and immunity. A. Phosphorylation at Ser-506 and Thr-446 oppositely regulate DGK5 kinase activity. In vitro enzymatic activity assay was performed by incubating GST-DGK5 or indicated aspartic acid substitution in DGK reaction buffer containing p32 ATP. Lipids in the reaction were separated on TLC plate and enzymatic activity was shown by converting with quantification of radiolabeled PA. Protein loading control was shown by Coomassie blue staining (bottom panel). **B**. Phosphorylation at Ser-506 and Thr-446 oppositely regulate DGK5 function in flg22-induced ROS production. Leaf discs were treated with 100 nM flg22, and the ROS production was measured with a plate reader over 40 min. Two independent homozygous transgenic lines, 1 & 2, of *pDGK5::DGK5-HA, pDGK5::DGK5*^{T446A}*-HA* and *pDGK5::DGK5*^{S506A}*-HA* in the *dgk5* mutant background are shown here. The data are shown as means ± standard errors from 20 leaf discs for flg22 treatment. **C.** Total photon counts from results in C. **D.** Phosphorylation at Ser-506 and Thr-446 oppositely regulate DGK5 function in disease resistance to *Pst* DC3000 infection. Four-week-old plants were hand-inoculated with *Pst* DC3000 at 5×10^5 cfu/ml. The *in planta* bacterial growth was measured at 2 days-post inoculation (dpi). Two independent homozygous transgenic lines, 1 & 2, of *pDGK5::DGK5-HA, pDGK5::DGK5*^{T446A}*-HA* and *pDGK5::DGK5*^{S506A}*-HA* in the *dgk5* mutant background are shown here. The data are shown as means ± standard errors.

4.3.7 Phosphorylation at Ser-506 and Thr-446 oppositely regulates DGK5 function in ROS and immunity

Considering the involvement of DGK5 in flg22-triggered ROS production and immunity, we tried to assess how the two phosphorylation events regulate DGK5 function. We first constructed transgenic complementation lines of WT DGK5, DGK5^{T446A} and DGK5^{S506A} driven by its own promoter into *dgk5* knock-out mutant plants. Next we performed flg22-induced ROS assay with different complementation lines. Indeed, DGK5-HA transgene rescued *dgk5* ROS to WT Col-0 level (Fig.4.9C). More importantly, DGK5^{S506A} failed to complement *dgk5* ROS production while DGK5^{T446A} transgenic plants produced much higher level of ROS than WT (Fig 4.9B). These results lead us to hypothesize that phosphorylation at Thr-446 may play a negative role on DGK5 while Ser-506 positively regulates it. Furthermore, we performed a disease assay with these transgenic complementation lines. DGK5-HA rescued *dgk5* disease resistance almost to the same level as WT Col-0 while DGK5^{S506A} failed to rescue *dgk5*. DGK5^{T446A} transgenic lines at least complemented *dgk5* disease resistance to WT level although they did not clearly enhance resistance (Fig 4.9C). Combining the *in vitro* DGK5 kinase activity assay and the result of the transgenic plants, we conclude that phosphorylation at Ser-506 positively regulates DGK5 activity which likely promotes PA production and plant defense. In contrast, phosphorylation at Thr-446 negatively regulates DGK5 activity to suppress PA production and innate immunity.

4.4 Discussion and conclusions

Lipid molecules not only serve as the building blocks to form biological membranes that provide the boundary between the cell and surrounding environment, but also play significant roles in monitoring intracellular signal transduction. One of the lipid phosphatidic acid, or PA, is actively involved in various signaling pathways and is especially indispensable in plants. Acting as a secondary messenger, PA is dynamically regulated by diverse developmental and environmental stimuli. Many microbe-derived molecules including PAMPs such as flg22, xylanase, bacteria effectors such as AvrRpm1, AvrRpt2, as well as Avr4 promote PA accumulation in plant (Andersson et al., 2006; de Jong et al., 2004; van der Luit et al., 2000). It has been proposed either a PLC-DGK pathway or PLD pathway is responsible for producing PA upon elicitation during these biotic stresses. Research in human has demonstrated G-protein coupled receptor could activate PLC to initiate the PLC-DGK pathway, but how the lipid signaling pathways in plants as mentioned above could be stimulated is completely unknown partly due to the absence of classic GPCR in plants (Urano and Jones, 2014). In a Y2H screen looking for proteins interacting with BIK1, a PTI signaling transducer, we identified DGK5 as a potential link between PRR complex activation and lipid signaling initiation. There are seven DGKs in arabidopsis and DGK5 is the unique member bearing an extra C-terminal domain in one of its splicing isoform-DGK5β (Fig 4.1A). Interestingly, BIK1 only directly interacts with DGK5β but not DGK5α. This suggests an evolutionary phenomenon as DGK5 appear to have acquired this extra CTD to enable its interaction with BIK1 and bridging PRR activation and lipid signaling.

More significantly, BIK1 not only interacts with DGK5, but also rapidly phosphorylates DGK5 upon flg22 perception and the phosphorylation site Ser-506 resides in the CTD. Because of the uniqueness of the CTD in terms of BIK1 interaction and phosphorylation, DGK5 alone plays an irreplaceable role in plant defense response as the *dgk5* mutant exhibits reduced ROS production and increased disease susceptibility to pathogenic bacteria. When the *in vitro* DGK activity assay was performed, DGK5^{S506D} showed higher activity compared to WT DGK5. This provides a mechanistic insight on how this BIK1-mediated phosphorylation could initiate lipid signaling. As the model suggests (Fig 4.10), flg22-activated BIK1 directly phosphorylates DGK5, which stimulates

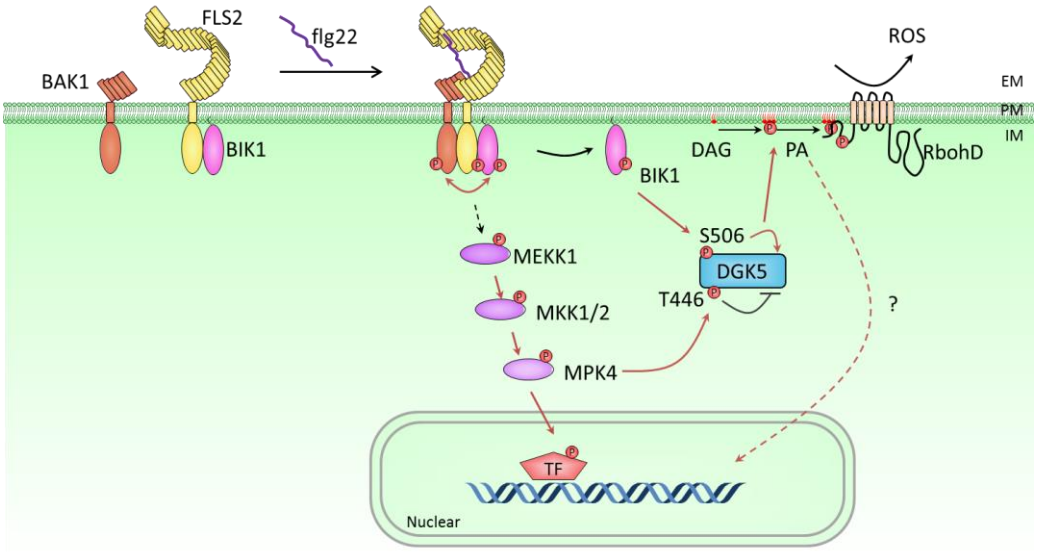

Figure 4.10 Model: Inverse regulation of DGK5 by protein kinase BIK1- and MPK4-mediated phosphorylation governs flg22-triggered PA signaling. Flg22 perception by FLS2/BAK1 receptor/co-receptor complex leads to phosphorylation and activation of BIK1 which in turn phosphorylates DGK5 at Ser-506 to promote PA production. Meanwhile flg22 also triggers activation of MAPK cascade including MPK4 whom phosphorylates DGK5 at Thr-446 to suppress DGK5 activity. PA level enhanced by FLS2 signaling regulates ROS production via direct binding to RbohD and contributes to plant immunity through other downstream effectors.

DGK5 activity likely via conformational change, and promotes phosphorylation of substrate DAG to synthesize PA. The elevated PA then positively influences the downstream signaling as well as disease resistance.

During the investigation to identify DGK5 phosphorylation sites, we unexpectedly discovered another residue, Thr-446. It is also quickly phosphorylated upon flg22 treatment and additional analysis demonstrated the corresponding kinase is MPK4. More surprisingly, phosphorylation of Thr-446 by MPK4 oppositely affects DGK5 and surrenders its kinase activity as well as its function in immunity. In addition, Thr-446 is also unique in DGK5 and not conserved in other DGKs. For plants, lacking robust immune responses risks the fitness of the host in the environment, while uncontrolled immune activation leads to excessive tissue damage and sacrificed development. By the differential phosphorylation of DGK5 by BIK1 and MPK4, plants likely gain the capability to precisely regulate the PA production to fine tune immune responses. It has been known MPK4 negatively regulates immunity but the exact mechanism is still not well understood (Kong et al., 2012). One report revealed that MPK4 directly phosphorylates ASR3, a transcriptional repressor which negatively regulates defense gene expression (Li et al., 2015). The involvement of MPK4 in lipid signaling provides another explanation how the negative regulatory role of MPK4 in immunity is achieved.

Besides the two phosphorylation sites studied in detail, we also detected additional phosphorylation sites by mass spectrometry (Fig 4.7A). Although phosphorylation of those sites did not cause a mobility band shift, they may still be

phosphorylated by other kinases and regulate DGK5 function in unknown circumstances such as abiotic stress. Regarding Ser-506 phosphorylation, although we observed great reduction in the *bik1* mutant, there was still remnant phosphorylation left (Fig 4.6B). Considering many RLCKs homologs function redundantly with BIK1, it is reasonable to speculate that other RLCKs may be involved in DGK5 phosphorylation.

In the PLC-DGK pathway, PIP2 is hydrolyzed by PLC into DAG and IP3. We discovered the direct transmission from the PRR complex ignition to DGK5 activation. However, it does not exclude the existence of other links between the PRR signaling and lipid signaling. Upon PAMP treatment, PA is accumulated while the amount of PIP2 is reduced (van der Luit et al., 2000). Activation of DGK alone could not explain the reduced amount of PIP2 so it is possible that specific PLCs could also be activated as quickly as DGKs. How the PLC is activated in plants without classic GPCR and which PLC is directly responsible for this PAMP-triggered PIP2 dynamic require further study. Considering the significant functions of RLCKs in PRR signaling, it is reasonable to question if BIK1 or its homologs are involved in this process.

While we now have more understanding of the early steps from PRR to lipid signaling activation, how PA orchestrates the defense responses remains largely unknown. PA could bind NADPH oxidase RbohD and which would explain the altered ROS production in the *dgk5* mutant. It was proposed that PA binds to MPK6 and influences its kinase activity in salt stress condition (Yu et al., 2010), however, we did not detect any activity change of MPK6 in the *dgk5* mutant (Fig 4.4). This suggests the convergent components such as the MAPK cascade could be divergently regulated in

different signaling networks. Future studies with more PA binding targets identified will provide more knowledge of the involvement of lipids in PTI responses and PRR signaling networks.

REFERENCES

Abuqamar, S., Chai, M.F., Luo, H., Song, F., and Mengiste, T. (2008). Tomato protein kinase 1b mediates signaling of plant responses to necrotrophic fungi and insect herbivory. The Plant Cell *20*, 1964-1983.

Al-Hakim, A.K., Zagorska, A., Chapman, L., Deak, M., Peggie, M., and Alessi, D.R. (2008). Control of AMPK-related kinases by USP9X and atypical Lys(29)/Lys(33)-linked polyubiquitin chains. The Biochemical Journal *411*, 249-260.

Albert, I., Bohm, H., Albert, M., Feiler, C.E., Imkampe, J., Wallmeroth, N., Brancato, C., Raaymakers, T.M., Oome, S., Zhang, H.Q., *et al.* (2015). An RLP23-SOBIR1-BAK1 complex mediates NLP-triggered immunity. Nature Plants *1*, 15140.

Andersson, M.X., Kourtchenko, O., Dangl, J.L., Mackey, D., and Ellerstrom, M. (2006). Phospholipase-dependent signalling during the AvrRpm1- and AvrRpt2-induced disease resistance responses in Arabidopsis thaliana. The Plant Journal *47*, 947-959.

Anthony, R.G., Henriques, R., Helfer, A., Meszaros, T., Rios, G., Testerink, C., Munnik, T., Deak, M., Koncz, C., and Bogre, L. (2004). A protein kinase target of a PDK1 signalling pathway is involved in root hair growth in Arabidopsis. The EMBO Journal *23*, 572-581.

Antolin-Llovera, M., Ried, M.K., Binder, A., and Parniske, M. (2012). Receptor kinase signaling pathways in plant-microbe interactions. Annual Review of Phytopathology *50*, 451-473.

Arisz, S.A., Testerink, C., and Munnik, T. (2009). Plant PA signaling via diacylglycerol kinase. Biochimica et Biophysica Acta (BBA) -Molecular and Cell Biology of Lipids *1791*, 869-875.

Ausubel, F.M. (2005). Are innate immune signaling pathways in plants and animals conserved? Nature Immunology *6*, 973-979.

Barberon, M., Zelazny, E., Robert, S., Conejero, G., Curie, C., Friml, J., and Vert, G. (2011). Monoubiquitin-dependent endocytosis of the iron-regulated transporter 1 (IRT1) transporter controls iron uptake in plants. Proceedings of the National Academy of Science of the United States of America *108*, E450-458.

Bergink, S., and Jentsch, S. (2009). Principles of ubiquitin and SUMO modifications in DNA repair. Nature *458*, 461-467.

Bethke, G., Pecher, P., Eschen-Lippold, L., Tsuda, K., Katagiri, F., Glazebrook, J., Scheel, D., and Lee, J. (2012). Activation of the Arabidopsis thaliana mitogen-activated

protein kinase MPK11 by the flagellin-derived elicitor peptide, flg22. Molecular Plant-Microbe Intereactions *25*, 471-480.

Bethke, G., Unthan, T., Uhrig, J.F., Poschl, Y., Gust, A.A., Scheel, D., and Lee, J. (2009). Flg22 regulates the release of an ethylene response factor substrate from MAP kinase 6 in Arabidopsis thaliana via ethylene signaling. Proceedings of the National Academy of Sciences of the United States of America *106*, 8067-8072.

Bhatnagar, S., Gazin, C., Chamberlain, L., Ou, J.H., Zhu, X.C., Tushir, J.S., Virbasius, C.M., Lin, L., Zhu, L.H.J., Wajapeyee, N., *et al.* (2014). TRIM37 is a new histone H2A ubiquitin ligase and breast cancer oncoprotein. Nature *516*, 116-U313.

Blackledge, N.P., Farcas, A.M., Kondo, T., King, H.W., McGouran, J.F., Hanssen, L.L., Ito, S., Cooper, S., Kondo, K., Koseki, Y., *et al.* (2014). Variant PRC1 complex-dependent H2A ubiquitylation drives PRC2 recruitment and polycomb domain formation. Cell *157*, 1445-1459.

Bohm, H., Albert, I., Oome, S., Raaymakers, T.M., Van den Ackerveken, G., and Nurnberger, T. (2014). A Conserved Peptide Pattern from a Widespread Microbial Virulence Factor Triggers Pattern-Induced Immunity in Arabidopsis. PLoS Pathogen *10*, 11.

Boller, T., and Felix, G. (2009). A renaissance of elicitors: perception of microbe-associated molecular patterns and danger signals by pattern-recognition receptors. Annual Review of Plant Biology *60*, 379-406.

Boname, J.M., Thomas, M., Stagg, H.R., Xu, P., Peng, J., and Lehner, P.J. (2010). Efficient internalization of MHC I requires lysine-11 and lysine-63 mixed linkage polyubiquitin chains. Traffic *11*, 210-220.

Boudsocq, M., Willmann, M.R., McCormack, M., Lee, H., Shan, L., He, P., Bush, J., Cheng, S.H., and Sheen, J. (2010). Differential innate immune signalling via Ca(2+) sensor protein kinases. Nature *464*, 418-422.

Brenkman, A.B., de Keizer, P.L.J., van den Broek, N.J.F., Jochemsen, A.G., and Burgering, B.M.T. (2008). Mdm2 Induces Mono-Ubiquitination of FOXO4. PloS One *3*, (7):e2819.

Bueso, E., Rodriguez, L., Lorenzo-Orts, L., Gonzalez-Guzman, M., Sayas, E., Munoz-Bertomeu, J., Ibanez, C., Serrano, R., and Rodriguez, P.L. (2014). The single-subunit RING-type E3 ubiquitin ligase RSL1 targets PYL4 and PYR1 ABA receptors in plasma membrane to modulate abscisic acid signaling. The Plant Journal *80*, 1057-1071.

Cao, Y.R., Liang, Y., Tanaka, K., Nguyen, C.T., Jedrzejczak, R.P., Joachimiak, A., and Stacey, G. (2014). The kinase LYK5 is a major chitin receptor in Arabidopsis and forms a chitin-induced complex with related kinase CERK1. Elife *3*: e03766.

Carter, R.S., Pennington, K.N., Arrate, P., Oltz, E.M., and Ballard, D.W. (2005). Site-specific monoubiquitination of IkappaB kinase IKKbeta regulates its phosphorylation and persistent activation. The Journal of Biological Chemistry *280*, 43272-43279.

Chen, Z.J., and Sun, L.J. (2009). Nonproteolytic functions of ubiquitin in cell signaling. Molecular Cell *33*, 275-286.

Cheng, Z.Y., Li, J.F., Niu, Y.J., Zhang, X.C., Woody, O.Z., Xiong, Y., Djonovic, S., Millet, Y., Bush, J., McConkey, B.J., *et al.* (2015). Pathogen-secreted proteases activate a novel plant immune pathway. Nature *521*, 213-216.

Chinchilla, D., Bauer, Z., Regenass, M., Boller, T., and Felix, G. (2006). The Arabidopsis receptor kinase FLS2 binds flg22 and determines the specificity of flagellin perception. The Plant Cell *18*, 465-476.

Chinchilla, D., Zipfel, C., Robatzek, S., Kemmerling, B., Nurnberger, T., Jones, J.D., Felix, G., and Boller, T. (2007). A flagellin-induced complex of the receptor FLS2 and BAK1 initiates plant defence. Nature *448*, 497-500.

Choi, J., Tanaka, K., Cao, Y.R., Qi, Y., Qiu, J., Liang, Y., Lee, S.Y., and Stacey, G. (2014). Identification of a Plant Receptor for Extracellular ATP. Science *343*, 290-294.

Ciechanover, A. (1994). The ubiquitin-proteasome proteolytic pathway. Cell *79*, 13-21.

Couto, D., Niebergall, R., Liang, X., Bucherl, C.A., Sklenar, J., Macho, A.P., Ntoukakis, V., Derbyshire, P., Altenbach, D., Maclean, D., *et al.* (2016). The Arabidopsis Protein Phosphatase PP2C38 Negatively Regulates the Central Immune Kinase BIK1. PLoS Pathogens *12*, e1005811.

Couto, D., and Zipfel, C. (2016). Regulation of pattern recognition receptor signalling in plants. Nature Reviews Immunology *16*, 537-552.

de Jong, C.F., Laxalt, A.M., Bargmann, B.O.R., de Wit, P.J.G.M., Joosten, M.H.A.J., and Munnik, T. (2004). Phosphatidic acid accumulation is an early response in the Cf-4/Avr4 interaction. The Plant Journal *39*, 1-12.

De Smet, I., Voss, U., Jurgens, G., and Beeckman, T. (2009). Receptor-like kinases shape the plant. Nature Cell Biology *11*, 1166-1173.

den Hartog, M., Verhoef, N., and Munnik, T. (2003). Nod factor and elicitors activate different phospholipid signaling pathways in suspension-cultured alfalfa cells. Plant Physiology *132*, 311-317.

Dodds, P.N., and Rathjen, J.P. (2010). Plant immunity: towards an integrated view of plant-pathogen interactions. Nature Reviews Genetics *11*, 539-548.

Downes, B.P., Stupar, R.M., Gingerich, D.J., and Vierstra, R.D. (2003). The HECT ubiquitin-protein ligase (UPL) family in Arabidopsis: UPL3 has a specific role in trichome development. The Plant Journal *35*, 729-742.

Dubiella, U., Seybold, H., Durian, G., Komander, E., Lassig, R., Witte, C.P., Schulze, W.X., and Romeis, T. (2013). Calcium-dependent protein kinase/NADPH oxidase activation circuit is required for rapid defense signal propagation. Proceedings of the National Academy of Sciences of the United States of America *110*, 8744-8749.

Dynek, J.N., Goncharov, T., Dueber, E.C., Fedorova, A.V., Izrael-Tomasevic, A., Phu, L., Helgason, E., Fairbrother, W.J., Deshayes, K., Kirkpatrick, D.S., *et al.* (2010). c-IAP1 and UbcH5 promote K11-linked polyubiquitination of RIP1 in TNF signalling. The EMBO Journal *29*, 4198-4209.

Espinosa, J.M. (2008). Histone H2B ubiquitination: the cancer connection. Genes & Development *22*, 2743-2749.

Felix, G., Duran, J.D., Volko, S., and Boller, T. (1999). Plants have a sensitive perception system for the most conserved domain of bacterial flagellin. The Plant Journal *18*, 265-276.

Feng, F., and Zhou, J.M. (2012). Plant-bacterial pathogen interactions mediated by type III effectors. Current Opinion in Plant Biology *15*, 469-476.

Freudenthal, B.D., Gakhar, L., Ramaswamy, S., and Washington, M.T. (2010). Structure of monoubiquitinated PCNA and implications for translesion synthesis and DNA polymerase exchange. Nature Structural & Molecular Biology *17*, 479-484.

Geisler, S., Holmstrom, K.M., Skujat, D., Fiesel, F.C., Rothfuss, O.C., Kahle, P.J., and Springer, W. (2010). PINK1/Parkin-mediated mitophagy is dependent on VDAC1 and p62/SQSTM1. Nature Cell Biology *12*, 119-131.

Glauser, L., Sonnay, S., Stafa, K., and Moore, D.J. (2011). Parkin promotes the ubiquitination and degradation of the mitochondrial fusion factor mitofusin 1. Journal of Neurochemistry *118*, 636-645.

Gomez-Gomez, L., and Boller, T. (2000). FLS2: an LRR receptor-like kinase involved in the perception of the bacterial elicitor flagellin in Arabidopsis. Molecular Cell *5*, 1003-1011.

Goto, E., Yamanaka, Y., Ishikawa, A., Aoki-Kawasumi, M., Mito-Yoshida, M., Ohmura-Hoshino, M., Matsuki, Y., Kajikawa, M., Hirano, H., and Ishido, S. (2010). Contribution of lysine 11-linked ubiquitination to MIR2-mediated major histocompatibility complex class I internalization. The Journal of Biological Chemistry *285*, 35311-35319.

Gust, A.A., and Felix, G. (2014). Receptor like proteins associate with SOBIR1-type of adaptors to form bimolecular receptor kinases. Current Opinion in Plant Biology *21*, 104-111.

Haglund, K., and Dikic, I. (2012). The role of ubiquitylation in receptor endocytosis and endosomal sorting. Journal of Cell Science *125*, 265-275.

Han, Z.F., Sun, Y.D., and Chai, J.J. (2014). Structural insight into the activation of plant receptor kinases. Current Opinion in Plant Biology *20*, 55-63.

Hanson, A.J., Wallace, H.A., Freeman, T.J., Beauchamp, R.D., Lee, L.A., and Lee, E. (2012). XIAP Monoubiquitylates Groucho/TLE to Promote Canonical Wnt Signaling. Molecular Cell *45*, 619-628.

He, P., Shan, L., and Sheen, J. (2007). The use of protoplasts to study innate immune responses. Methods in Molecular Biology *354*, 1-9.

Heese, A., Hann, D.R., Gimenez-Ibanez, S., Jones, A.M., He, K., Li, J., Schroeder, J.I., Peck, S.C., and Rathjen, J.P. (2007). The receptor-like kinase SERK3/BAK1 is a central regulator of innate immunity in plants. Proceedings of the National Academy of Sciences of the United States of America *104*, 12217-12222.

Hislop, J.N., and von Zastrow, M. (2011). Role of ubiquitination in endocytic trafficking of G-protein-coupled receptors. Traffic *12*, 137-148.

Hoege, C., Pfander, B., Moldovan, G.L., Pyrowolakis, G., and Jentsch, S. (2002). RAD6-dependent DNA repair is linked to modification of PCNA by ubiquitin and SUMO. Nature *419*, 135-141.

Huang, H., Jeon, M.S., Liao, L., Yang, C., Elly, C., Yates, J.R., 3rd, and Liu, Y.C. (2010). K33-linked polyubiquitination of T cell receptor-zeta regulates proteolysis-independent T cell signaling. Immunity *33*, 60-70.

Hunter, T. (2007). The age of crosstalk: phosphorylation, ubiquitination, and beyond. Molecular Cell *28*, 730-738.

Jin, H.S., Lee, D.H., Kim, D.H., Chung, J.H., Lee, S.J., and Lee, T.H. (2009). cIAP1, cIAP2, and XIAP Act Cooperatively via Nonredundant Pathways to Regulate Genotoxic Stress-Induced Nuclear Factor-kappa B Activation. Cancer Research *69*, 1782-1791.

Jones, J.D., and Dangl, J.L. (2006). The plant immune system. Nature *444*, 323-329.

Kadota, Y., Sklenar, J., Derbyshire, P., Stransfeld, L., Asai, S., Ntoukakis, V., Jones, J.D.G., Shirasu, K., Menke, F., Jones, A., *et al.* (2014). Direct Regulation of the NADPH Oxidase RBOHD by the PRR-Associated Kinase BIK1 during Plant Immunity. Molecular Cell *54*, 43-55.

Kaiser, S.E., Riley, B.E., Shaler, T.A., Trevino, R.S., Becker, C.H., Schulman, H., and Kopito, R.R. (2011). Protein standard absolute quantification (PSAQ) method for the measurement of cellular ubiquitin pools. Nature Methods *8*, 691-696.

Kang, S., Yang, F., Li, L., Chen, H., Chen, S., and Zhang, J. (2015). The Arabidopsis transcription factor BRASSINOSTEROID INSENSITIVE1-ETHYL METHANESULFONATE-SUPPRESSOR1 is a direct substrate of MITOGEN-ACTIVATED PROTEIN KINASE6 and regulates immunity. Plant Physiology *167*, 1076-1086.

Kim, D.Y., Scalf, M., Smith, L.M., and Vierstra, R.D. (2013). Advanced proteomic analyses yield a deep catalog of ubiquitylation targets in Arabidopsis. The Plant Cell *25*, 1523-1540.

Kinoshita, T., Cano-Delgado, A.C., Seto, H., Hiranuma, S., Fujioka, S., Yoshida, S., and Chory, J. (2005). Binding of brassinosteroids to the extracellular domain of plant receptor kinase BRI1. Nature *433*, 167-171.

Komander, D. (2009). The emerging complexity of protein ubiquitination. Biochemical Society Transactions *37*, 937-953.

Komander, D., and Rape, M. (2012). The ubiquitin code. Annual Review of Biochemistry *81*, 203-229.

Kong, Q., Qu, N., Gao, M., Zhang, Z., Ding, X., Yang, F., Li, Y., Dong, O.X., Chen, S., Li, X., *et al.* (2012). The MEKK1-MKK1/MKK2-MPK4 kinase cascade negatively regulates immunity mediated by a mitogen-activated protein kinase kinase kinase in Arabidopsis. The Plant Cell *24*, 2225-2236.

Krol, E., Mentzel, T., Chinchilla, D., Boller, T., Felix, G., Kemmerling, B., Postel, S., Arents, M., Jeworutzki, E., Al-Rasheid, K.A.S., *et al.* (2010). Perception of the Arabidopsis Danger Signal Peptide 1 Involves the Pattern Recognition Receptor AtPEPR1 and Its Close Homologue AtPEPR2. The Journal of Biological Chemistry *285*, 13471-13479.

Kwaaitaal, M., Huisman, R., Maintz, J., Reinstadler, A., and Panstruga, R. (2011). Ionotropic glutamate receptor (iGluR)-like channels mediate MAMP-induced calcium influx in Arabidopsis thaliana. The Biochemical Journal *440*, 355-365.

Leitner, J., Petrasek, J., Tomanov, K., Retzer, K., Parezova, M., Korbei, B., Bachmair, A., Zazimalova, E., and Luschnig, C. (2012). Lysine63-linked ubiquitylation of PIN2 auxin carrier protein governs hormonally controlled adaptation of Arabidopsis root growth. Proceedings of the National Academy of Science of the United States of America *109*, 8322-8327.

Li, B., Jiang, S., Yu, X., Cheng, C., Chen, S., Cheng, Y., Yuan, J.S., Jiang, D., He, P., and Shan, L. (2015). Phosphorylation of trihelix transcriptional repressor ASR3 by MAP KINASE4 negatively regulates Arabidopsis immunity. The Plant Cell *27*, 839-856.

Li, B., Lu, D., and Shan, L. (2014a). Ubiquitination of pattern recognition receptors in plant innate immunity. Molecular Plant Pathology *15*, 737-746.

Li, B., Meng, X., Shan, L., and He, P. (2016). Transcriptional Regulation of Pattern-Triggered Immunity in Plants. Cell Host & Microbe *19*, 641-650.

Li, F., Cheng, C., Cui, F., de Oliveira, M.V., Yu, X., Meng, X., Intorne, A.C., Babilonia, K., Li, M., Li, B., *et al.* (2014). Modulation of RNA polymerase II phosphorylation downstream of pathogen perception orchestrates plant immunity. Cell Host & Microbe *16*, 748-758.

Li, J., Wen, J., Lease, K.A., Doke, J.T., Tax, F.E., and Walker, J.C. (2002). BAK1, an Arabidopsis LRR receptor-like protein kinase, interacts with BRI1 and modulates brassinosteroid signaling. Cell *110*, 213-222.

Li, J.F., Zhang, D., and Sheen, J. (2014). Epitope-tagged protein-based artificial miRNA screens for optimized gene silencing in plants. Nature Protocols *9*, 939-949.

Li, L., Li, M., Yu, L., Zhou, Z., Liang, X., Liu, Z., Cai, G., Gao, L., Zhang, X., Wang, Y., *et al.* (2014). The FLS2-Associated Kinase BIK1 Directly Phosphorylates the NADPH Oxidase RbohD to Control Plant Immunity. Cell Host & Microbe *15*, 329-338.

Liang, X., Ding, P., Lian, K., Wang, J., Ma, M., Li, L., Li, L., Li, M., Zhang, X., Chen, S., *et al.* (2016). Arabidopsis heterotrimeric G proteins regulate immunity by directly coupling to the FLS2 receptor. Elife *5*, e13568.

Liebrand, T.W.H., van den Burg, H.A., and Joosten, M.H.A.J. (2014). Two for all: receptor-associated kinases SOBIR1 and BAK1. Trends in Plant Science *19*, 123-132.

Lin, W., Li, B., Lu, D., Chen, S., Zhu, N., He, P., and Shan, L. (2014). Tyrosine phosphorylation of protein kinase complex BAK1/BIK1 mediates Arabidopsis innate

immunity. Proceedings of the National Academy of Science of the United States of America *111*, 3632-3637.

Lin, W., Lu, D., Gao, X., Jiang, S., Ma, X., Wang, Z., Mengiste, T., He, P., and Shan, L. (2013a). Inverse modulation of plant immune and brassinosteroid signaling pathways by the receptor-like cytoplasmic kinase BIK1. Proceedings of the National Academy of Sciences of the United States of America *110*, 12114-12119.

Lin, W., Ma, X., Shan, L., and He, P. (2013b). Big Roles of Small Kinases: The Complex Functions of Receptor-like Cytoplasmic Kinases in Plant Immunity and Development. Journal of Integrative Plant Biology *55*, (12):1188-1197.

Liu, T., Liu, Z., Song, C., Hu, Y., Han, Z., She, J., Fan, F., Wang, J., Jin, C., Chang, J., *et al.* (2012). Chitin-induced dimerization activates a plant immune receptor. Science *336*, 1160-1164.

Liu, Z., Wu, Y., Yang, F., Zhang, Y., Chen, S., Xie, Q., Tian, X., and Zhou, J.M. (2013). BIK1 interacts with PEPRs to mediate ethylene-induced immunity. Proceedings of the National Academy of Sciences of the United States of America *110*, 6205-6210.

Lu, D., Lin, W., Gao, X., Wu, S., Cheng, C., Avila, J., Heese, A., Devarenne, T.P., He, P., and Shan, L. (2011). Direct ubiquitination of pattern recognition receptor FLS2 attenuates plant innate immunity. Science *332*, 1439-1442.

Lu, D., Wu, S., Gao, X., Zhang, Y., Shan, L., and He, P. (2010a). A receptor-like cytoplasmic kinase, BIK1, associates with a flagellin receptor complex to initiate plant innate immunity. Proceedings of the National Academy of Sciences of the United States of America *107*, 496-501.

Lu, D., Wu, S., He, P., and Shan, L. (2010b). Phosphorylation of receptor-like cytoplasmic kinases by bacterial flagellin. Plant Signaling & Behavior *5*, (5):598-600.

Ma, Y., Walker, R.K., Zhao, Y., and Berkowitz, G.A. (2012). Linking ligand perception by PEPR pattern recognition receptors to cytosolic Ca2+ elevation and downstream immune signaling in plants. Proceedings of the National Academy of Sciences of the United States of America *109*, 19852-19857.

Macho, A.P., and Zipfel, C. (2014). Plant PRRs and the activation of innate immune signaling. Molecular Cell *54*, 263-272.

Mao, G., Meng, X., Liu, Y., Zheng, Z., Chen, Z., and Zhang, S. (2011). Phosphorylation of a WRKY transcription factor by two pathogen-responsive MAPKs drives phytoalexin biosynthesis in Arabidopsis. The Plant Cell *23*, 1639-1653.

Martins, S., Dohmann, E.M., Cayrel, A., Johnson, A., Fischer, W., Pojer, F., Satiat-Jeunemaitre, B., Jaillais, Y., Chory, J., Geldner, N., *et al.* (2015). Internalization and vacuolar targeting of the brassinosteroid hormone receptor BRI1 are regulated by ubiquitination. Nature Communication *6*, 6151.

Meng, X., Xu, J., He, Y., Yang, K.Y., Mordorski, B., Liu, Y., and Zhang, S. (2013). Phosphorylation of an ERF transcription factor by Arabidopsis MPK3/MPK6 regulates plant defense gene induction and fungal resistance. The Plant Cell *25*, 1126-1142.

Meng, X., and Zhang, S. (2013). MAPK Cascades in Plant Disease Resistance Signaling. Annual Review of Phytopathology *51*, 245-266.

Miao, Y., and Zentgraf, U. (2010). A HECT E3 ubiquitin ligase negatively regulates Arabidopsis leaf senescence through degradation of the transcription factor WRKY53. The Plant Journal *63*, 179-188.

Miranda, M., and Sorkin, A. (2007). Regulation of receptors and transporters by ubiquitination: new insights into surprisingly similar mechanisms. Molecular Interventions *7*, 157-167.

Monaghan, J., Matschi, S., Shorinola, O., Rovenich, H., Matei, A., Segonzac, C., Malinovsky, F.G., Rathjen, J.P., MacLean, D., Romeis, T., *et al.* (2014). The calcium-dependent protein kinase CPK28 buffers plant immunity and regulates BIK1 turnover. Cell Host & Microbe *16*, 605-615.

Monaghan, J., and Zipfel, C. (2012). Plant pattern recognition receptor complexes at the plasma membrane. Current Opinion of Plant Biology *15*, 349-357.

Morris, J.R., and Solomon, E. (2004). BRCA1 : BARD1 induces the formation of conjugated ubiquitin structures, dependent on K6 of ubiquitin, in cells during DNA replication and repair. Human Molecular Genetics *13*, 807-817.

Munnik, T., and Testerink, C. (2009). Plant phospholipid signaling: "in a nutshell". The Journal of Lipid Research *50*, S260-S265.

Munnik, T., and Zarza, X. (2013). Analyzing plant signaling phospholipids through 32Pi-labeling and TLC. Methods in Molecular Biology *1009*, 3-15.

Nakagawa, T., Kajitani, T., Togo, S., Masuko, N., Ohdan, H., Hishikawa, Y., Koji, T., Matsuyama, T., Ikura, T., Muramatsu, M., *et al.* (2008). Deubiquitylation of histone H2A activates transcriptional initiation via trans-histone cross-talk with H3K4 di- and trimethylation. Genes & Development *22*, 37-49.

Nakagawa, T., and Nakayama, K. (2015). Protein monoubiquitylation: targets and diverse functions. Genes to Cells *20*, 543-562.

Nam, K.H., and Li, J. (2002). BRI1/BAK1, a receptor kinase pair mediating brassinosteroid signaling. Cell *110*, 203-212.

Nie, L., Sasaki, M., and Maki, C.G. (2007). Regulation of p53 nuclear export through sequential changes in conformation and ubiquitination. The Journal of Biological Chemistry *282*, 14616-14625.

Oome, S., Raaymakers, T.M., Cabral, A., Samwel, S., Bohm, H., Albert, I., Nurnberger, T., and Van den Ackerveken, G. (2014). Nep1-like proteins from three kingdoms of life act as a microbe-associated molecular pattern in Arabidopsis. Proceedings of the National Academy of Sciences of the United States of America *111*, 16955-16960.

Ranf, S., Eschen-Lippold, L., Pecher, P., Lee, J., and Scheel, D. (2011). Interplay between calcium signalling and early signalling elements during defence responses to microbe- or damage-associated molecular patterns. The Plant Journal *68*, 100-113.

Ranf, S., Gisch, N., Schaffer, M., Illig, T., Westphal, L., Knirel, Y.A., Sanchez-Carballo, P.M., Zahringer, U., Huckelhoven, R., Lee, J., *et al.* (2015). A lectin S-domain receptor kinase mediates lipopolysaccharide sensing in Arabidopsis thaliana. Nature Immunology *16*, 426-433.

Robatzek, S., Chinchilla, D., and Boller, T. (2006). Ligand-induced endocytosis of the pattern recognition receptor FLS2 in Arabidopsis. Genes & Development *20*, 537-542.

Roberts, D., Pedmale, U.V., Morrow, J., Sachdev, S., Lechner, E., Tang, X.B., Zheng, N., Hannink, M., Genschik, P., and Liscum, E. (2011). Modulation of Phototropic Responsiveness in Arabidopsis through Ubiquitination of Phototropin 1 by the CUL3-Ring E3 Ubiquitin Ligase CRL3(NPH3). The Plant Cell *23*, 3627-3640.

Rotin, D., and Kumar, S. (2009). Physiological functions of the HECT family of ubiquitin ligases. Nature Reviews Molecular Cell Biology *10*, 398-409.

Roux, M., Schwessinger, B., Albrecht, C., Chinchilla, D., Jones, A., Holton, N., Malinovsky, F.G., Tor, M., de Vries, S., and Zipfel, C. (2011). The Arabidopsis Leucine-Rich Repeat Receptor-Like Kinases BAK1/SERK3 and BKK1/SERK4 Are Required for Innate Immunity to Hemibiotrophic and Biotrophic Pathogens. The Plant Cell *23*, 2440-2455.

Santiago, J., Henzler, C., and Hothorn, M. (2013). Molecular mechanism for plant steroid receptor activation by somatic embryogenesis co-receptor kinases. Science *341*, 889-892.

Schulz, P., Herde, M., and Romeis, T. (2013). Calcium-dependent protein kinases: hubs in plant stress signaling and development. Plant Physiology *163*, 523-530.

Schulze, B., Mentzel, T., Jehle, A.K., Mueller, K., Beeler, S., Boller, T., Felix, G., and Chinchilla, D. (2010). Rapid heteromerization and phosphorylation of ligand-activated plant transmembrane receptors and their associated kinase BAK1. The Journal of Biological Chemistry *285*, 9444-9451.

Schwessinger, B., and Ronald, P.C. (2012). Plant innate immunity: perception of conserved microbial signatures. Annual Review of Plant Biology *63*, 451-482.

Schwessinger, B., Roux, M., Kadota, Y., Ntoukakis, V., Sklenar, J., Jones, A., and Zipfel, C. (2011). Phosphorylation-dependent differential regulation of plant growth, cell death, and innate immunity by the regulatory receptor-like kinase BAK1. PLoS Genetics *7*, e1002046.

Seybold, H., Trempel, F., Ranf, S., Scheel, D., Romeis, T., and Lee, J. (2014). Ca2+ signalling in plant immune response: from pattern recognition receptors to Ca2+ decoding mechanisms. The New Phytologist *204*, 782-790.

Shabek, N., Herman-Bachinsky, Y., Buchsbaum, S., Lewinson, O., Haj-Yahya, M., Hejjaoui, M., Lashuel, H.A., Sommer, T., Brik, A., and Ciechanover, A. (2012). The size of the proteasomal substrate determines whether its degradation will be mediated by mono- or polyubiquitylation. Molecular Cell *48*, 87-97.

Shan, L., He, P., and Sheen, J. (2007). Intercepting host MAPK signaling cascades by bacterial type III effectors. Cell Host & Microbe *1*, 167-174.

Shi, H., Shen, Q., Qi, Y., Yan, H., Nie, H., Chen, Y., Zhao, T., Katagiri, F., and Tang, D. (2013). BR-SIGNALING KINASE1 physically associates with FLAGELLIN SENSING2 and regulates plant innate immunity in Arabidopsis. The Plant Cell *25*, 1143-1157.

Shinya, T., Yamaguchi, K., Desaki, Y., Yamada, K., Narisawa, T., Kobayashi, Y., Maeda, K., Suzuki, M., Tanimoto, T., Takeda, J., *et al.* (2014). Selective regulation of the chitin-induced defense response by the Arabidopsis receptor-like cytoplasmic kinase PBL27. The Plant Journal *79*, 56-66.

Shiu, S.H., and Bleecker, A.B. (2001). Receptor-like kinases from Arabidopsis form a monophyletic gene family related to animal receptor kinases. Proceedings of the National Academy of Science of the United States of America *98*, 10763-10768.

Shiu, S.H., and Bleecker, A.B. (2003). Expansion of the receptor-like kinase/Pelle gene family and receptor-like proteins in Arabidopsis. Plant Physiology *132*, 530-543.

Shiu, S.H., Karlowski, W.M., Pan, R., Tzeng, Y.H., Mayer, K.F., and Li, W.H. (2004). Comparative analysis of the receptor-like kinase family in Arabidopsis and rice. The Plant Cell *16*, 1220-1234.

Skaug, B., Jiang, X., and Chen, Z.J. (2009). The role of ubiquitin in NF-kappaB regulatory pathways. Annual Review Biochemistry *78*, 769-796.

Smith, H., Peggie, M., Campbell, D.G., Vandermoere, F., Carrick, E., and Cohen, P. (2009). Identification of the phosphorylation sites on the E3 ubiquitin ligase Pellino that are critical for activation by IRAK1 and IRAK4. Proceedings of the National Academy of Science of the United States of America *106*, 4584-4590.

Sreekanta, S., Bethke, G., Hatsugai, N., Tsuda, K., Thao, A., Wang, L., Katagiri, F., and Glazebrook, J. (2015). The receptor-like cytoplasmic kinase PCRK1 contributes to pattern-triggered immunity against Pseudomonas syringae in Arabidopsis thaliana. The New Phytologist *207*, 78-90.

Stegmann, M., Anderson, R.G., Ichimura, K., Pecenkova, T., Reuter, P., Zarsky, V., McDowell, J.M., Shirasu, K., and Trujillo, M. (2012). The ubiquitin ligase PUB22 targets a subunit of the exocyst complex required for PAMP-triggered responses in Arabidopsis. The Plant Cell *24*, 4703-4716.

Strzalka, W., Bartnicki, F., Pels, K., Jakubowska, A., Tsurimoto, T., and Tanaka, K. (2013). RAD5a ubiquitin ligase is involved in ubiquitination of Arabidopsis thaliana proliferating cell nuclear antigen. Journal of Experimental Botany *64*, 859-869.

Sun, Y., Han, Z., Tang, J., Hu, Z., Chai, C., Zhou, B., and Chai, J. (2013a). Structure reveals that BAK1 as a co-receptor recognizes the BRI1-bound brassinolide. Cell Research *23*, 1326-1329.

Sun, Y., Li, L., Macho, A.P., Han, Z., Hu, Z., Zipfel, C., Zhou, J.M., and Chai, J. (2013b). Structural basis for flg22-induced activation of the Arabidopsis FLS2-BAK1 immune complex. Science *342*, 624-628.

Takeuchi, O., and Akira, S. (2010). Pattern recognition receptors and inflammation. Cell *140*, 805-820.

Tanaka, K., Swanson, S.J., Gilroy, S., and Stacey, G. (2010). Extracellular nucleotides elicit cytosolic free calcium oscillations in Arabidopsis. Plant Physiology *154*, 705-719.

Tang, J., Han, Z., Sun, Y., Zhang, H., Gong, X., and Chai, J. (2015). Structural basis for recognition of an endogenous peptide by the plant receptor kinase PEPR1. Cell Research *25*, 110-120.

Tang, L.Y., Yamashita, M., Coussens, N.P., Tang, Y., Wang, X., Li, C., Deng, C.X., Cheng, S.Y., and Zhang, Y.E. (2011). Ablation of Smurf2 reveals an inhibition in TGF-beta signalling through multiple mono-ubiquitination of Smad3. The EMBO Journal *30*, 4777-4789.

Testerink, C., Larsen, P.B., van der Does, D., van Himbergen, J.A.J., and Munnik, T. (2007). Phosphatidic acid binds to and inhibits the activity of Arabidopsis CTR1. Journal of Experimental Botany *58*, 3905-3914.

Testerink, C., and Munnik, T. (2011). Molecular, cellular, and physiological responses to phosphatidic acid formation in plants. Journal of Experimental Botany *62*, 2349-2361.

Trotman, L.C., Wang, X., Alimonti, A., Chen, Z., Teruya-Feldstein, J., Yang, H., Pavletich, N.P., Carver, B.S., Cordon-Cardo, C., Erdjument-Bromage, H., *et al.* (2007). Ubiquitination regulates PTEN nuclear import and tumor suppression. Cell *128*, 141-156.

Trujillo, M., Ichimura, K., Casais, C., and Shirasu, K. (2008). Negative regulation of PAMP-triggered immunity by an E3 ubiquitin ligase triplet in Arabidopsis. Current Biology *18*, 1396-1401.

Urano, D., and Jones, A.M. (2014). Heterotrimeric G protein-coupled signaling in plants. Annual Review of Plant Biology *65*, 365-384.

van der Horst, A., de Vries-Smits, A.M.M., Brenkman, A.B., van Triest, M.H., van den Broek, N., Colland, F., Maurice, M.M., and Burgering, B.M.T. (2006). FOXO4 transcriptional activity is regulated by monoubiquitination and USP7/HAUSP. Nature Cell Biology *8*, 1064-U1040.

van der Luit, A.H., Piatti, T., van Doorn, A., Musgrave, A., Felix, G., Boller, T., and Munnik, T. (2000). Elicitation of suspension-cultured tomato cells triggers the formation of phosphatidic acid and diacylglycerol pyrophosphate. Plant Physiology *123*, 1507-1515.

Vierstra, R.D. (2009). The ubiquitin-26S proteasome system at the nexus of plant biology. Nature Reviews Molecular Cell Biology *10*, 385-397.

Wang, C., Zien, C.A., Afitlhile, M., Welti, R., Hildebrand, D.F., and Wang, X. (2000). Involvement of phospholipase D in wound-induced accumulation of jasmonic acid in arabidopsis. The Plant Cell *12*, 2237-2246.

Wang, G.D., Ellendorff, U., Kemp, B., Mansfield, J.W., Forsyth, A., Mitchell, K., Bastas, K., Liu, C.M., Woods-Tor, A., Zipfel, C., *et al.* (2008). A genome-wide functional investigation into the roles of receptor-like proteins in Arabidopsis. Plant Physiology *147*, 503-517.

Wang, H.B., Wang, L.J., Erdjument-Bromage, H., Vidal, M., Tempst, P., Jones, R.S., and Zhang, Y. (2004). Role of histone H2A ubiquitination in polycomb silencing. Nature *431*, 873-878.

Wang, Y.S., Pi, L.Y., Chen, X.H., Chakrabarty, P.K., Jiang, J., De Leon, A.L., Liu, G.Z., Li, L.C., Benny, U., Oard, J., *et al.* (2006). Rice XA21 binding protein 3 is a ubiquitin ligase required for full Xa21-mediated disease resistance. The Plant Cell *18*, 3635-3646.

Wickliffe, K.E., Williamson, A., Meyer, H.J., Kelly, A., and Rape, M. (2011). K11-linked ubiquitin chains as novel regulators of cell division. Trends in Cell Biology *21*, 656-663.

Willmann, R., Lajunen, H.M., Erbs, G., Newman, M.A., Kolb, D., Tsuda, K., Katagiri, F., Fliegmann, J., Bono, J.J., Cullimore, J.V., *et al.* (2011). Arabidopsis lysin-motif proteins LYM1 LYM3 CERK1 mediate bacterial peptidoglycan sensing and immunity to bacterial infection. Proceedings of the National Academy of Sciences of the United States of America *108*, 19824-19829.

Wu-Baer, F., Lagrazon, K., Yuan, W., and Baer, R. (2003). The BRCA1/BARD1 heterodimer assembles polyubiquitin chains through an unconventional linkage involving lysine residue K6 of ubiquitin. The Journal of Biological Chemistry *278*, 34743-34746.

Wu, S., Shan, L., and He, P. (2014). Microbial signature-triggered plant defense responses and early signaling mechanisms. Plant Science *228C*, 118-126.

Xu, G.Y., Greene, G.H., Yoo, H.J., Liu, L.J., Marques, J., Motley, J., and Dong, X.N. (2017). Global translational reprogramming is a fundamental layer of immune regulation in plants. Nature *545*, 487-490.

Xu, P., Duong, D.M., Seyfried, N.T., Cheng, D., Xie, Y., Robert, J., Rush, J., Hochstrasser, M., Finley, D., and Peng, J. (2009). Quantitative proteomics reveals the function of unconventional ubiquitin chains in proteasomal degradation. Cell *137*, 133-145.

Yamada, K., Yamaguchi, K., Shirakawa, T., Nakagami, H., Mine, A., Ishikawa, K., Fujiwara, M., Narusaka, M., Narusaka, Y., Ichimura, K., *et al.* (2016). The Arabidopsis CERK1-associated kinase PBL27 connects chitin perception to MAPK activation. The EMBO Journal *35*, 2468-2483.

Yamaguchi, Y., Huffaker, A., Bryan, A.C., Tax, F.E., and Ryan, C.A. (2010). PEPR2 Is a Second Receptor for the Pep1 and Pep2 Peptides and Contributes to Defense Responses in Arabidopsis. The Plant Cell *22*, 508-522.

Yamaguchi, Y., Pearce, G., and Ryan, C.A. (2006). The cell surface leucine-rich repeat receptor for AtPep1, an endoaenous peptide elicitor in Arabidopsis, is functional in transgenic tobacco cells. Proceedings of the National Academy of Sciences of the United States of America *103*, 10104-10109.

Yang, Y., Kitagaki, J., Dai, R.M., Tsai, Y.C., Lorick, K.L., Ludwig, R.L., Pierre, S.A., Jensen, J.P., Davydov, I.V., Oberoi, P., *et al.* (2007). Inhibitors of ubiquitin-activating enzyme (E1), a new class of potential cancer therapeutics. Cancer Research *67*, 9472-9481.

Yu, L., Nie, J., Cao, C., Jin, Y., Yan, M., Wang, F., Liu, J., Xiao, Y., Liang, Y., and Zhang, W. (2010). Phosphatidic acid mediates salt stress response by regulation of MPK6 in Arabidopsis thaliana. The New Phytologist *188*, 762-773.

Yu, X., Feng, B., He, P., and Shan, L. (2017). From Chaos to Harmony: Responses and Signaling upon Microbial Pattern Recognition. Annual Review of Phytopathology *55*, 109-137.

Zhang, H.W., Cui, F., Wu, Y.R., Lou, L.J., Liu, L.J., Tian, M.M., Ning, Y., Shu, K., Tang, S.Y., and Xie, Q. (2015). The RING Finger Ubiquitin E3 Ligase SDIR1 Targets SDIR1-INTERACTING PROTEIN1 for Degradation to Modulate the Salt Stress Response and ABA Signaling in Arabidopsis. The Plant Cell *27*, 214-227.

Zhang, J., Li, W., Xiang, T., Liu, Z., Laluk, K., Ding, X., Zou, Y., Gao, M., Zhang, X., Chen, S., *et al.* (2010). Receptor-like cytoplasmic kinases integrate signaling from multiple plant immune receptors and are targeted by a Pseudomonas syringae effector. Cell Host & Microbe *7*, 290-301.

Zhang, W.D., Chen, J., Zhang, H.J., and Song, F.M. (2008). Overexpression of a rice diacylglycerol kinase gene OsBIDK1 enhances disease resistance in transgenic tobacco. Molecules and Cells *26*, 258-264.

Zhang, X.R., Garreton, V., and Chua, N.H. (2005). The AIP2 E3 ligase acts as a novel negative regulator of ABA signaling by promoting ABI3 degradation. Genes & Development *19*, 1532-1543.

Zhang, Y.Y., Zhu, H.Y., Zhang, Q., Li, M.Y., Yan, M., Wang, R., Wang, L.L., Welti, R., Zhang, W.H., and Wang, X.M. (2009). Phospholipase D alpha 1 and Phosphatidic Acid Regulate NADPH Oxidase Activity and Production of Reactive Oxygen Species in ABA-Mediated Stomatal Closure in Arabidopsis. The Plant Cell *21*, 2357-2377.

Zhou, J., He, P., and Shan, L. (2014). Ubiquitination of plant immune receptors. Methods in Molecular Biology *1209*, 219-231.

Zipfel, C., Kunze, G., Chinchilla, D., Caniard, A., Jones, J.D.G., Boller, T., and Felix, G. (2006). Perception of the bacterial PAMP EF-Tu by the receptor EFR restricts Agrobacterium-mediated transformation. Cell *125*, 749-760.

APPENDIX

SUPPLEMENTAL DATA

Supplemental Table 1. Primers used in this study.

Supplemental Table 2. Y2H screen result (unique to BIK1).

Supplemental Table 1. Primers used in this study.

BIK1K41R-F	CGGCGGCTCAGAGGACGGAAGGGGAG
BIK1K41R-R	CTCCCCTTCCGTCCTCTGAGCCGCCG
BIK1K358R-F	GGACAACTTGGGACGGCCGAGTCAGACC
BIK1K358R-R	GGTCTGACTCGGCCGTCCCAAGTTGTCC
BIK1KK105RR-F	GGTCATCGCCGTTCGCCGGCTTAACCAAGAAG
BIK1KK105RR-F	CTTCTTGGTTAAGCCGGCGAACGGCGATGACC
BIK1 K105R-F	GGTTTGGTCATCGCCGTTAGAAAGCTTAACCAAG
BIK1 K105R-R	CTTGGTTAAGCTTTCTAACGGCGATGACCAAACC
BIK1 K186R-F	GCGCTTGATGCAGCAAGGGGGCTTGCTTTTCTTC
BIK1 K186R-R	GAAGAAAAGCAAGCCCCCTTGCTGCATCAAGCGC
BIK1 K204R-F	GATATACCGAGACATTAGAGCCTCGAACATCTTA C
BIK1 K204R-R	GTAAGATGTTCGAGGCTCTAATGTCTCGGTATATC
BIK1 K217R-F	GCGGACTACAACGCAAGACTTTCTGACTTTGGAC
BIK1 K217R-R	GTCCAAAGTCAGAAAGTCTTGCGTTGTAGTCCGC
BIK1 K303R-F	CCTCACAAGCAAACGTAGGGTTCTCCTAATCGTGG
BIK1 K303R-R	CCACGATTAGGAGAACCCTACGTTTGCTTGTGAGG
BIK1 K10R-F	CTTCAGTTCTCGAGTCAGAGCAGACATCTTCCAC
BIK1 K10R-R	GTGGAAGATGTCTGCTCTGACTCGAGAACTGAAG
BIK1 K18R-F	CATCTTCCACAATGGTAGGAGCAGCGATCTTTATG
BIK1 K18R-R	CATAAAGATCGCTGCTCCTACCATTGTGGAAGATG
BIK1 K31R-F	GTCTCTCAAGTCGGAGATCGTCTTCGACTGTAG
BIK1 K31R-R	CTACAGTCGAAGACGATCTCCGACTTGAGAGAC
BIK1 K53R-F	GAGTTCGACCCCTGTCAGAAGCTTCACCTTTAACG
BIK1 K53R-R	CGTTAAAGGTGAAGCTTCTGACAGGGGTCGAACT C
BIK1 K61R-F	CACCTTTAACGAACTCAGACTCGCCACAAGAAAC
BIK1 K61R-R	GTTTCTTGTGGCGAGTCTGAGTTCGTTAAAGGTG
BIK1 K83R-F	CTTTGGTTGTGTCTTTAGAGGCTGGTTAGATGAG
BIK1 K83R-R	CTCATCTAACCAGCCTCTAAAGACACAACCAAAG
BIK1 K95R-F	CACTCTCACTCCGACTAGACCTGGAACCGGTTTG
BIK1 K95R-R	CAAACCGGTTCCAGGTCTAGTCGGAGTGAGAGTG
BIK1 K135R-F	CACCCAAATCTAGTTAGACTGATCGGTTATTGC
BIK1 K135R-R	GCAATAACCGATCAGTCTAACTAGATTTGGGTG
BIK1 K155R-F	CTACGAGTTTATGCAAAGAGGAAGTCTTGAGAAT C

BIK1 K155R-R	GATTCTCAAGACTTCCTCTTTGCATAAACTCGTAG
BIK1 K170R-F	GAGGTGCATATTTTAGGCCACTCCCATGGTTTC
BIK1 K170R-R	GAAACCATGGGAGTGGCCTAAAATATGCACCTC
BIK1 K197R-F	CACAGCGATCCCGTCAGAGTGATATACCGAGAC
BIK1 K197R-R	GTCTCGGTATATCACTCTGACGGGATCGCTGTG
BIK1 K276R-F	GAGATTTTATCTGGTAGGCGAGCGTTGGATC
BIK1 K276R-R	GATCCAACGCTCGCCTACCAGATAAAATCTC
BIK1 K286R-F	CATAACAGACCGGCTAGAGAAGAAAACCTTGTG
BIK1 K286R-R	CACAAGGTTTTCTTCTCTAGCCGGTCTGTTATG
BIK1 K301R-F	CGTACCTCACAAGCAGACGTAAGGTTCTCCTAATC
BIK1 K301R-R	GATTAGGAGAACCTTACGTCTGCTTGTGAGGTACG
BIK1 K337R-F	CTCTCATTTGAACCCAGGTCGCGCCCGACCATG
BIK1 K337R-R	CATGGTCGGGCGCGACCTGGGTTCAAATGAGAG
BIK1 K366R-F	CAGACCAATCCGGTTAGGGATACCAAGAAACTTG
BIK1 K366R-R	CAAGTTTCTTGGTATCCCTAACCGGATTGGTCTG
BIK1 K369R-F	CGGTTAAGGATACCAGGAGACTTGGTTTTAAAAC TG
BIK1 K369R-R	CAGTTTTAAAACCAAGTCTCCTGGTATCCTTAACC G
BIK1 K374R-F	CAAGAAACTTGGTTTTAGAACTGGTACTACTAAG
BIK1 K374R-R	CTTAGTAGTACCAGTTCTAAAACCAAGTTTCTTG
BIK1 K379R-F	GTTTTAAAACTGGTACTACTAGGTCATCCGAAAAA CG
BIK1 K379R-R	CGTTTTTCGGATGACCTAGTAGTACCAGTTTTAAA AC
BIK1 K383R-F	CTAAGTCATCCGAAAGACGGTTTACACAAAAAC
BIK1 K383R-R	GTTTTTGTGTAAACCGTCTTTCGGATGACTTAG
BIK1 K388R-F	GAAAAACGGTTTACACAAAGACCTTTTGGCAGGC
BIK1 K388R-R	GCCTGCCAAAAGGTCTTTGTGTAAACCGTTTTTC
BIK1-KK379374RR-F	GAACTGGTACTACTAGGTCATCCGAAAAACG
BIK1-KK379374RR-R	CGTTTTTCGGATGACCTAGTAGTACCAGTTC
BIK1-KK369370RR-K366RK374R-F	CGGTTAGGGATACCAGGAGACTTGGTTTTAGAAC
BIK1-KK369370RR-K366RK374R-R	GTTCTAAAACCAAGTCTCCTGGTATCCCTAACCG
BIK1-KK383388RR-F	GTCATCCGAAAGACGGTTTACACAAAGACCTTTTG
BIK1-KK383388RR-R	CAAAAGGTCTTTGTGTAAACCGTCTTTCGGATGAC
BIK1-KK303301RR-F	CTCACAAGCAGACGTAGGGTTCTCCTAATCG
BIK1-KK303301RR-R	CGATTAGGAGAACCCTACGTCTGCTTGTGAG

PBL1 K199R-F	TCATTTACAGAGACATCAGGGCGTCAAACATCTTAC
PBL1 K199R-R	GTAAGATGTTTGACGCCCTGATGTCTCTGTAAATGA
LUCKY1-BAMHI-F	CGGGATCCATGACTCGACCGTCAAGATTAC
LUCKY1-STUI-R	GAAGGCCTAGGAAGAAACGTAGGAATGGTAG
LUCKY2-BAMHI-F	CGGGATCCATGACTCGCTCCTCTAGATTC
LUCKY2-SMAI-R	TCCCCCGGGAGGAAGAAAAGCAGGAATAATG
LUCKY1-CD-BAMHI-F	CGGGATCCCGATGCGCTTGGCTCCGGCG
LUCKY2-CD-BAMHI-F	CGGGATCCGCTCGCTGCGCTTGGCTCCGC
LUCKY1-STOP-HA-F	CATTCCTACGTTTCTTCCTTAGCCTTACCCATACGAC
LUCKY1-STOP-HA-R	GTCGTATGGGTAAGGCTAAGGAAGAAACGTAGGAATG
LUCKY1AMIRNA480-1	GATTTTGTCAATACACTCCACGGTCTCTCTTTTGTATTCC
LUCKY1AMIRNA480-2	GACCGTGGAGTGTATTGACAAAATCAAAGAGAATCAATGA
LUCKY1AMIRNA480-3	GACCATGGAGTGTATAGACAAATTCACAGGTCGTGATATG
LUCKY1AMIRNA480-4	GAATTTGTCTATACACTCCATGGTCTACATATATATTCCT
LUCKY1AMIRNA109-1	GATCAAGTAATCTTGACGGTCGTTCTCTCTTTTGTATTCC
LUCKY1AMIRNA109-2	GAACGACCGTCAAGATTACTTGATCAAAGAGAATCAATGA
LUCKY1AMIRNA109-3	GAACAACCGTCAAGAATACTTGTTCACAGGTCGTGATATG
LUCKY1AMIRNA109-4	GAACAAGTATTCTTGACGGTTGTTCTACATATATATTCCT
LUCKY1AMIRNA211-1	GATCAACGCAGATAAGAGCGCTATCTCTCTTTTGTATTCC
LUCKY1AMIRNA211-2	GATAGCGCTCTTATCTGCGTTGATCAAAGAGAATCAATGA
LUCKY1AMIRNA211-3	GATAACGCTCTTATCAGCGTTGTTCACAGGTCGTGATATG
LUCKY1AMIRNA211-4	GAACAACGCTGATAAGAGCGTTATCTACATATATATTCCT
LUCKY2AMIRNA444-1	GATTATGCATATTGCACACTCCGTCTCTCTTTTGTATTCC
LUCKY2AMIRNA444-2	GACGGAGTGTGCAATATGCATAATCAAAGAGAATCAATGA

LUCKY2AMIRNA444-3	GACGAAGTGTGCAATTTGCATATTCACAGGTCGTGATATG
LUCKY2AMIRNA444-4	GAATATGCAAATTGCACACTTCGTCTACATATATATTCCT
LUCKY2AMIRNA113-1	GATAATCTAGAGGAGCGAGTCAGTCTCTCTTTTGTATTCC
LUCKY2AMIRNA113-2	GACTGACTCGCTCCTCTAGATTATCAAAGAGAATCAATGA
LUCKY2AMIRNA113-3	GACTAACTCGCTCCTGTAGATTTTCACAGGTCGTGATATG
LUCKY2AMIRNA113-4	GAAAATCTACAGGAGCGAGTTAGTCTACATATATATTCCT
LUCKY2AMIRNA214-1	GATCTACGCATACGAGAGCGCATTCTCTCTTTTGTATTCC
LUCKY2AMIRNA214-2	GAATGCGCTCTCGTATGCGTAGATCAAAGAGAATCAATGA
LUCKY2AMIRNA214-3	GAATACGCTCTCGTAAGCGTAGTTCACAGGTCGTGATATG
LUCKY2AMIRNA214-4	GAACTACGCTTACGAGAGCGTATTCTACATATATATTCCT
PLUCKY1-SACI-F	CCGGAGCTCCTCAATTTGATAGAATTTCTCCG
PLUCKY1-BAMHI-R	CGGGATCCTGCTTTTTGAGCTTTGGAGAC
PLUCKY2-SACI-F	TCCGAGCTCGCTTCCGTTCTCAATTATTG
PLUCKY2-BAMHI-R	CGGGATCCTTTGTTTTGGTTTTGAGTTC
DGK5-BAMHI-F	CGGGATCCATGGAGAAATACAACAGTTTATC
DGK5-STUI-R	GAAGGCCTGAGCACATGTGACCAACCATGAAC
DGK5-S267A-F	GCTGGTTAATCAGGCTACGTATGTAAAGC
DGK5-S267A-R	GCTTTACATACGTAGCCTGATTAACCAGC
DGK5-T398A-F	GTGCAACCGACCATGCATTCATGAGGATG
DGK5-T398A-R	CATCCTCATGAATGCATGGTCGGTTGCAC
DGK5-S463A-F	GATAATGAAGACGACGCAGTGGCTGAAGGC
DGK5-S463A-R	GCCTTCAGCCACTGCGTCGTCTTCATTATC
DGK5-S478A-F	GTTTGGTGCTGCGGATGCCTTCAAGATTCCTG
DGK5-S478A-R	CAGGAATCTTGAAGGCATCCGCAGCACCAAAC
DGK5-S495A-F	TAAAAAAGGAAGGGCTGCAAGGAGGAGAAATTC
DGK5-S495A-R	GAATTTCTCCTCCTTGCAGCCCTTCCTTTTTTA
DGK5-S500A-F	CAAGGAGGAGAAATGCAAATGTTCATGGTTG
DGK5-S500A-R	CAACCATGAACATTTGCATTTCTCCTCCTTG
DGK5-S506A-F	ATGTTCATGGTTGGGCACATGTGCTCAGGC
DGK5-S506A-R	GCCTGAGCACATGTGCCCAACCATGAACAT

DGK5SV-NO-INTRON-F	TATTTCTCAACTTAGTAGGCCTTACCCATAC
DGK5SV-NO-INTRON-R	GTATGGGTAAGGCCTACTAAGTTGAGAAATA
PDGK5-SACI-F	CCGGAGCTCTCACAATAGATAGGTACAAATG
PDGK5-BAMHI-R	CGGGATCCTGTCGCGCAACAATTTTGGTAG
DGK5-T446A-F	GTGTTTGACCCTTCAGCACCCCGCCATCAG
DGK5-T446A-R	CTGATGGCGGGGTGCTGAAGGGTCAAACAC
DGK5-T446D-F	GTGTTTGACCCTTCAGACCCCCGCCATCAGGATG
DGK5-T446D-R	CATCCTGATGGCGGGGGTCTGAAGGGTCAAACAC
DGK5-S488A-F	GAGGGAGAACACGCTAATAAAAAAGGAAG
DGK5-S488A-R	CTTCCTTTTTTATTAGCGTGTTCTCCCTC
DGK5-S506D-FP	GTTCATGGTTGGGACCATGTGCTCAGG
DGK5-S506D-RP	CCTGAGCACATGGTCCCAACCATGAAC
SAIL_1212_E10 LP	TTCAGAGCACATGTGACCAAC
SAIL_1212_E10 RP	TCCAATTCGGACATTTGTTTC
SAIL_127_B03 LP	CAAATAGTCATCAGTGACGACCA
SAIL_127_B03 RP	GGTGTAGGACGACTCTCCTCC

Supplemental Table 2. Y2H screen result (unique to BIK1).

# of colonies	Gene	Gene annotation
14	AT2G20900	DGK5, ATDGK5 | diacylglycerol kinase 5
8	AT1G05135	pseudogene of unknown protein
7	AT3G56360	unkown protein
5	AT5G60670	Ribosomal protein L11 family protein
5	AT1G20340	DRT112, PETE2 | Cupredoxin superfamily protein
5	AT4G34230	CAD5, ATCAD5, CAD-5 | cinnamyl alcohol dehydrogenase 5
3	AT1G02920	ATGSTF7, GST11, ATGSTF8, GSTF7, ATGST11 | glutathione S-transferase 7
2	AT5G66930	ATG101, AUTOPHAGY-RELATED 101
2	AT3G53430	Ribosomal protein L11 family protein
2	AT2G14260	PIP | proline iminopeptidase
2	AT4G12480	pEARLI 1 | Bifunctional inhibitor/lipid-transfer protein/seed storage 2S albumin superfamily protein
2	AT1G11530	ATCXXS1, CXXS1 | C-terminal cysteine residue is changed to a serine 1
2	AT5G56260	Ribonuclease E inhibitor RraA/Dimethylmenaquinone Methyltransferase
2	AT1G47250	PAF2 | 20S proteasome alpha subunit F2
2	AT3G17390	MTO3, SAMS3, MAT4 | S-adenosylmethionine synthetase family protein
2	AT5G01750	Protein of unknown function (DUF567)
1	AT1G13990	unknown protein
1	AT5G41800	Transmembrane amino acid transporter family protein
1	AT3G52340	SPP2 | sucrose-6F-phosphate phosphohydrolase 2
1	AT1G02500	SAM1, SAM-1, MAT1, AtSAM1 | S-adenosylmethionine synthetase 1
1	AT2G17450	RHA3A | RING-H2 finger A3A
1	AT5G44250	Protein of unknown function DUF829, transmembrane 53
1	AT1G11200	Protein of unknown function (DUF300)
1	AT5G42790	PAF1, ATPSM30, ARS5 | proteasome alpha subunit F1
1	AT1G10590	Nucleic acid-binding, OB-fold-like protein
1	AT1G22190	Integrase-type DNA-binding superfamily protein
1	AT1G69740	HEMB1 | Aldolase superfamily protein
1	AT4G23730	Galactose mutarotase-like superfamily protein
1	AT5G47840	AMK2 | adenosine monophosphate kinase

1	AT3G22231	PCC1 | pathogen and circadian controlled 1
1	AT1G12900	GAPA-2
1	AT1G78830	Curculin-like (mannose-binding) lectin family protein
1	AT2G35980	YLS9, NHL10, ATNHL10 | Late embryogenesis abundant (LEA) hydroxyproline-rich glycoprotein family
1	AT5G17560	BolA-like family protein
1	AT3G54870	MRH2, ARK1, CAE1 | Armadillo/beta-catenin repeat family protein / kinesin motor family protein